Molecular Therapy
Original Article

In vivo CRISPR gene editing in patients with herpetic stromal keratitis

Anji Wei,[1,7] Di Yin,[2,7] Zimeng Zhai,[1,7] Sikai Ling,[3,7] Huangying Le,[2] Lijia Tian,[1] Jianjiang Xu,[1] Soren R. Paludan,[4] Yujia Cai,[2] and Jiaxu Hong[1,5,6]

[1]Department of Ophthalmology and Visual Science, Eye, and ENT Hospital, Shanghai Medical College, Fudan University, Shanghai, China; [2]Key Laboratory of Systems Biomedicine (Ministry of Education), Shanghai Center for Systems Biomedicine, Shanghai Jiao Tong University, Shanghai, China; [3]BDgene Therapeutics, Shanghai, China; [4]Department of Biomedicine, Aarhus University, Aarhus, Denmark; [5]Shanghai Key Laboratory of Visual Impairment and Restoration, Science and Technology Commission of Shanghai Municipality, Shanghai, China; [6]Shanghai Engineering Research Center of Synthetic Immunology, Shanghai, China

***In vivo* CRISPR gene therapy holds large clinical potential, but the safety and efficacy remain largely unknown. Here, we injected a single dose of herpes simplex virus 1 (HSV-1)-targeting CRISPR formulation in the cornea of three patients with severe refractory herpetic stromal keratitis (HSK) during corneal transplantation. Our study is an investigator-initiated, open-label, single-arm, non-randomized interventional trial at a single center (NCT04560790). We found neither detectable CRISPR-induced off-target cleavages by GUIDE-seq nor systemic adverse events for 18 months on average in all three patients. The HSV-1 remained undetectable during the study. Our preliminary clinical results suggest that *in vivo* gene editing targeting the HSV-1 genome holds acceptable safety as a potential therapy for HSK.**

INTRODUCTION

Herpes simplex virus type 1 (HSV-1) is a common human virus, with a global seroprevalence of 50%–90%.[1–3] Ocular HSV-1 infection is the major cause of herpetic stromal keratitis (HSK), which is one of the leading causes of infectious blindness in developed countries.[4] Approximately 40,000 people develop visual disability among the 1.5 million new cases of ocular HSV infection each year.[4] After primary infection in the cornea, HSV-1 establishes a latent reservoir in the trigeminal ganglia (TGs), which can be reactivated, leading to the recurrence.[5]

Currently, no vaccine is available against HSV infection.[6] Acyclovir (ACV) and analogs that target the viral DNA polymerase are the first-choice treatments for HSK.[7] However, as the antiviral molecules do not change the existing viral DNA, recurrences are still common. Additionally, resistance to ACV has been associated with longer disease duration and subsequent failure of prophylaxis in patients with recurrent ocular HSV episodes.[7,8] Other strategies, including antibodies, peptides, and small molecules, are still under development.[9] Corneal transplantation is recommended for HSK-induced corneal leucoma or perforation. However, the postoperative prognosis is compromised by high rates of virus recurrence.[10] According to previous studies, there is a high incidence of herpetic keratitis recurrence following penetrating keratoplasty (PK), even with the topical ACV, the recurrent rate is still over 55%.[10,11] Various studies have reported the recurrence rate of HSV infection in grafts with prophylactic oral ACV therapy ranging from 12% to 33%.[11–13] Notably, systemic ACV has been associated with kidney injury and neurotoxicity.[11,14] Essentially, neither the drugs nor surgical treatments can diminish the virus in the corneas or TG reservoir and cleave the virus genome directly, which drives the exploration of next-generation antiviral strategies with meganucleases and CRISPR.[15–17]

CRISPR has been remarkably successful in preclinical research.[18–22] So far, it has been applied in clinical trials for treating hemoglobin diseases, cancers, and HIV infection.[23–27] However, the published trials are all *ex vivo* except the recent report by Gillmore et al. in which CRISPR was used for *in vivo* treatment of transthyretin amyloidosis.[28] Still, the broader *in vivo* safety and efficacy profile of CRISPR remains to be established. To overcome the delivery obstacle for *in vivo* CRISPR therapy, several groups, including ours, have reported engineered virus-like particles that are able to transport mRNA or ribonucleoprotein, allowing transient gene editing.[29–31] Our group has developed an mRNA-carrying lentiviral particle (mLP) capable of incorporating an mRNA of interest such as SpCas9 in the producer cells via the interaction between aptamer in the mRNA and adaptor in the viral structural protein.[32] We further designed the SpCas9 mRNA-carrying lentiviral particle, termed HSV-1-erasing lentiviral particle (HELP), to specifically cleave two essential genes for the HSV-1 life cycle, UL8 and UL29, for HSK therapy.[33] A single intracorneal injection of HELP significantly diminished HSV-1 in the corneas and TG in mice.[33]

Received 4 May 2023; accepted 29 August 2023;
https://doi.org/10.1016/j.ymthe.2023.08.021.

[7]These authors contributed equally

Correspondence: Yujia Cai, Key Laboratory of Systems Biomedicine (Ministry of Education), Shanghai Center for Systems Biomedicine, Shanghai Jiao Tong University, Shanghai, China.
E-mail: yujia.cai@sjtu.edu.cn
Correspondence: Jiaxu Hong, Department of Ophthalmology and Visual Science, Eye, and ENT Hospital, Shanghai Medical College, Fudan University, Shanghai, China.
E-mail: Jiaxu.hong@fdeent.org

Although we have shown HELP efficiently controlled the HSV replication *in vitro*, in animal models and *ex vivo* human corneas, it may be difficult to clear all the viruses in the reservoir in humans. We hypothesized that reducing the virus load to a certain threshold will change the balance between virus and host so that the immune system can control the remaining virus and achieve a functional cure.[34,35] Here, we reported data from a clinical trial evaluating the safety and efficacy of one-dose HELP injection during the PK for three patients with severe refractory HSK and acute corneal perforation (Figure 1), all three had completed the 12-month follow-up (21 months, 18 months, and 14 months for patients 1, 2, and 3, respectively).

RESULTS

Preclinical results

The presence of HSV-1 in the corneas of the participants was determined by quantitative polymerase chain reaction (qPCR) analysis of the viral genome in tear-swabbed samples. The positive result was a precondition for enrollment (Table 1). HELP was given by intrastromal injection at a dose of 2.4 μg of p24 during PK, as illustrated in Figure 1. The perforated cornea was removed from the patient during the operation for subsequent fluorescence microscopy and immunohistochemistry analysis. The viral capsid protein VP5 was detected in the corneas of three patients by confocal imaging (Figure S1). As HSK is the consequence of excessive virus-induced corneal infiltration of inflammatory cells,[36] we therefore stained the removed corneal button for T cells (CD4+ and CD8+), myeloid-derived cells (CD11b+), and macrophages (F4/80+). Immunohistochemistry showed their infiltration in the cornea stroma of three patients (Figure S2). We sequenced HSV-1 strains isolated from three participants for genes encoding thymidine kinase (TK) and DNA polymerase (DNA pol). We found changes in amino acids in TK or in DNA pol, but they were not drug-resistance mutations (Figure S3 in the supplemental information). Additionally, we used an HSV-1-infected healthy cornea to evaluate the functionality of CRISPR and found a significant reduction of HSV-1 genome and viable viruses in addition to the barely detectable VP5 antigen (Figures 2A–2E). Also, we found direct evidence of viral genome cleavage in UL8 and UL29 loci with indel frequencies 28.8% and 14.4%, respectively, by deep sequencing (Figure 2F).

Patient demographics and outcomes

Patient 1

Patient 1 was a senior male in his early 70s who was admitted in November 2020 for corneal perforation due to recurrent HSK in the right eye and had initial HSK nearly 30 years ago with a recurrence interval of every 1–2 years. He had been prescribed a high dose of antiviral medications yet still failed to ameliorate the keratitis. His left eye was diagnosed with traumatic corneal leucoma. On examination, uncorrected visual acuity was light perception for both eyes. The slit-lamp image of the right eye showed an ill-defined central corneal ulcer of about 3 × 3 mm with iris incarcerated in the perforation. The left eye showed a cloudy cornea without conjunctival congestion. Patient 1 had mild anemia and a history of diabetes with a slightly high glycated hemoglobin of 6.2%.

Topical ganciclovir eye gel was discontinued for the patient 1 day before the uncomplicated PK. During the PK operation, the iris was carefully separated and severe lens opacity was found in the surgical eye. Patient 1 received HELP injection according to the protocol (Figure 3A). Topical 0.5% levofloxacin and 1% prednisolone acetate were administered three times per day after the surgery. Postoperative hyphema was identified immediately after the surgery and was absorbed on day 7. His visual acuity of the right eye has remained finger count owing to the severe cataract since day 3. At 6 months after PK, patient 1 developed an uncontrolled corneal ulcer related to neurotrophic keratopathy (NK), which mainly resulted from the long-lasting damage to the corneal sensory nerve induced by chronic HSV infection. In accordance with his decrease in corneal sensitivity, *in vivo* confocal microscopy (IVCM) showed significantly impaired corneal subbasal nerves in the central cornea graft at the latest follow-up (Figure S4). To further improve the patient's vision, we therefore conducted the second corneal transplantation and phacoemulsification with intraocular lens implantation on his right eye. He had regained an uncorrected visual acuity (decimal) of 20/100 in the surgical eye by the time of discharge (Figure 3B). The postoperative intraocular pressure was within the normal range (Table S1 in the supplemental information). Optical coherence tomography (OCT) showed a relatively shallow anterior chamber in patient 1 (Figure S5). His corneal graft had remained transparent since the second PK after 12 months post injection (Figure 3A).

Before treatment, both the corneal button and aqueous humor were diagnosed positive for HSV-1 using a Triplex HSV-1 DNA Diagnostic Kit with cycle threshold (Ct) values of 21.35 and 28.37, respectively (Table S1). However, tear swabs had maintained negative since his 2-month visit (Table 1). Interestingly, the second corneal transplantation in the sixth month gave us a unique opportunity to explore whether the HELP can diminish the HSV-1 genome *in vivo* by examining the excised corneal button. Indeed, we found VP5 signals neither around the rim nor in the center of the removed corneal button via fluorescence microscopy and immunohistochemistry analysis (Figures S6 and S7).

Patient 2

Patient 2 was a male in his early 50s who had an acute corneal perforation in the right eye caused by recurrent HSK. His right eye had been suffering from repeated redness and pain for more than a decade with a recurrence interval of 2–3 months, which could not be effectively controlled by various antiviral and glucocorticoid eye drops. Five days before admission in January 2021, the patient complained of sharp, sudden pain and fluid leakage in the right eye. On examination, uncorrected visual acuity (decimal) was 20/20 in the left eye yet only hand motion in the right eye. The slit-lamp image of the right eye revealed a 4-mm-diameter lower paracentral corneal ulcer with a pinpoint leakage but no hypopyon in the anterior chamber. The lens of the right eye was slightly cloudy. His left eye was unremarkable. Patient 2 had a history of chronic B-related hepatitis and hyperlipidemia.

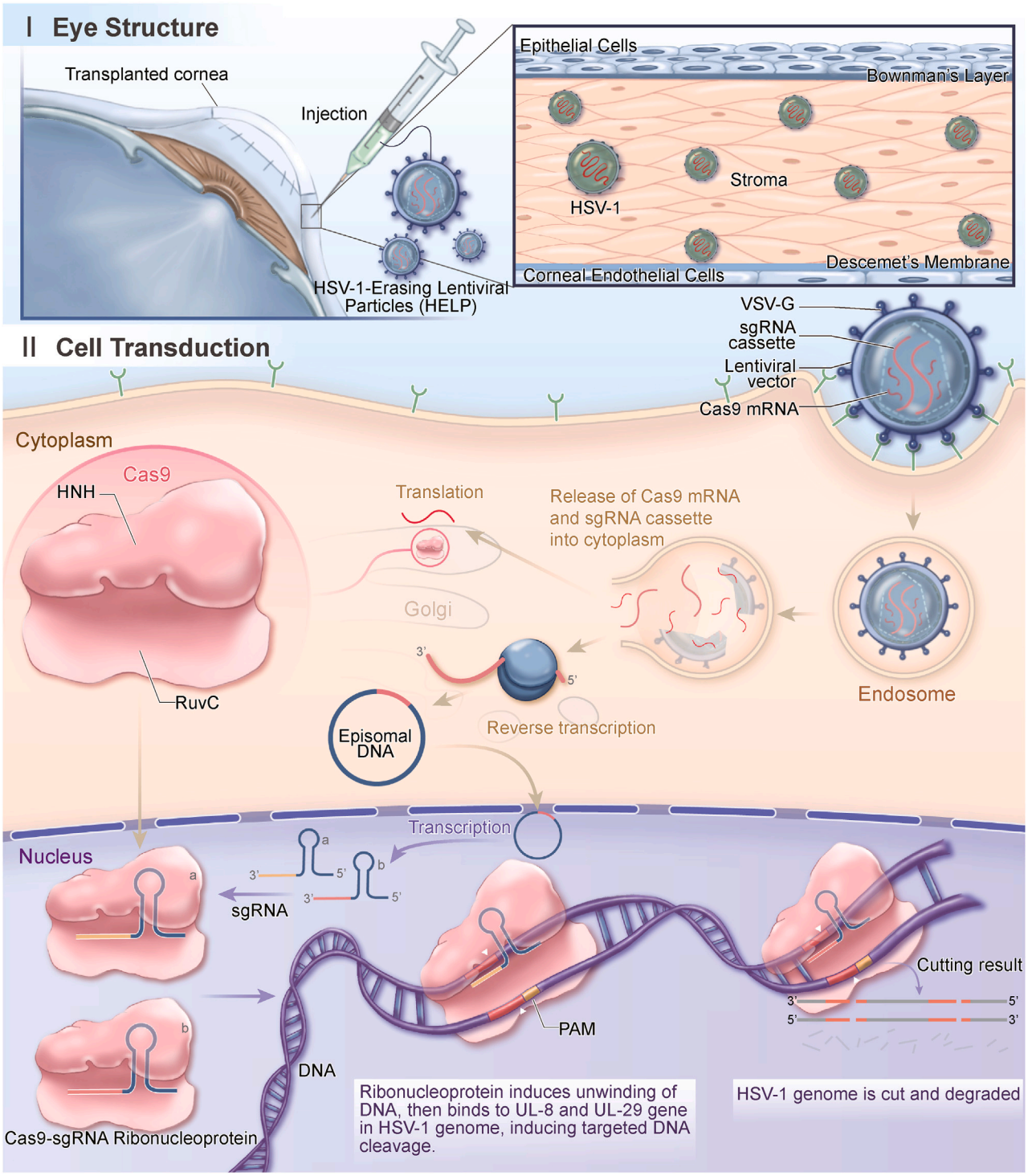

Figure 1. The antiviral mechanism of CRISPR in human corneas

HELP is a lentiviral viral particle carrying SpCas9 mRNA and a gRNA-expression cassette. The SpCas9 protein translated from mRNA directly and the gRNA expressed from the reverse transcribed viral DNA assemble into ribonucleoproteins (RNPs), which cleave the HSV-1 genome at UL8 and UL29 loci for degradation. A total of 0.2 mL (2.4 μg of p24) of HELP formulation was injected into the recipient graft bed in six to eight locations by using a 27G ophthalmic syringe after corneal transplantation.

Table 1. HSV-1 diagnosis

Number	Sex	Age range	Cornea	Aqueous	Tear swab (time post injection)							
					−1 day	1 week	1 month	2 months	3 months	6 months	12 months	Last visit[a]
1	male	70–74	+	+	+	−	+	−	−	−	−	−
					+	+	+	−	−	−	−	−
					+	−	+	−	−	−	−	−
2	male	50–54	+	+/−	+	−	−	−	−	−	−	−
					+	−	−	−	−	−	−	−
					+	−	−	−	−	−	−	−
3	male	65–69	+	−	+	−	−	−	−	−	−	−
					−	−	−	−	−	−	−	−
					−	−	−	−	−	−	−	−

+, positive, Ct value ≤36.
+/−, weak positive, 36 < Ct value < 40.
−, negative, Ct value = 40 or "no Ct."
HSV-1 diagnosis was via nucleic acids detection by qPCR.
[a]Last visit: patient 1, 21 months; patient 2, 18 months; patient 3, 14 months.

Uncomplicated PK was performed for patient 2 who also received HELP injection subsequently according to the protocol. After the surgery, topical 0.5% levofloxacin and 1% prednisolone acetate were applied three times a day, whereas the traditional ACV eye drops (every 2 h) and oral tablets (twice daily) were discontinued. One day after surgery, topical prednisolone acetate was increased to four times daily due to corneal graft edema. Two days later, intraocular pressure of the right eye was 11 mm Hg and visual acuity raised to finger count. OCT at this time confirmed a flat iris and open anterior angle in all directions (Figure S8). At later visits, his visual acuity improved to 20/167 immediately at the 1-month visit and stabilized as 20/67 at 3 months after the surgery (Figure 3B). In the sixth month after PK, patient 2 was diagnosed with staphylococcal endophthalmitis, which was confirmed by bacterial and fungal cultures (Table S2) and subsequently contained by the combination of vitrectomy and antibiotic injection. His uncorrected visual acuity had decreased to 20/133 because of the secondary cataract in the surgical eye (Figure 3B). IVCM revealed partial regeneration of corneal nerves at his 12-month follow-ups (Figure S9). No relapse of herpetic keratitis or graft rejection was identified at the final visit.

Before treatment, the patient was positive for HSV-1 by qPCR analysis of the removed corneal tissue (Ct = 26.34) and tear swabs (Ct = 35.01) and the aqueous humor, which was weakly positive (Ct = 36.50) (Table S1). In the subsequent 12- and 18-month follow-ups, however, we found the tear swab samples during the postoperative visits showed that the HSV-1 tests were all negative by qPCR examination (Table 1).

Patient 3

Patient 3 was a male in his late 60s who had 6-year history of HSK and eventual corneal perforation in the left eye 10 days before admission in May 2021. His HSK relapsed every 2–3 months. The same eye had phacoemulsification with intraocular lens implantation 8 years ago. His right eye was unremarkable. On examination, uncorrected visual acuity (decimal) was 20/50 in the right eye and hand motion in the left eye. Conjunctiva congestion and limbal neovascularization were severe in his left eye, with a gray ulcer of 5 × 5 mm at the center of the opaque cornea. Subacute cornea perforation and hypopyon indicated a high-risk corneal transplantation. OCT confirmed partial perforation on the cornea (Figure S10). Patient 3 had a history of hypertension.

After the uneventful PK and HELP injection, the patient had been prescribed 0.3% tobramycin and 0.1% dexamethasone ophthalmic ointment four times daily. Brinzolamide timolol drops (twice per day) were prescribed for his elevated intraocular pressure owing to postoperative hyphema. Ganciclovir eye gel (four times daily) and ACV oral tablets (twice daily) were discontinued after treatment. One day after the surgery, 0.5% cyclosporine eye drops were added to suppress inflammation of the ocular surface. Due to the intraocular lens opacity induced by corneal perforation, the visual acuity of patient 3 had been hand motion since PK operation and finger count at 12-month follow-up (Figure 3B). On his 3-month follow-up, we observed corneal edema and inflammatory cell infiltration around the corneal sutures, indicating an occurring graft rejection, which was controlled after receiving topical treatment for the graft rejection and secondary glaucoma. Postoperative B-scan ultrasonography suggested no significant abnormal changes in the retina (Figure S12).

Although we did not detect HSV-1 in aqueous humor in patient 3 before CRISPR treatment, the patient was diagnosed as HSV-1 positive for detecting HSV-1 in the tear swab (Ct = 29.5) and the removed corneal tissue (Ct = 34.9) during PK by qPCR and the viral VP5 antigen using confocal imaging (Tables 1 and S1; Figure S1). However, in the 12- and 14-month follow-ups, we found the swab samples during the postoperative visits were all negative for HSV-1 (Table 1).

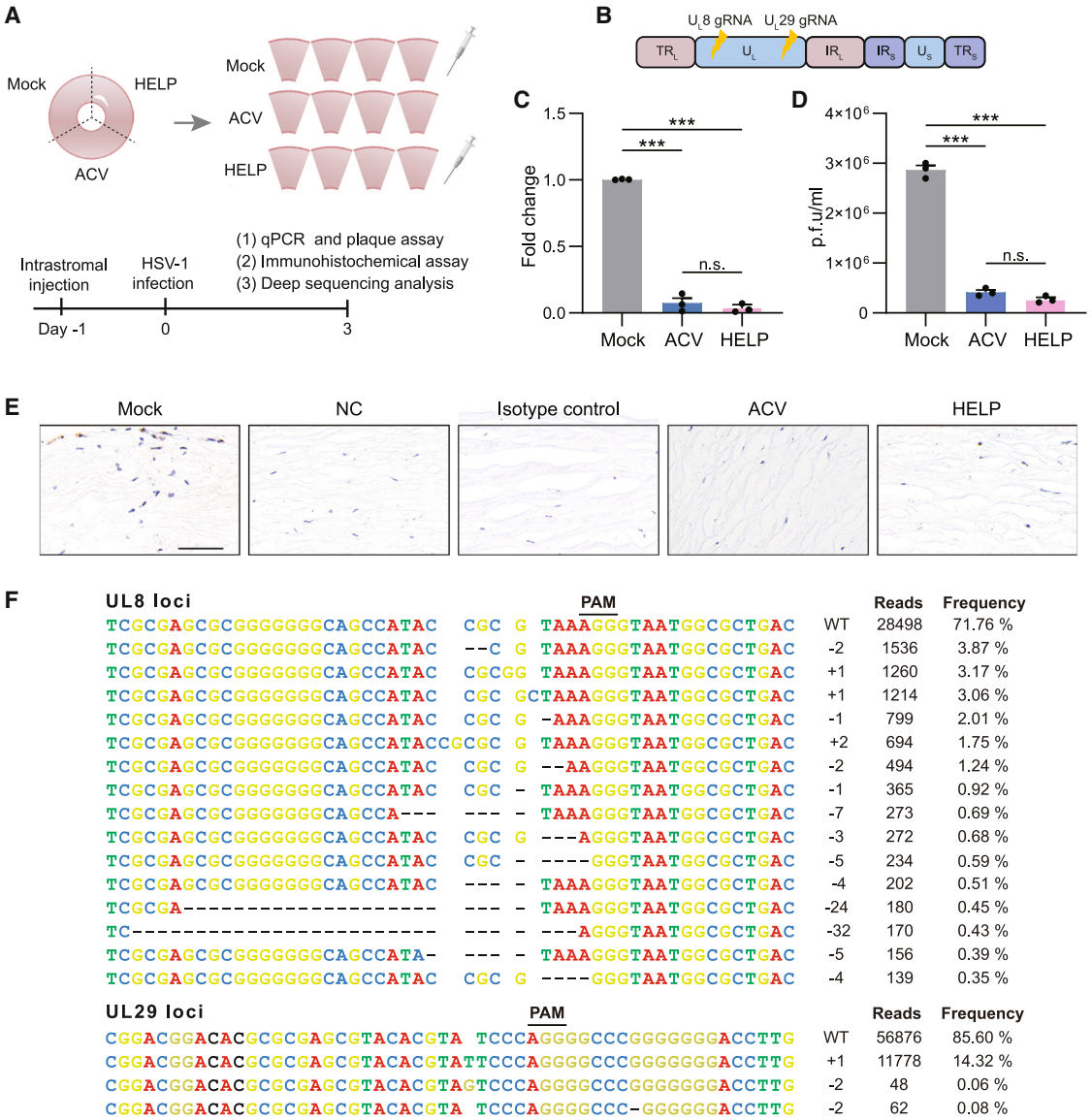

Figure 2. Preclinical results of HELP eliminating HSV-1 in tissue culture of a healthy cornea

(A) Flowchart for evaluating the antiviral effects of HELP in HSV-1-infected healthy human cornea. (B) Schematic illustration of the HSV-1 genome and gRNA loci. TRL, terminal repeat long; UL, unique long; IRL, internal repeat long; IRS, internal repeat short; US, unique short; TRS, terminal repeat short. (C) qPCR analysis of HSV-1 genome (fold change); $p < 0.0001$. (D) HSV-1 titer of supernatants from human corneal cultures measured by plaque assay; mock versus ACV and HELP, $p < 0.0001$, respectively. (E) Immunohistochemistry analysis of HSV-1 dissemination in a human cornea; scale bar, 20 μm. (F) The profile of HELP-induced mutations in HSV-1 UL8 and UL29 loci in a human cornea. Frequencies >0.035% and 0.07% in UL8 and UL29 loci are shown, respectively. The minus symbol indicates a deletion and the plus symbol indicates an insertion. PAM, protospacer adjacent motif; WT, wild type. Data and error bars represent mean ± SEM; n.s., not significant. One-way ANOVA with Dunnett's multiple comparisons test was performed.

Additional safety assessment

The potential HELP (CRISPR)-relevant side effects are the immune response attacking the CRISPR-transduced cells expressing Cas9 and off-target cleavages. ELISA showed intrastromal injection of HELP did not provoke an anti-vector immune response as no p24-specific immunoglobulin (Ig) G was induced (Table S3). Interestingly, by examining the blood samples, all the patients were SpCas9 positive before treatment, while the Cas9-specific IgG was not significantly enhanced after treatment (Figure S20). To analyze the potential off-target effects of our virus-targeting HELP in the human genome, we performed genome-wide, unbiased identification of DNA double-stranded breaks enabled by GUIDE-seq to reveal genome-wide integrations of double-stranded oligodeoxynucleotides in the double-strand DNA breaks caused by CRISPR (Figure 3C).[37] However, in subsequent deep

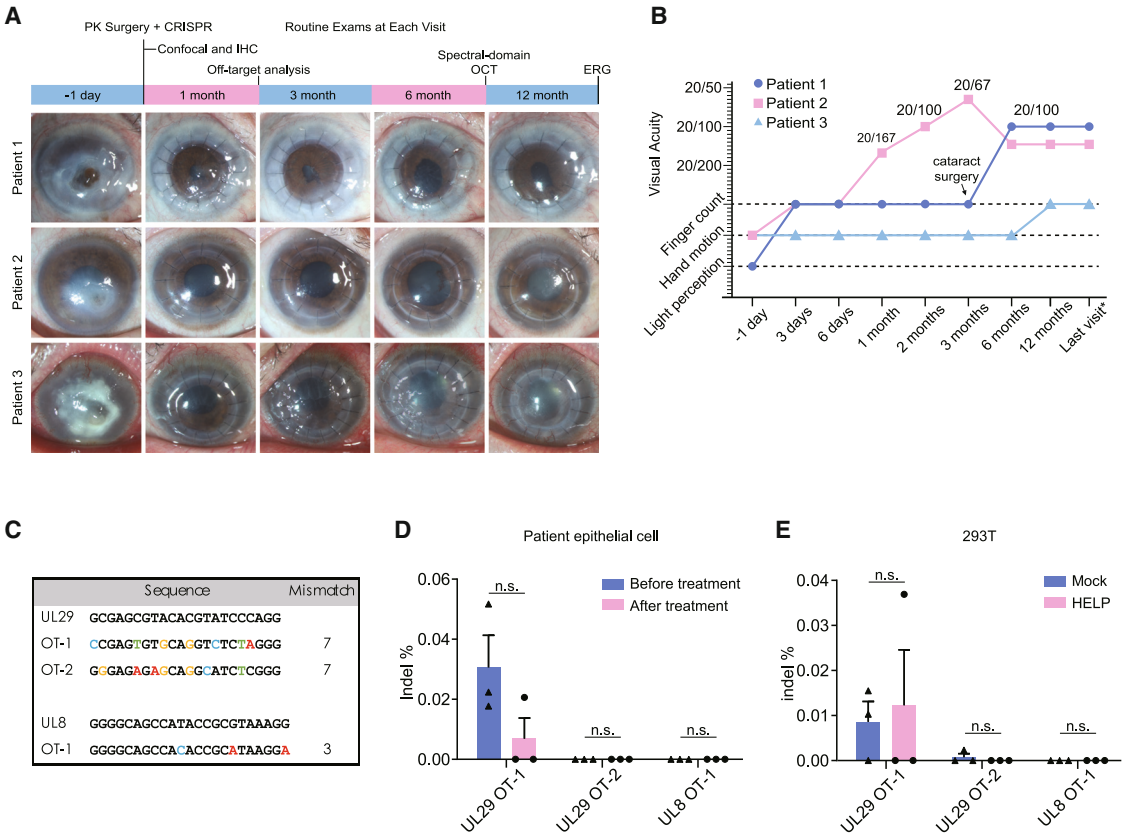

Figure 3. The main clinical results of CRISPR-treated HSK patients

(A) The time scheme and corresponding anterior segment photographs of three participants. (B) The changes of visual acuity in each participant during follow-ups, wherein last visit means 14 months, 18 months, and 21 months for patients 1, 2, and 3, respectively. (C) Potential off-target loci of HELP in the human genome identified by the GUIDE-seq. (D) Deep-sequencing results on the potential off-target sites in the patients' corneal epithelial cells at 1 month post HELP treatment. (E) Deep-sequencing results on the potential off-target sites in 293T cells. The genome was isolated 48 h post HELP transduction. OT, off-target site. Data and error bars represent mean ± SEM; n.s., non-significant; unpaired two-tailed Student's t tests.

sequencing, we did not detect indels on the three GUIDE-seq-identified sites in the detached epithelial cells from wiping the cornea of the patients 1 week after the treatment as well as in 293T cells (Figures 3D and 3E). The whole-genome sequencing (WGS) analysis of off-target sites identified only one potential off-target site for UL29 single guide RNA (sgRNA), whereas no potential off-target sites for UL8 sgRNA were found (supplemental results of WGS are in the supplemental information). As shown in Table S6, the potential off-target site was located in the intergenic region and would not change the gene function. Structural variants (SVs) analysis revealed that all the SVs have a low risk of affecting the gene function and causing pathogenicity (Tables S7–S9), suggesting that HELP has a minimal risk of inducing off-target effects. For the rest, we performed a complete ophthalmic examination on three patients after HELP treatment (supplemental information). The ocular adverse events (AEs) we observed included corneal graft edema, hyphema, post-herpes NK, concurrent cataract, and secondary glaucoma, which were mainly attributed to the high-risk PK with acute corneal perforation (Table S2).[38–40] B-scan ultrasonography of the patients on 7 days, 1 month, 6 months, and 12 months post injection showed no abnormal changes in the vitreous body and retina (Figures S12–S14). Retinal OCT demonstrated relatively intact fundus in HELP-injected eyes (Figures S15 and S16). Additionally, we found no apparent change in rod or cone responses in the participants by electroretinography (ERG) (Figures S17–S19). No systemic AEs were found during the study period.

Deficiencies of current work

To fulfill the ethics requirements by the committee as the first *in vivo* CRISPR human trial in infectious disease, the severe HSK participants enrolled in this pioneering study with corneal perforation demanded PK, which is prone to causing a myriad of postoperative manifestations and HSK recurrence for the surgery alone.[38] Additionally, the recurrent cases who urgently need corneal transplantation with definitive etiological evidence of HSV-1 infection, as suggested inclusion criteria by the ethical committee of China, brought limited participants in this prospective study, which is attributed to the single-arm nature of our work with a primary goal to explore the CRISPR-related safety and initial conclusion regarding the efficacy

of HELP. Once the safety and effectiveness of CRISPR is preliminarily determined, less severe HSK cases and subsequently more participants would be treated with HELP. By then, negative and positive control groups in the later-stage clinical trials would be embedded.

DISCUSSION

We report three refractory HSK cases with acute corneal perforation receiving *in vivo* CRISPR therapeutics. After a single intrastromal injection of HELP in combination with corneal transplantation, corneal grafts and tear swabs in the three patients were still free of viral relapse at their last visits, with the average follow-ups reaching 18 months even though we discontinued the antiviral therapy after the CRISPR injection. In the HSV-1-infected healthy corneas, HELP efficiently diminish the HSV-1 in terms of genome, viable viruses, and antigen (Figure 2). Moreover, we did not detect HSV-1 in the removed corneal button from patient 1 at 6 months post HELP treatment due to NK, supporting that the HELP could diminish the HSV-1 in the corneas (Figure S6). The laboratory data suggested no CRISPR off-target cleavage in the human genome or Cas9 and vector-specific immune response induced by intrastromal injection of HELP. These results suggest that HELP might be an effective strategy in restricting HSV-1 replication in the human corneas with no remarkable CRISPR-related side effects.

Although the HSV-1 DNA levels became undetectable immediately after treatment in patients 2 and 3, the virus was still detected in the first month for patient 1 but not at later time points. We reason several mechanisms may be responsible for this phenomenon. It is likely that HELP reduces viral load by targeting both productive replication and the latent reservoir without achieving full elimination, especially in cases such as patient 1 who had a much higher virus load than patient 2 and patient 3 (Table S1; Figure S1). Therefore, the acute stress-associated host response is likely to augment viral replication.[41,42] Second, immune activities are also likely required to fully inhibit the virus after the HELP treatment. Patient 1 was in his 70s and therefore might have a relatively weak immune system not fully capable of controlling residual viruses in the corneas and TG the first months after treatment. To balance the benefit-risk of the first antiviral CRISPR therapy, patient 1 was chosen because he had very high pre-operational viral loads in the cornea, aqueous humor, and tear swabs. Therefore, it is not surprising that HELP was unable to clear the virus completely in this patient but only reduce the virus burden *in vivo*. However, as the cornea of patient 1 was transparent at the 1-month visit without signs of recurrence, we continued an antiviral-drugs-free protocol on the patient. Notably, his swabs of both cornea and tear film remained negative for HSV-1 from 2 months to the final visit. According to the current study, patients 2 and 3, who had lower pre-operational HSV-1 loads compared with patient 1, had obtained a more thorough HSV-1 clearance by HELP judging from their virus tests. Future studies enrolling more patients with different degrees of HSK will answer whether patients with lower pre-operational corneal virus load than the three patients in this study will have an even more beneficial outcome after HELP treatment.

The participants enrolled in our study were all experiencing recurrent HSK episodes for decades, raising the possibility of drug-resistant HSV-1 infection. Accordingly, we found respective rather than simultaneously changes of amino acids in TK and DNA pol in the patients' isolates that were different from both the KOS and 17syn+ strains of HSV-1 (Figure S3), suggesting that the constant release of HSV-1 from the reservoir, instead of drug resistance, may have contributed to the refractory HSK in these patients. To date, the HSV-1 reservoir in TGs has still been untargetable with antiviral drugs. We have previously shown in the preclinical model that HELP is capable of modulating the virus in the reservoir via retrograde transportation of CRISPR to TG.[33] High-risk corneal transplantation for the perforated cornea is prone to HSK recurrence and corneal rejection. Therefore, the discontinuation of antiviral therapy after PK could make participants more vulnerable to HSV-1 recurrence than other patients. However, among the 21 tests of HSV-1 on three participants, except two tests in the first month of patient 1 that were positive without any clinical symptoms, all the other tests with the longest follow-up up to 21 months after treatment were negative. Thus, all three participants had no HSK recurrence during this study, although the specific role of HELP on HSV-1 in the human TG reservoir remains elusive.

We summarized all the AEs divided by the patients and by follow-up visits in a table (supplementary information Table S2). Although HELP treatment may not be fully excluded from the observed complications due to the limited cases and lack of controls, this was very unlikely except for corneal edema. Numerous complications, such as graft rejection, hyphema, glaucoma, or cataract, could be found in postoperative treatment of PK despite the progress of surgical techniques, especially in the high-risk cases with acute corneal perforation.[38] Hyphema in patient 1 is mainly attributed to the tear of the iris during the surgery, which finally resolved. Cataract in our three cases may happen because of acute corneal perforation and the usage of corticosteroid after the surgery. The incidence of glaucoma in patients 1 and 3 is not rare after corneal transplantation. Several etiologic factors have been identified, the most common being synechial angle closure and corticosteroid-induced intraocular pressure (IOP) elevation. IVCM revealed HSV-related corneal epithelium abnormality and low nerve density in all three participants, indicating their high susceptibility to post-herpes NK. Damage to the sensory nerve ending of the trigeminal nerve by HSV-1 could result in decreased corneal sensitivity, loss of epithelial integrity, and corneal ulceration in severe cases.[43] This possibly could explain why patient 1, a senior male with 30 years of HSK history, ultimately developed NK 6 months after PK. The endophthalmitis of patient 2 stemmed from bacterial infection, identified as gram-positive cocci (*Staphylococcus caprea*) using bacterial culture. The HELP product was produced and stored under GMP-like regulation, with a quality-control report (Table S11). Additionally, the HELP was injected into the cornea of patient 2, which remained transparent during the 18-month follow-up. To sum up, the potential HELP-relevant clinical AEs were minimal after CRISPR treatment.

Immune responses against the viral vector or Cas9 can be problematic for *in vivo* CRISPR gene therapy.[44,45] In our study, no vector-specific

IgG was detected after the HELP treatment. Indeed, prednisolone acetate has been prescribed throughout the follow-up course of the patients, as instructed by the standards for corneal transplantation to prevent rejection, which may have played a role in the restrained inflammatory and immune reactions in the patients.[9] Additionally, we have previously characterized that HELP is low immunogenic,[33] so both the low immunogenicity and prednisolone acetate may have contributed to the absence of inflammatory and immune reactions after the HELP treatment. Finally, the lack of HELP-related adverse effects may also be due to the transient nature of SpCas9 mRNA delivered by HELP.

HELP was originally designed for a single-dose administration. In the case of repeated dosing, the effectiveness of HELP may be compromised if the vector-specific IgG antibodies were induced, as they may block HELP at the entry level. However, the intracorneal injection may not be an effective route to induce anti-vector IgG as all three patients were p24 negative after HELP treatment (Table S3). Additionally, repeated administration may not cause safety problems for HELP as the SpCas9 expressed from mRNA exists only for several days, thus minimizing the chance to be attacked by cytotoxic T cells.[32] A preclinical study by Aubert and colleagues showed that adeno-associated virus (AAV)-delivered meganucleases have the potential to cure latent HSV infection.[15] Although the efficacy may not be a challenge for this method, the long-term expression of nucleases from AAV may cause safety concerns. In certain scenarios, our HELP or other similar technologies may be administered *ex vivo* to remove the virus that existed in the infected corneas from donors before the cornea transplantation surgeries. In conclusion, our clinical results from three HSK patients with an average of 18-month follow-up after receiving HELP suggest that *in vivo* CRISPR gene editing targeting the HSV-1 genome holds promise as a safe antiviral adjuvant therapy for which the efficacy may further be improved in combination with existing antiviral molecules such as ACV for severe refractory HSK to prevent the virus recurrence.[46] Dose escalation may clear the virus in high-virus-load patients more thoroughly than was achieved in patient 1. As our study is a single-arm pilot trial, a more complete study including a head-to-head comparison to the conventional ACV treatment and longer-term follow-up is necessary to fully evaluate the safety and efficacy of *in vivo* CRISPR therapy. It will also be interesting to adapt neuron tropic vial envelopes such as the envelope from rabies virus to pseudotype HELP, which might gain the additional advantage to target TGs where the latent HSV-1 hid. Future studies may also expand the treatment to patients with less severe HSK to protect them from getting refractory HSK and corneal perforation complications. Overall, our study provides clinical proof of concept for *in vivo* CRISPR gene editing as a potential antiviral strategy.

MATERIALS AND METHODS

Study oversight

The study is designed to evaluate the safety and efficacy of HELP for *in vivo* treatment of refractory HSK patients. This clinical practice was approved by the ethics committee of the Eye & ENT Hospital of Fudan University, China, and the National Health Commission, China (IRB-220113), and is registered with ClinicalTrials.gov (NCT04560790). Written informed consent was provided by the patients under video recording. The healthy donors involved in this study all signed the informed consent for biological sample donation and data sharing before the operation, with an agreement that the samples should be used for biomedical research. All the authors had access to the data and vouch for their accuracy and completeness. The manuscript was written and revised by the corresponding authors with help from all authors and was approved for publication by each of the authors.

Trial design and eligibility

In this investigator-initiated, open-label, single-arm, non-randomized interventional trial of 12 months at a single center, participants with refractory HSK were designed to receive a single dose of HELP formulation via intrastromal injection during the PK for acute corneal perforation. The trial is a completed analysis for this pilot study. Adult (ages 1870 years) patients with refractory keratitis who were repeatedly infected with HSV-1 virus (more than three times per year) and unresponsive to the standard regimen for HSK (oral ACV, 800 mg twice a day for 10 days, then 400 mg twice a day for at least 1 year) or those who were suffering from relapsed HSV infections with corneal perforation requiring corneal transplantation were enrolled. Patients who had serious ocular or systemic comorbidities (i.e., trauma, other infections, immune diseases, tumors) judged by investigators to be were unsuitable for the trial were excluded from this study. The follow-up strategy of this study consisted of two stages, a treatment period (1 day to 12 months) and a monitoring period (1–15 years). Participants entered the treatment follow-up period on the day after operation, from which researchers monitored predefined indicators according to the study protocol. After the end of the clinical trial (12 months post injection) patients transitioned into the monitoring period. Every 12 months, researchers would appoint a follow-up visit or phone call to acquire the latest data of patient status, continuing for 15 years or until the death of participants.

Compared with the original protocol, the major revisions on the current one were listed as adjusting the contents and priorities of outcomes and modifying the inclusion criteria (Table S11). These revisions will not increase the risk to subjects and have been approved by the ethics committee. From April 2020 to April 2022, a total of six HSK patients had provided informed consent: two did not meet eligibility criteria, one withdrew before undergoing HELP injection on their own decision, and three received intervention and had >12 months of follow-up; the preliminary analysis of our study was based on these last three patients (trials flow diagram from supplemental information).

Main outcomes and safety

The primary outcome was the ocular surface HSV-1 of the intervention eye on 1 week, 1 month, 2 months, 3 months, 6 months, and 12 months post operation and serious AEs post injection. The secondary outcome was cornea graft survival and best corrected visual acuity

(BCVA) at every follow-up visit. Safety assessment included HELP-provoked humoral immune reaction, off-target effects of CRISPR-Cas9 technology, tolerability assessments based on HELP-related AEs, clinical ophthalmic examinations and vital signs, and all-cause mortality. Owing to the small sample size (n = 3), the data are primarily descriptive. More details are provided in the supplemental information. Routine assessments included a complete ophthalmic examination (measurement of BCVA and intraocular pressure; slit-lamp examination), IVCM to analyze the corneal structures at the cellular level (corneal epithelium/endothelium and corneal subbasal nerves), time-domain OCT to investigate the anterior segment, the spectral-domain OCT to document the retinal status, postoperative B-scan ultrasonography to evaluate the status of the posterior segment of the eye, and ERG to measure the electrical activity generated by the retina in response to a light stimulus. Aqueous humor and the surgically removed corneal button were collected for HSV-1 genome detection. Tear swabs of pre-injection and at 1 week, 1 month, 2 months, 3 months, 6 months, and 12 months post injection were also collected and quantified for HSV-1 genome by qPCR using HSV-1 DNA Diagnostic Kit (Triplex International Bioscience). The virus testing outcome was indicated as positive (+) or negative (−) by Ct values that are equal or above 40 for negative, 36–40 for weakly positive, and equal or below 36 for positive according to the manufacturer's instruction. Blood samples of the participants were collected at 1-month, 3-month, 6-month, and 12-month visits to confirm whether intrastromal injection of HELP induces SpCas9-specific IgG and vector-specific IgG, which were determined by ELISA.[44] Deep sequencing of the detached epithelial cells by wipes was used for analyzing the potential off-target effects caused by CRISPR in the human genome.

Preparation and administration of HELP

The SpCas9 mRNA-carrying HELP was produced and quality controlled following Good Manufacturing Practice (GMP) guidelines by OBiO Technology. To manufacture the GMP-like level HELP, 293T cells were seeded in cell factories 24 h before polyethylenimine (PEI) transfection. Six hours after transfection, the media were refreshed and the supernatants were harvested 48 h post transfection. The virus-rich supernatants were filtered through a 0.45-μm filter and treated with Benzonase. After ultrafiltration/diafiltration using tangential flow filtration, the viral particles were purified by chromatography and then passed through 0.22-μm filters for sterilization.

The final formulation of HELP is a phosphate buffered saline (PBS)-dissolved lentiviral vector that contains two types of RNA all in one; one is SpCas9 mRNA (four copies on average in each particle) and the other is a guide RNA (gRNA)-expression viral RNA cassette.[33] A D64V mutation was introduced in the integrase so that the gRNA-expression cassette will not integrate into the host genome. The gRNA-expression cassette is reverse transcribed in the host cells and maintained as circular episomal DNA, which encodes two gRNAs targeting UL8 and UL29, respectively. The formulation was kept at −80°C for long-term storage. It was recovered to room temperature 10 min before injection. Each formulation, 0.2 mL in total, was drawn into a 27G ophthalmic syringe for the injection. PK was performed following the routine procedures. After sewing up the donor cornea, the graft bed of the recipient was injected with the HELP formulation in six to eight locations (Figure 1; Video S1).

HSV-1 plaque assay

Vero cells were seeded in a 12-well plate and infected with various dilutions of culture supernatants on the following day. Two hours after infection, cells were overlaid with 1% agarose solution. The cells were cultured for 3 days before being fixed with 4% formaldehyde and stained with 1% crystal violet solution. After three washes with water, the number of plaques was counted. HSV-1 titers were calculated as plaque-forming units (PFU) per milliliter. Each biological sample was performed in triplicate in a plaque assay.

ELISA

The humoral immune response to p24 was evaluated by an HIV p24 ELISA kit according to the manufacturer's protocol (Abnove). To detect the humoral immune response to SpCas9 in three patients, recombinant SpCas9 protein (Novoprotein), human albumin (Sigma), or tetanus toxoid (Astarte Biologics) were used to coat the ELISA plates, respectively. The plates were washed five times using ELISA wash buffer after incubation at 4°C overnight. One-percent BSA blocking solution was used to block plates at room temperature for 1 h, and then washed five times. Fifty-fold diluted serum samples were added to each well and incubated for 2 h. Plates were washed three times before adding HRP-conjugated goat anti-human antibody (Sangon), which was diluted 1,000-fold in blocking buffer. Plates incubated for 1 h at room temperature and then washed five times with washing buffer. TMB Single-Component Substrate solution (Solarbio) was added to the plate and developed for 15 min. The reaction was stopped by ELISA Stop Solution (Solarbio). The optical density (OD) value of each sample was analyzed by a microplate reader.

HSV-1 infection diagnosis

HSV-1 DNA in tear swabs, corneal buttons, and aqueous humor was amplified using HSV-1 DNA Diagnostic Kit (Triplex International Bioscience) according to the manufacturer's instructions. Quantitative PCR was performed using a LightCycler 96 real-time PCR system (Roche).

Immunofluorescence microscopy

An immunofluorescence protocol was adapted from a previous study.[33] Briefly, the corneal buttons were fixed in 4% paraformaldehyde (PFA) overnight at 4°C and then transferred to 30% sucrose. The optimal cutting temperature compound-embedded tissues were sectioned to 10-μm thickness using a freezing microtome (Leica) and processed for immunofluorescence. Slides were blocked in blocking buffer and incubated with primary antibody against HSV-1 VP5 (Santa Cruz Biotechnology, sc56989) overnight at 4°C. After washing five times, the slides were incubated with Alexa Fluor 488-conjugated secondary antibody (Jackson ImmunoResearch, 711-545-152).

Fluorescent images were collected using a laser scanning confocal microscope (Nikon).

Immunohistochemistry

Corneal button fixed in 4% formaldehyde and embedded in paraffin. The sections were then blocked with 1% BSA at room temperature for 30 min and incubated with anti-HSV-1 VP5 (Santa Cruz Biotechnology, sc56989), anti-CD4 (Servicebio, gb13064), anti-CD8 (Servicebio, gb11068), anti-CDllb antibody (Servicebio, gb11058), or anti-F4/80 antibody (Servicebio, gb11027) at 4°C overnight. The sections were then incubated with an anti-rabbit secondary antibody (Servicebio, gb23303) or anti-mouse secondary antibody (Servicebio, gb23301) followed by incubation with freshly prepared diaminobenzidine (DAB) substrate solution to detect the antibody. Sections were counterstained with hematoxylin, blued with ammonia water, and then dehydrated and coverslipped.

CRISPR off-target analysis

The off-target analysis was designed according to the original GUIDE-seq protocol.[37] Briefly, 293T cells (5×10^5) were electric transfected with 2 μL of double-stranded oligodeoxynucleotide (100 μM), 1.5 μg of SpCas9-expressing plasmid, and 0.75 μg of UL29-UL8 gRNA-expressing plasmid or an empty plasmid. Genomic DNA was isolated 72 h after transfection to generate a DNA sequencing library. The remaining steps for sequencing were completed following the GUIDE-seq method described in the study of Montagna et al.[47] The potential off-target sites identified by GUIDE-seq were PCR amplified and pooled for double-end sequencing using an Illumina nova-seq6000 (Genefund Biotech). Raw data of deep sequencing were analyzed by Cas-analyzer.

Human corneal HSV-1 infection

Human corneas were supplied by the Eye Bank of the Eye, Ear, Nose and Throat Hospital, Fudan University, under the approval of the hospital ethics committee (EENTIRB-2017-06-07-01). Experiments were conducted according to the Declaration of Helsinki and in compliance with Chinese law. Corneas were evenly divided into 12 halves, and four halves were dosed with 1.5 μg of p24 HELP or the same volume of PBS by intrastromal injection while the other four halves were incubated with 20 μM ACV. Corneas were infected with 2×10^6 PFU of HSV-1 17syn+ at 24 h post treatment. The media were refreshed at 2 h post infection and maintained with minimum essential medium (MEM) (containing 10% FBS and 1% P/S). The culture supernatant and cornea were harvested on day 3 to perform the plaque assay, immunohistochemical analysis, and RNA/DNA isolation (TaKaRa MiniBEST viral RNA/DNA extraction kit). The UL8 and UL29 on-target sites were PCR amplified and pooled for double-end sequencing using an Illumina nova-seq6000 (Genefund Biotech). Raw data from deep sequencing were analyzed by Cas-analyzer online (version 2016/12/14).

WGS

Human corneal stromal cells (HCSCs) were used to assess the potential effect of HELP in the genome. HCSCs (Qingqi (Shanghai) Biotechnology Development, #BFN60804061) were transduced with 4.5 μg of p24 HELP (36.1 μg p24/mL, BD111VD20220601) per well 24 h after being seeded in a 12-well plate at a density of 3×10^5 cells per well. Cells were cultured in DMEM (Gibco) supplemented with 10% FBS (Gibco) and 1% penicillin- streptomycin-amphotericin B solution (BFB, BFNS001) at 37°C in a 5% CO_2 incubator. Two weeks later, a total of 1.0×10^6 HCSCs from the experimental (HELP-treated) group were collected and WGS was conducted. Untreated HCSCs were used as negative control groups (wild-type [WT] group). WGS as well as off-target and SV analysis were performed in Sequanta Technologies.

To construct a sequence library, DNA was extracted from the cells and fragmented into 350- to 450-bp fragments randomly using sonication. The library was subjected to 2×150 paired-end sequencing on an Illumina NovaSeq 6000 system. The raw data underwent quality-control analysis using FastQC (v0.11.9) software and were then aligned to the reference genome (hg19) using the maximal exact matched algorithm in BWA (v0.7.17) software. Following sequence alignment, Sentieon (202010.01) was employed to detect SNV and InDel. To predict potential off-target sites across the genome for identifying whether the detect SNV and InDel caused by CRISPR, the Cas-OFFinder software was utilized. The tool accepted NGG protospacer adjacent motif (PAM) sequence and searched sgRNA (UL8 and UL29 sgRNA) homology regions across the genome. During the homology region search, a maximum of five mismatches were allowed between the query sequence and target sequence. By calling out all SNP/InDel sites detected by Sentieon within 500 bp upstream and downstream of the sgRNA homology region predicted by Cas-OFFinder,[48] potential off-target sites were screened out. Manta software (version 1.6.0) was used to analyze the structural variations of samples. The potential off-target site and structural variations were annotated by using the software annovar (date 20180416).

BCVA

BCVA was assessed at day −1 (pre-injection), week 1, month 1 (M1), M2, M3, M6, and M12 using a standard visual acuity chart via the logMAR method. It was scored as the number of correctly read opening directions of letter E after adjusting for distance (4 or 1 m) and described as logMAR to measure the range of acuities from 20/10 to 20/800 (or from −0.30 to +1.6 logMAR). For patients unable to correctly distinguish the opening direction of letter E at 1 m, the Berkeley Rudimentary Vision Test battery was performed[49] at distances of 1 and 0.25 m to measure the range of acuities from +1.4 to +2.9 log10 MAR. Light perception was assigned +4.0 log10 MAR, and hand motion and counting fingers were assigned +3.0 logMAR and +2.0 logMAR, respectively.[50,51]

Time-domain OCT

An OCT system (Stratus OCT, Carl Zeiss Meditec, Dublin, CA) developed for ophthalmology research was used to visualize the anterior segment (cornea, anterior chamber, iris, etc.) of participants in this trial at day −1 (pre-injection), week 1, M6, and M12. In this clinical trial, time-domain OCT was mainly used for confirmation of

corneal perforation, assessment for synechia of iris, and postoperative status of the anterior segment using a 12-mm high-resolution telecentric lens designed for imaging the anterior segment of the eye.

Electroretinogram

A full-field cone and rod ERG was performed via Espion (E2, E3) systems (Diagnosys LLC, Lowell, MA) 12 months post injection. As described earlier,[52] ERG recordings were obtained in nondilated eyes using DTL electrodes secured deep in the conjunctival sac. Ground and reference electrodes were taped to the forehead and external canthi of participants, respectively. Flashes and background light were induced by a Ganzfeld color dome to achieve full-field stimulation. By convention, the amplitude and latency of both the a-wave and b-wave generate a total of four parameters to define an ERG waveform.

IVCM

Laser IVCM (Heidelberg Retina Tomograph 3 with the Rostock Cornea Module, Heidelberg Engineering, Germany) was routinely conducted on participants 12 months post injection. As described,[53] IVCM images were recorded at 30 frames/s. Adjacent images were separated by 1 μm with a lateral resolution of 1 μm/pixel. Performed eyes were topically anesthetized and administered with a layer of gel before reaching the equipment. Fifty to 100 images of the corneal subbasal layer were obtained and the most representative images were selected by the same masked observer.

Spectral-domain OCT

Spectral-domain OCT (Cirrus OCT 5000, Zeiss) was used for the cross-sectional imaging of the retina, which were aligned by straightening the major retinal pigment epithelium reflection.[54,55] Participants were measured for full retinal thickness, outer nuclear layer thickness, photoreceptor outer segment layer thickness, and presence of macular edema on the sixth month post injection. Quantitative analyses of the photoreceptor cilial anatomy was performed via longitudinal reflectivity profiles. En face imaging with near-infrared illumination was conducted with autofluorescence mode or reflectance mode via a confocal scanning laser ophthalmoscope.[54,55]

Statistics

Data were analyzed using GraphPad Prism 8 and presented as mean ± SEM in all experiments (n = 3). Unpaired two-tailed Student's t tests and one-way ANOVA with Dunnett's multiple comparisons test were performed to determine the p values (95% confidence interval).

DATA AND CODE AVAILABILITY

The authors declare that all data supporting the findings of this study are available within the paper and its extended data and supplemental information files. The deep-sequencing data for 293T and patient samples are available at NCBI BioProject. The BioProject IDs are PRJNA823566 and PRJNA823861, respectively. The GUIDE-seq preliminary data are shown on NCBI BioProject with an ID of PRJNA857843. No custom code or mathematical algorithm is used for this study.

SUPPLEMENTAL INFORMATION

Supplemental information can be found online at https://doi.org/10.1016/j.ymthe.2023.08.021.

ACKNOWLEDGMENTS

This work was supported by National Natural Science Foundation of China (81970766 and 82171102 to J.H., 31971364 to Y.C.), the Shanghai Medical Innovation Research Program (22Y21900900 to J.H.), the Shanghai Xuhui Intelligent Medicine Research Program (2022 to J.H.), key forward-looking layout fund from Shanghai Jiao Tong University (AF4150049 to Y.C.), and National Key R&D Program of China (2022YFC3400205 to Y.C.).

AUTHOR CONTRIBUTIONS

Conceptualization, Y.C. and J.H.; methodology, Y.C., J.H., X.J., and S.P.; investigation, A.W., D.Y., Z.Z., S.L., H.L., and L.T.; visualization, A.W., S.L., H.L., and L.T.; funding acquisition, Y.C. and J.H.; project administration, A.W., D.Y., and Z.Z.; supervision, Y.C. and J.H.; writing – original draft, D.Y. and Z.Z.; writing – review & editing, Y.C., J.H., A.W., D.Y., Z.Z., and S.L.

DECLARATION OF INTERESTS

Y.C. is a co-founder and advisor of BDgene Therapeutics. S.L. is currently an employee of BDgene Therapeutics.

REFERENCES

1. Liesegang, T.J. (2001). Herpes simplex virus epidemiology and ocular importance. Cornea *20*, 1–13. https://doi.org/10.1097/00003226-200101000-00001.
2. Bradley, H., Markowitz, L.E., Gibson, T., and McQuillan, G.M. (2014). Seroprevalence of herpes simplex virus types 1 and 2--United States, 1999-2010. J. Infect. Dis. *209*, 325–333. https://doi.org/10.1093/infdis/jit458.
3. Zhang, W., Gao, P., Gui, X., Zhou, L., Ge, X., Guo, X., Wills, J.W., Han, J., and Yang, H. (2020). Induction of Rod-Shaped Structures by Herpes Simplex Virus Glycoprotein I. J. Virol. *94*, e00231-20. https://doi.org/10.1128/jvi.00231-20.
4. Farooq, A.V., and Shukla, D. (2012). Herpes simplex epithelial and stromal keratitis: an epidemiologic update. Surv. Ophthalmol. *57*, 448–462. https://doi.org/10.1016/j.survophthal.2012.01.005.
5. Singh, N., and Tscharke, D.C. (2020). Herpes Simplex Virus Latency Is Noisier the Closer We Look. J. Virol. *94*, e01701-19. https://doi.org/10.1128/jvi.01701-19.
6. Xu, X., Zhang, Y., and Li, Q. (2019). Characteristics of herpes simplex virus infection and pathogenesis suggest a strategy for vaccine development. Rev. Med. Virol. *29*, e2054. https://doi.org/10.1002/rmv.2054.
7. Rousseau, A., Boutolleau, D., Titier, K., Bourcier, T., Chiquet, C., Weber, M., Colin, J., Gueudry, J., M'Garrech, M., Bodaghi, B., Burrel, S., et al. (2017). Recurrent herpetic keratitis despite antiviral prophylaxis: A virological and pharmacological study. Antivir. Res. *146*, 205–212. https://doi.org/10.1016/j.antiviral.2017.09.013.
8. Rousseau, A., Pharm, S.B., Gueudry, J., Deback, C., Haigh, O., Schweitzer, C., Boutolleau, D., and Labetoulle, M. (2022). Acyclovir-Resistant Herpes Simplex Virus 1 Keratitis: A Concerning and Emerging Clinical Challenge. Am. J. Ophthalmol. *238*, 110–119. https://doi.org/10.1016/j.ajo.2022.01.010.
9. Koganti, R., Yadavalli, T., and Shukla, D. (2019). Current and Emerging Therapies for Ocular Herpes Simplex Virus Type-1 Infections. Microorganisms *7*, 429. https://doi.org/10.3390/microorganisms7100429.
10. Kanclerz, P., and Alio, J.L. (2020). Ocular surgery after herpes simplex and herpes zoster keratitis. Int. Ophthalmol. *40*, 3599–3612. https://doi.org/10.1007/s10792-020-01539-6.
11. Ghosh, S., Jhanji, V., Lamoureux, E., Taylor, H.R., and Vajpayee, R.B. (2008). Acyclovir therapy in prevention of recurrent herpetic keratitis following penetrating

keratoplasty. Am. J. Ophthalmol. *145*, 198–202. https://doi.org/10.1016/j.ajo.2007.10.005.

12. Akova, Y.A., Onat, M., and Duman, S. (1999). Efficacy of low-dose and long-term oral acyclovir therapy after penetrating keratoplasty for herpes simplex heratitis. Ocul. Immunol. Inflamm. *7*, 51–60. https://doi.org/10.1076/ocii.7.1.51.8113.

13. Simon, A.L., and Pavan-Langston, D. (1996). Long-term oral acyclovir therapy. Effect on recurrent infectious herpes simplex keratitis in patients with and without grafts. Ophthalmology *103*, 1399–1404. https://doi.org/10.1016/s0161-6420(96)30492-2.

14. Brandariz-Nuñez, D., Correas-Sanahuja, M., Maya-Gallego, S., and Martín Herranz, I. (2021). Neurotoxicity associated with acyclovir and valacyclovir: A systematic review of cases. J. Clin. Pharm. Ther. *46*, 918–926. https://doi.org/10.1111/jcpt.13464.

15. Aubert, M., Strongin, D.E., Roychoudhury, P., Loprieno, M.A., Haick, A.K., Klouser, L.M., Stensland, L., Huang, M.L., Makhsous, N., Tait, A., et al. (2020). Gene editing and elimination of latent herpes simplex virus in vivo. Nat. Commun. *11*, 4148. https://doi.org/10.1038/s41467-020-17936-5.

16. van Diemen, F.R., Kruse, E.M., Hooykaas, M.J.G., Bruggeling, C.E., Schürch, A.C., van Ham, P.M., Imhof, S.M., Nijhuis, M., Wiertz, E.J.H.J., and Lebbink, R.J. (2016). CRISPR/Cas9-Mediated Genome Editing of Herpesviruses Limits Productive and Latent Infections. Plos Pathog. *12*, e1005701. https://doi.org/10.1371/journal.ppat.1005701.

17. Soppe, J.A., and Lebbink, R.J. (2017). Antiviral Goes Viral: Harnessing CRISPR/Cas9 to Combat Viruses in Humans. Trends Microbiol. *25*, 833–850. https://doi.org/10.1016/j.tim.2017.04.005.

18. Rossidis, A.C., Stratigis, J.D., Chadwick, A.C., Hartman, H.A., Ahn, N.J., Li, H., Singh, K., Coons, B.E., Li, L., Lv, W., et al. (2018). In utero CRISPR-mediated therapeutic editing of metabolic genes. Nat. Med. *24*, 1513–1518. https://doi.org/10.1038/s41591-018-0184-6.

19. Santiago-Fernández, O., Osorio, F.G., Quesada, V., Rodríguez, F., Basso, S., Maeso, D., Rolas, L., Barkaway, A., Nourshargh, S., Folgueras, A.R., et al. (2019). Development of a CRISPR/Cas9-based therapy for Hutchinson-Gilford progeria syndrome. Nat. Med. *25*, 423–426. https://doi.org/10.1038/s41591-018-0338-6.

20. Nelson, C.E., Wu, Y., Gemberling, M.P., Oliver, M.L., Waller, M.A., Bohning, J.D., Robinson-Hamm, J.N., Bulaklak, K., Castellanos Rivera, R.M., Collier, J.H., et al. (2019). Long-term evaluation of AAV-CRISPR genome editing for Duchenne muscular dystrophy. Nat. Med. *25*, 427–432. https://doi.org/10.1038/s41591-019-0344-3.

21. Maeder, M.L., Stefanidakis, M., Wilson, C.J., Baral, R., Barrera, L.A., Bounoutas, G.S., Bumcrot, D., Chao, H., Ciulla, D.M., DaSilva, J.A., et al. (2019). Development of a gene-editing approach to restore vision loss in Leber congenital amaurosis type 10. Nat. Med. *25*, 229–233. https://doi.org/10.1038/s41591-018-0327-9.

22. Beyret, E., Liao, H.K., Yamamoto, M., Hernandez-Benitez, R., Fu, Y., Erikson, G., Reddy, P., and Izpisua Belmonte, J.C. (2019). Single-dose CRISPR-Cas9 therapy extends lifespan of mice with Hutchinson-Gilford progeria syndrome. Nat. Med. *25*, 419–422. https://doi.org/10.1038/s41591-019-0343-4.

23. Frangoul, H., Altshuler, D., Cappellini, M.D., Chen, Y.S., Domm, J., Eustace, B.K., Foell, J., de la Fuente, J., Grupp, S., Handgretinger, R., et al. (2021). CRISPR-Cas9 Gene Editing for Sickle Cell Disease and β-Thalassemia. N. Engl. J. Med. *384*, 252–260. https://doi.org/10.1056/NEJMoa2031054.

24. Xu, L., Wang, J., Liu, Y., Xie, L., Su, B., Mou, D., Wang, L., Liu, T., Wang, X., Zhang, B., et al. (2019). CRISPR-Edited Stem Cells in a Patient with HIV and Acute Lymphocytic Leukemia. N. Engl. J. Med. *381*, 1240–1247. https://doi.org/10.1056/NEJMoa1817426.

25. Lu, Y., Xue, J., Deng, T., Zhou, X., Yu, K., Deng, L., Huang, M., Yi, X., Liang, M., Wang, Y., et al. (2020). Safety and feasibility of CRISPR-edited T cells in patients with refractory non-small-cell lung cancer. Nat. Med. *26*, 732–740. https://doi.org/10.1038/s41591-020-0840-5.

26. Stadtmauer, E.A., Fraietta, J.A., Davis, M.M., Cohen, A.D., Weber, K.L., Lancaster, E., Mangan, P.A., Kulikovskaya, I., Gupta, M., Chen, F., et al. (2020). CRISPR-engineered T cells in patients with refractory cancer. Science *367*, eaba7365. https://doi.org/10.1126/science.aba7365.

27. Narayan, V., Barber-Rotenberg, J.S., Jung, I.Y., Lacey, S.F., Rech, A.J., Davis, M.M., Hwang, W.T., Lal, P., Carpenter, E.L., Maude, S.L., Plesa, G., Vapiwala, N., Chew, A., Moniak, M., Sebro, R.A., Farwell, M.D., Marshall, A., Gilmore, J., Lledo, L., Dengel, K., Church, S.E., Hether, T.D., Xu, J., Gohil, M., Buckingham, T.H., Yee, S.S., Gonzalez, V.E., Kulikovskaya, I., Chen, F., Tian, L., Tien, K., Gladney, W., Nobles, C.L., Raymond, H.E., Prostate Cancer Cellular Therapy Program Investigators, Hexner, E.O., Siegel, D.L., Bushman, F.D., June, C.H., Fraietta, J.A., and Haas, N.B. (2022). PSMA-targeting TGFβ-insensitive armored CAR T cells in metastatic castration-resistant prostate cancer: a phase 1 trial. Nat. Med. *28*, 724–734. https://doi.org/10.1038/s41591-022-01726-1.

28. Gillmore, J.D., Gane, E., Taubel, J., Kao, J., Fontana, M., Maitland, M.L., Seitzer, J., O'Connell, D., Walsh, K.R., Wood, K., et al. (2021). CRISPR-Cas9 In Vivo Gene Editing for Transthyretin Amyloidosis. N. Engl. J. Med. *385*, 493–502. https://doi.org/10.1056/NEJMoa2107454.

29. Hamilton, J.R., Tsuchida, C.A., Nguyen, D.N., Shy, B.R., McGarrigle, E.R., Sandoval Espinoza, C.R., Carr, D., Blaeschke, F., Marson, A., and Doudna, J.A. (2021). Targeted delivery of CRISPR-Cas9 and transgenes enables complex immune cell engineering. Cell Rep. *35*, 109207. https://doi.org/10.1016/j.celrep.2021.109207.

30. Segel, M., Lash, B., Song, J., Ladha, A., Liu, C.C., Jin, X., Mekhedov, S.L., Macrae, R.K., Koonin, E.V., and Zhang, F. (2021). Mammalian retrovirus-like protein PEG10 packages its own mRNA and can be pseudotyped for mRNA delivery. Science *373*, 882–889. https://doi.org/10.1126/science.abg6155.

31. Banskota, S., Raguram, A., Suh, S., Du, S.W., Davis, J.R., Choi, E.H., Wang, X., Nielsen, S.C., Newby, G.A., Randolph, P.B., et al. (2022). Engineered virus-like particles for efficient in vivo delivery of therapeutic proteins. Cell *185*, 250–265.e16. https://doi.org/10.1016/j.cell.2021.12.021.

32. Ling, S., Yang, S., Hu, X., Yin, D., Dai, Y., Qian, X., Wang, D., Pan, X., Hong, J., Sun, X., et al. (2021). Lentiviral delivery of co-packaged Cas9 mRNA and a Vegfa-targeting guide RNA prevents wet age-related macular degeneration in mice. Nat. Biomed. Eng. *5*, 144–156. https://doi.org/10.1038/s41551-020-00656-y.

33. Yin, D., Ling, S., Wang, D., Dai, Y., Jiang, H., Zhou, X., Paludan, S.R., Hong, J., and Cai, Y. (2021). Targeting herpes simplex virus with CRISPR-Cas9 cures herpetic stromal keratitis in mice. Nat. Biotechnol. *39*, 567–577. https://doi.org/10.1038/s41587-020-00781-8.

34. Lafaille, F.G., Harschnitz, O., Lee, Y.S., Zhang, P., Hasek, M.L., Kerner, G., Itan, Y., Ewaleifoh, O., Rapaport, F., Carlile, T.M., et al. (2019). Human SNORA31 variations impair cortical neuron-intrinsic immunity to HSV-1 and underlie herpes simplex encephalitis. Nat. Med. *25*, 1873–1884. https://doi.org/10.1038/s41591-019-0672-3.

35. Ott, M., Jing, L., Lorenzo, L., Casanova, J.L., Zhang, S.Y., and Koelle, D.M. (2017). T-cell Responses to HSV-1 in Persons Who Have Survived Childhood Herpes Simplex Encephalitis. Pediatr. Infect. Dis. J. *36*, 741–744. https://doi.org/10.1097/inf.0000000000001631.

36. Wang, L., Wang, R., Xu, C., and Zhou, H. (2020). Pathogenesis of Herpes Stromal Keratitis: Immune Inflammatory Response Mediated by Inflammatory Regulators. Front. Immunol. *11*, 766. https://doi.org/10.3389/fimmu.2020.00766.

37. Tsai, S.Q., Zheng, Z., Nguyen, N.T., Liebers, M., Topkar, V.V., Thapar, V., Wyvekens, N., Khayter, C., Iafrate, A.J., Le, L.P., et al. (2015). GUIDE-seq enables genome-wide profiling of off-target cleavage by CRISPR-Cas nucleases. Nat. Biotechnol. *33*, 187–197. https://doi.org/10.1038/nbt.3117.

38. Serna-Ojeda, J.C., Loya-Garcia, D., Navas, A., Lichtinger, A., Ramirez-Miranda, A., and Graue-Hernandez, E.O. (2017). Long-term Outcomes of Pediatric Penetrating Keratoplasty for Herpes Simplex Virus Keratitis. Am. J. Ophthalmol. *173*, 139–144. https://doi.org/10.1016/j.ajo.2016.09.037.

39. Maier, A.K.B., Ozlügedik, S., Rottler, J., Heussen, F.M.A., Klamann, M.K.J., Huber, K.K., Joussen, A.M., and Winterhalter, S. (2011). Efficacy of postoperative immunosuppression after keratoplasty in herpetic keratitis. Cornea *30*, 1398–1405. https://doi.org/10.1097/ICO.0b013e31821e65b3.

40. Saad, S., Abdelmassih, Y., Saad, R., Guindolet, D., Khoury, S.E., Doan, S., Cochereau, I., and Gabison, E.E. (2020). Neurotrophic keratitis: Frequency, etiologies, clinical management and outcomes. Ocul. Surf. *18*, 231–236. https://doi.org/10.1016/j.jtos.2019.11.008.

41. Moshirfar, M., Milner, D.C., Baker, P.A., McCabe, S.E., Ronquillo, Y.C., and Hoopes, P.C. (2020). Corneal Refractive Surgery in Patients with a History of Herpes Simplex Keratitis: A Narrative Review. Clin. Ophthalmol. *14*, 3891–3901. https://doi.org/10.2147/opth.S282070.

42. Lomholt, J.A., Baggesen, K., and Ehlers, N. (1995). Recurrence and rejection rates following corneal transplantation for herpes simplex keratitis. Acta Ophthalmol. Scand. *73*, 29–32. https://doi.org/10.1111/j.1600-0420.1995.tb00008.x.

43. Moein, H.R., Kheirkhah, A., Muller, R.T., Cruzat, A.C., Pavan-Langston, D., and Hamrah, P. (2018). Corneal nerve regeneration after herpes simplex keratitis: A longitudinal in vivo confocal microscopy study. Ocul. Surf. *16*, 218–225. https://doi.org/10.1016/j.jtos.2017.12.001.

44. Charlesworth, C.T., Deshpande, P.S., Dever, D.P., Camarena, J., Lemgart, V.T., Cromer, M.K., Vakulskas, C.A., Collingwood, M.A., Zhang, L., Bode, N.M., et al. (2019). Identification of preexisting adaptive immunity to Cas9 proteins in humans. Nat. Med. *25*, 249–254. https://doi.org/10.1038/s41591-018-0326-x.

45. Wagner, D.L., Amini, L., Wendering, D.J., Burkhardt, L.M., Akyüz, L., Reinke, P., Volk, H.D., and Schmueck-Henneresse, M. (2019). High prevalence of Streptococcus pyogenes Cas9-reactive T cells within the adult human population. Nat. Med. *25*, 242–248. https://doi.org/10.1038/s41591-018-0204-6.

46. Bhatt, U.K., Abdul Karim, M.N., Prydal, J.I., Maharajan, S.V., and Fares, U. (2016). Oral antivirals for preventing recurrent herpes simplex keratitis in people with corneal grafts. Cochrane Database Syst. Rev. *11*, Cd007824. https://doi.org/10.1002/14651858.CD007824.pub2.

47. Montagna, C., Petris, G., Casini, A., Maule, G., Franceschini, G.M., Zanella, I., Conti, L., Arnoldi, F., Burrone, O.R., Zentilin, L., et al. (2018). VSV-G-Enveloped Vesicles for Traceless Delivery of CRISPR-Cas9. Mol. Ther. Nucleic Acids *12*, 453–462. https://doi.org/10.1016/j.omtn.2018.05.010.

48. Bae, S., Park, J., and Kim, J.S. (2014). Cas-OFFinder: a fast and versatile algorithm that searches for potential off-target sites of Cas9 RNA-guided endonucleases. Bioinformatics *30*, 1473–1475. https://doi.org/10.1093/bioinformatics/btu048.

49. Bailey, I.L., Jackson, A.J., Minto, H., Greer, R.B., and Chu, M.A. (2012). The Berkeley Rudimentary Vision Test. Optom. Vis. Sci. *89*, 1257–1264. https://doi.org/10.1097/OPX.0b013e318264e85a.

50. Holladay, J.T. (2004). Visual acuity measurements. J. Cataract Refract. Surg. *30*, 287–290. https://doi.org/10.1016/j.jcrs.2004.01.014.

51. Lange, C., Feltgen, N., Junker, B., Schulze-Bonsel, K., and Bach, M. (2009). Resolving the clinical acuity categories "hand motion" and "counting fingers" using the Freiburg Visual Acuity Test (FrACT). Graefes Arch. Clin. Exp. Ophthalmol. *247*, 137–142. https://doi.org/10.1007/s00417-008-0926-0.

52. Adams, S.A., and Nasrallah, H.A. (2018). Multiple retinal anomalies in schizophrenia. Schizophr. Res. *195*, 3–12. https://doi.org/10.1016/j.schres.2017.07.018.

53. Cruzat, A., Witkin, D., Baniasadi, N., Zheng, L., Ciolino, J.B., Jurkunas, U.V., Chodosh, J., Pavan-Langston, D., Dana, R., and Hamrah, P. (2011). Inflammation and the nervous system: the connection in the cornea in patients with infectious keratitis. Invest. Ophthalmol. Vis. Sci. *52*, 5136–5143. https://doi.org/10.1167/iovs.10-7048.

54. Cideciyan, A.V., Rachel, R.A., Aleman, T.S., Swider, M., Schwartz, S.B., Sumaroka, A., Roman, A.J., Stone, E.M., Jacobson, S.G., and Swaroop, A. (2011). Cone photoreceptors are the main targets for gene therapy of NPHP5 (IQCB1) or NPHP6 (CEP290) blindness: generation of an all-cone Nphp6 hypomorph mouse that mimics the human retinal ciliopathy. Hum. Mol. Genet. *20*, 1411–1423. https://doi.org/10.1093/hmg/ddr022.

55. Jacobson, S.G., Cideciyan, A.V., Sumaroka, A., Roman, A.J., Charng, J., Lu, M., Choi, W., Sheplock, R., Swider, M., Kosyk, M.S., et al. (2017). Outcome Measures for Clinical Trials of Leber Congenital Amaurosis Caused by the Intronic Mutation in the CEP290 Gene. Invest. Ophthalmol. Vis. Sci. *58*, 2609–2622. https://doi.org/10.1167/iovs.17-21560.

YMTHE, Volume *31*

Supplemental Information

In vivo CRISPR gene editing

in patients with herpetic stromal keratitis

Anji Wei, Di Yin, Zimeng Zhai, Sikai Ling, Huangying Le, Lijia Tian, Jianjiang Xu, Soren R. Paludan, Yujia Cai, and Jiaxu Hong

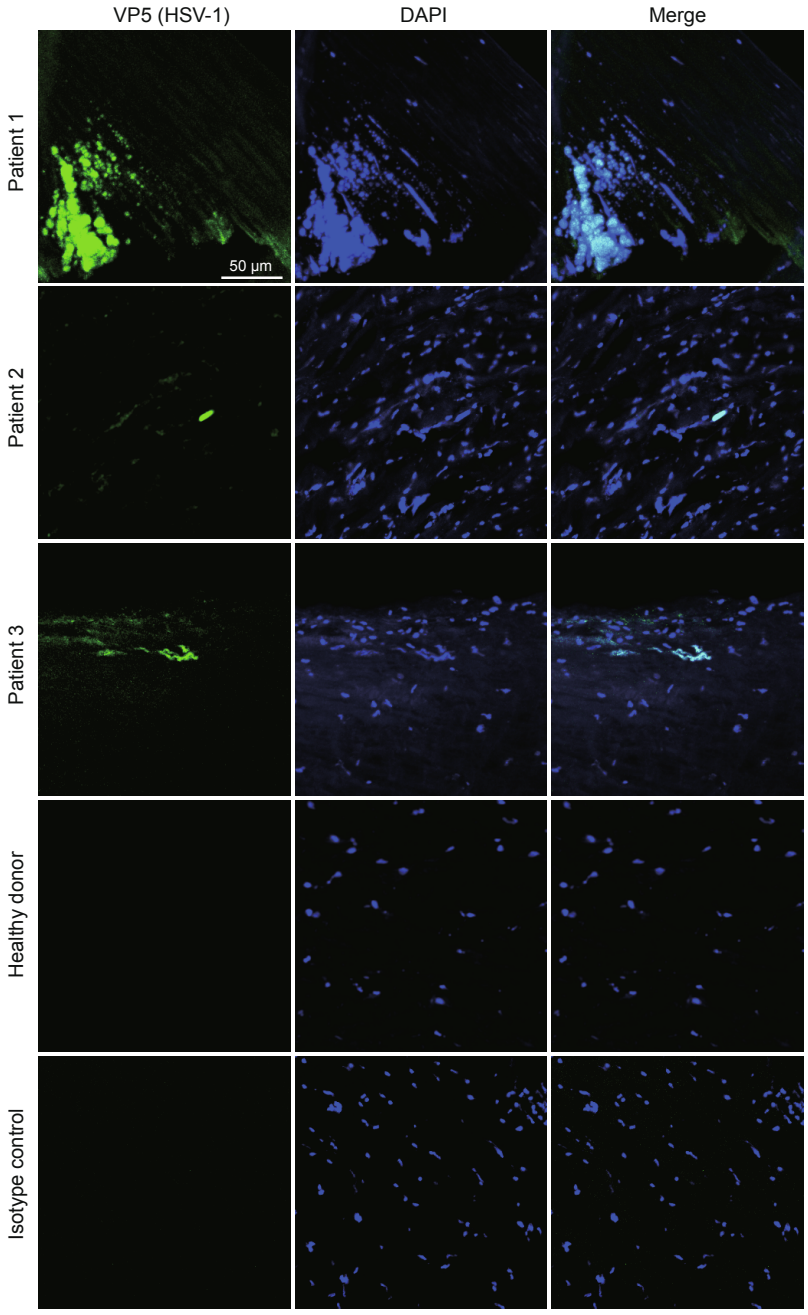

Fig. S1. Fluorescence microscopy analysis of HSV-1 in the removed corneal buttons. HSV-1 capsid protein VP5 was presented in green while DAPI was in blue. Their perfect overlap after merging suggests the presence of HSV-1 in the patient corneal tissue before CRISPR treatment.

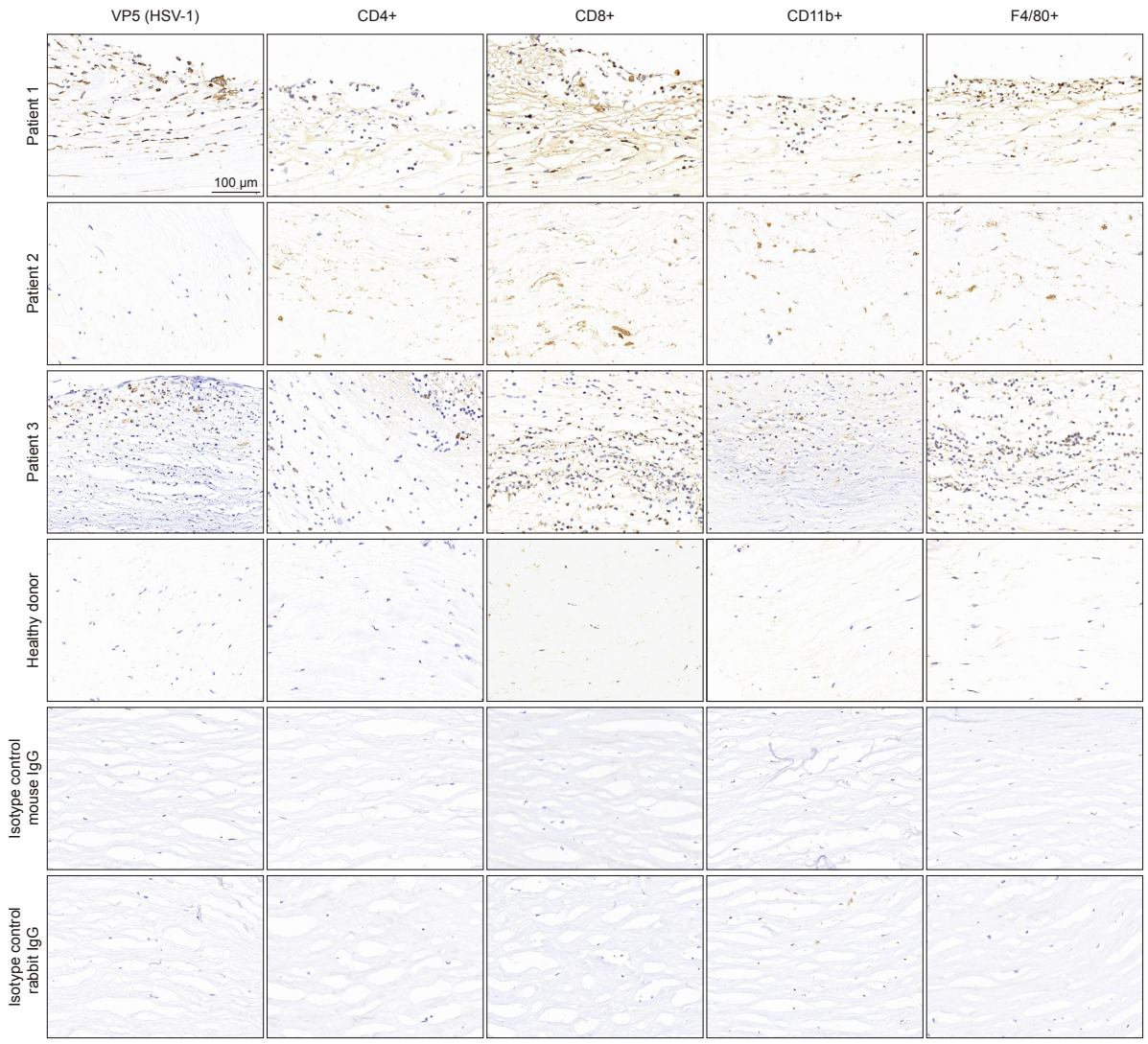

Fig. S2. Immunohistochemistry analysis of immune cells in the corneal button. The removed corneal buttons from the patients were stained for T cells (CD4+ and CD8+), myeloid-derived cells (CD11b+) and macrophages (F4/80+). Immunohistochemistry confirmed excess infiltration of inflammatory cells compared to the healthy cornea.

A

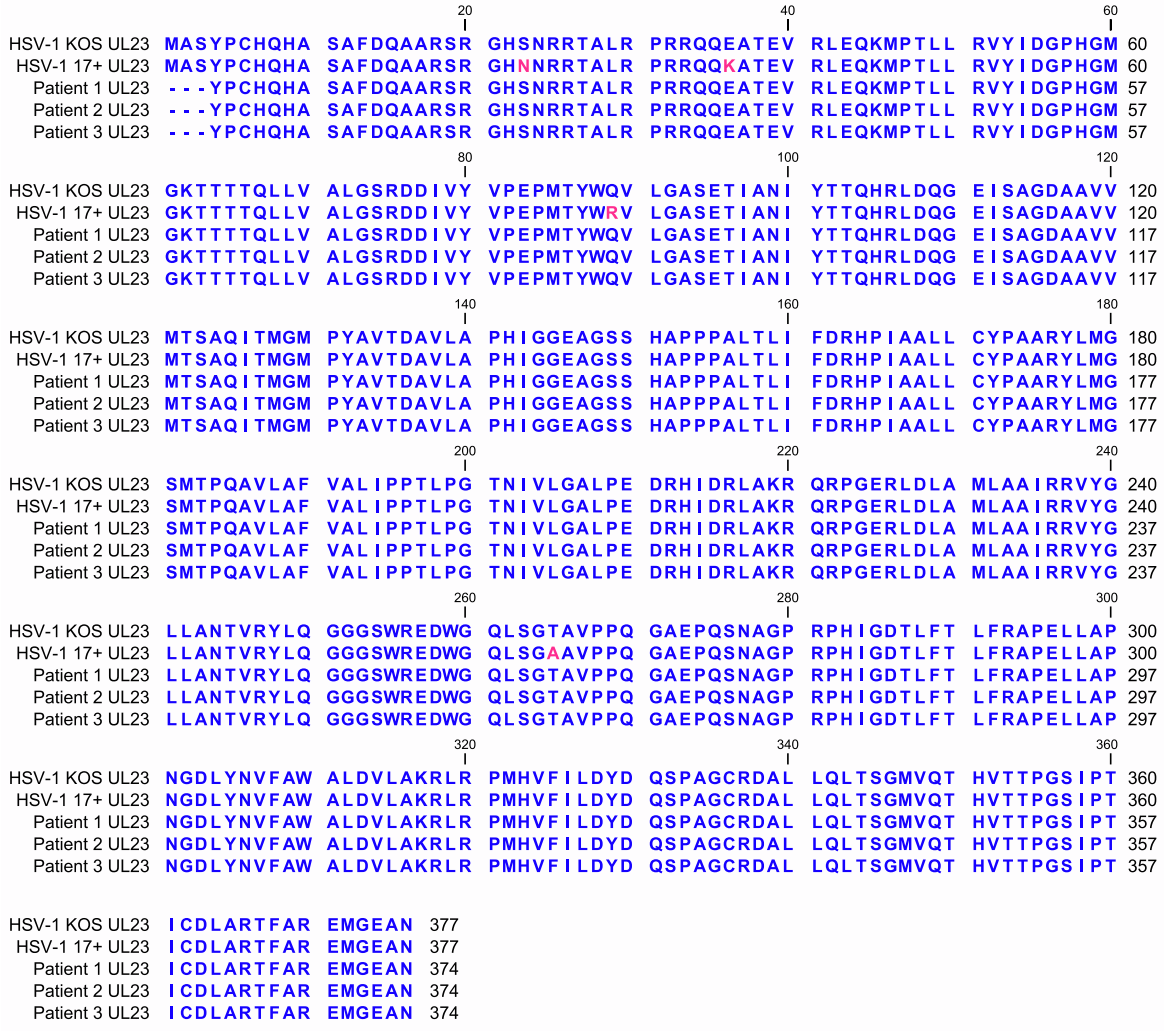
20 40 60
HSV-1 KOS UL23 MASYPCHQHA SAFDQAARSR GHSNRRTALR PRRQQEATEV RLEQKMPTLL RVYIDGPHGM 60
HSV-1 17+ UL23 MASYPCHQHA SAFDQAARSR GHNNRRTALR PRRQQKATEV RLEQKMPTLL RVYIDGPHGM 60
Patient 1 UL23 ---YPCHQHA SAFDQAARSR GHSNRRTALR PRRQQEATEV RLEQKMPTLL RVYIDGPHGM 57
Patient 2 UL23 ---YPCHQHA SAFDQAARSR GHSNRRTALR PRRQQEATEV RLEQKMPTLL RVYIDGPHGM 57
Patient 3 UL23 ---YPCHQHA SAFDQAARSR GHSNRRTALR PRRQQEATEV RLEQKMPTLL RVYIDGPHGM 57
80 100 120
HSV-1 KOS UL23 GKTTTTQLLV ALGSRDDIVY VPEPMTYWQV LGASETIANI YTTQHRLDQG EISAGDAAVV 120
HSV-1 17+ UL23 GKTTTTQLLV ALGSRDDIVY VPEPMTYWRV LGASETIANI YTTQHRLDQG EISAGDAAVV 120
Patient 1 UL23 GKTTTTQLLV ALGSRDDIVY VPEPMTYWQV LGASETIANI YTTQHRLDQG EISAGDAAVV 117
Patient 2 UL23 GKTTTTQLLV ALGSRDDIVY VPEPMTYWQV LGASETIANI YTTQHRLDQG EISAGDAAVV 117
Patient 3 UL23 GKTTTTQLLV ALGSRDDIVY VPEPMTYWQV LGASETIANI YTTQHRLDQG EISAGDAAVV 117
140 160 180
HSV-1 KOS UL23 MTSAQITMGM PYAVTDAVLA PHIGGEAGSS HAPPPALTLI FDRHPIAALL CYPAARYLMG 180
HSV-1 17+ UL23 MTSAQITMGM PYAVTDAVLA PHIGGEAGSS HAPPPALTLI FDRHPIAALL CYPAARYLMG 180
Patient 1 UL23 MTSAQITMGM PYAVTDAVLA PHIGGEAGSS HAPPPALTLI FDRHPIAALL CYPAARYLMG 177
Patient 2 UL23 MTSAQITMGM PYAVTDAVLA PHIGGEAGSS HAPPPALTLI FDRHPIAALL CYPAARYLMG 177
Patient 3 UL23 MTSAQITMGM PYAVTDAVLA PHIGGEAGSS HAPPPALTLI FDRHPIAALL CYPAARYLMG 177
200 220 240
HSV-1 KOS UL23 SMTPQAVLAF VALIPPTLPG TNIVLGALPE DRHIDRLAKR QRPGERLDLA MLAAIRRVYG 240
HSV-1 17+ UL23 SMTPQAVLAF VALIPPTLPG TNIVLGALPE DRHIDRLAKR QRPGERLDLA MLAAIRRVYG 240
Patient 1 UL23 SMTPQAVLAF VALIPPTLPG TNIVLGALPE DRHIDRLAKR QRPGERLDLA MLAAIRRVYG 237
Patient 2 UL23 SMTPQAVLAF VALIPPTLPG TNIVLGALPE DRHIDRLAKR QRPGERLDLA MLAAIRRVYG 237
Patient 3 UL23 SMTPQAVLAF VALIPPTLPG TNIVLGALPE DRHIDRLAKR QRPGERLDLA MLAAIRRVYG 237
260 280 300
HSV-1 KOS UL23 LLANTVRYLQ GGGSWREDWG QLSGTAVPPQ GAEPQSNAGP RPHIGDTLFT LFRAPELLAP 300
HSV-1 17+ UL23 LLANTVRYLQ GGGSWREDWG QLSGAAVPPQ GAEPQSNAGP RPHIGDTLFT LFRAPELLAP 300
Patient 1 UL23 LLANTVRYLQ GGGSWREDWG QLSGTAVPPQ GAEPQSNAGP RPHIGDTLFT LFRAPELLAP 297
Patient 2 UL23 LLANTVRYLQ GGGSWREDWG QLSGTAVPPQ GAEPQSNAGP RPHIGDTLFT LFRAPELLAP 297
Patient 3 UL23 LLANTVRYLQ GGGSWREDWG QLSGTAVPPQ GAEPQSNAGP RPHIGDTLFT LFRAPELLAP 297
320 340 360
HSV-1 KOS UL23 NGDLYNVFAW ALDVLAKRLR PMHVFILDYD QSPAGCRDAL LQLTSGMVQT HVTTPGSIPT 360
HSV-1 17+ UL23 NGDLYNVFAW ALDVLAKRLR PMHVFILDYD QSPAGCRDAL LQLTSGMVQT HVTTPGSIPT 360
Patient 1 UL23 NGDLYNVFAW ALDVLAKRLR PMHVFILDYD QSPAGCRDAL LQLTSGMVQT HVTTPGSIPT 357
Patient 2 UL23 NGDLYNVFAW ALDVLAKRLR PMHVFILDYD QSPAGCRDAL LQLTSGMVQT HVTTPGSIPT 357
Patient 3 UL23 NGDLYNVFAW ALDVLAKRLR PMHVFILDYD QSPAGCRDAL LQLTSGMVQT HVTTPGSIPT 357
HSV-1 KOS UL23 ICDLARTFAR EMGEAN 377
HSV-1 17+ UL23 ICDLARTFAR EMGEAN 377
Patient 1 UL23 ICDLARTFAR EMGEAN 374
Patient 2 UL23 ICDLARTFAR EMGEAN 374
Patient 3 UL23 ICDLARTFAR EMGEAN 374

B

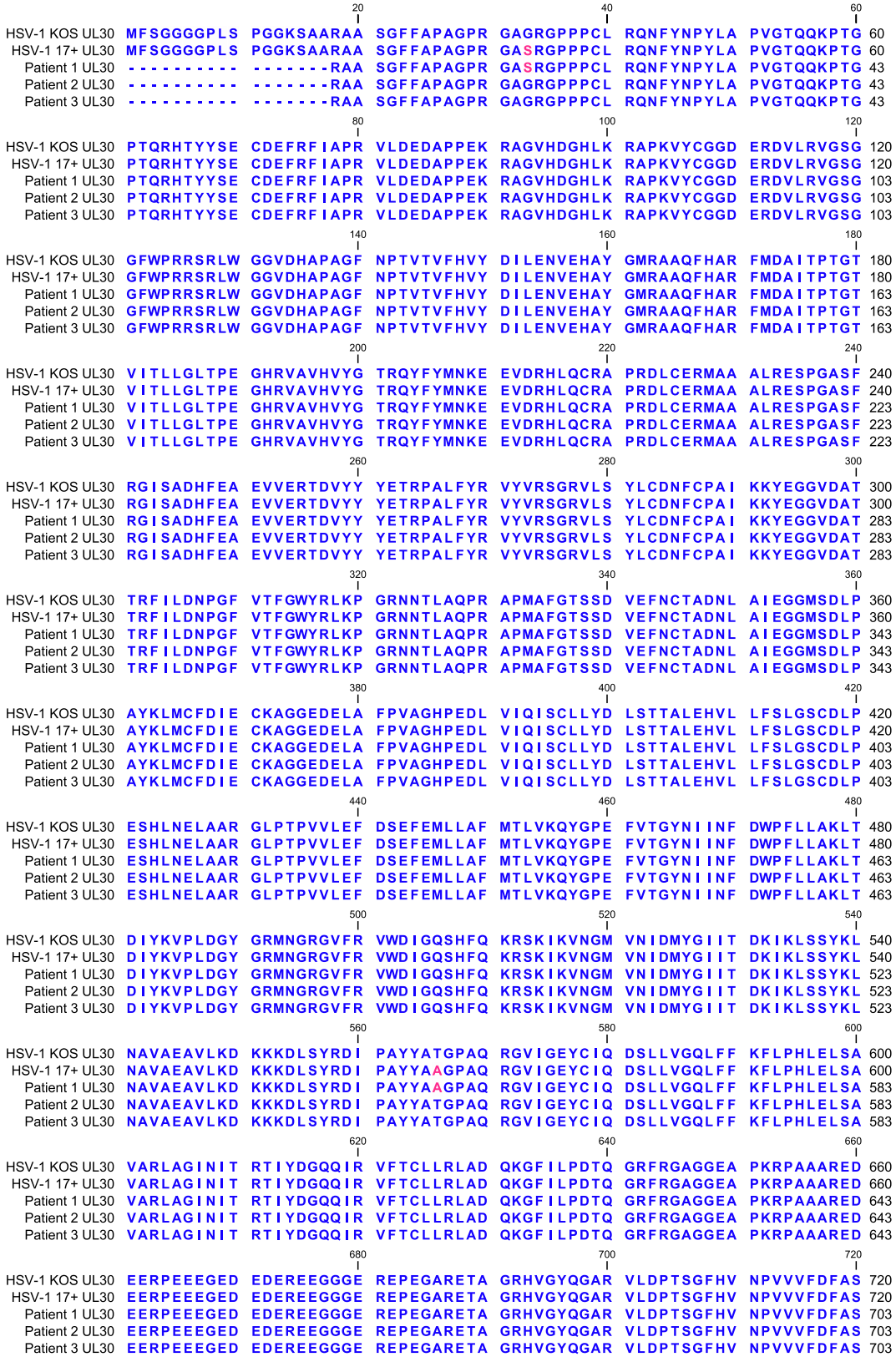
20 40 60
HSV-1 KOS UL30 MFSGGGGPLS PGGKSAARAA SGFFAPAGPR GAGRGPPPCL RQNFYNPYLA PVGTQQKPTG 60
HSV-1 17+ UL30 MFSGGGGPLS PGGKSAARAA SGFFAPAGPR GASRGPPPCL RQNFYNPYLA PVGTQQKPTG 60
Patient 1 UL30 ---------- -------RAA SGFFAPAGPR GASRGPPPCL RQNFYNPYLA PVGTQQKPTG 43
Patient 2 UL30 ---------- -------RAA SGFFAPAGPR GAGRGPPPCL RQNFYNPYLA PVGTQQKPTG 43
Patient 3 UL30 ---------- -------RAA SGFFAPAGPR GAGRGPPPCL RQNFYNPYLA PVGTQQKPTG 43
80 100 120
HSV-1 KOS UL30 PTQRHTYYSE CDEFRFIAPR VLDEDAPPEK RAGVHDGHLK RAPKVYCGGD ERDVLRVGSG 120
HSV-1 17+ UL30 PTQRHTYYSE CDEFRFIAPR VLDEDAPPEK RAGVHDGHLK RAPKVYCGGD ERDVLRVGSG 120
Patient 1 UL30 PTQRHTYYSE CDEFRFIAPR VLDEDAPPEK RAGVHDGHLK RAPKVYCGGD ERDVLRVGSG 103
Patient 2 UL30 PTQRHTYYSE CDEFRFIAPR VLDEDAPPEK RAGVHDGHLK RAPKVYCGGD ERDVLRVGSG 103
Patient 3 UL30 PTQRHTYYSE CDEFRFIAPR VLDEDAPPEK RAGVHDGHLK RAPKVYCGGD ERDVLRVGSG 103
140 160 180
HSV-1 KOS UL30 GFWPRRSRLW GGVDHAPAGF NPTVTVFHVY DILENVEHAY GMRAAQFHAR FMDAITPTGT 180
HSV-1 17+ UL30 GFWPRRSRLW GGVDHAPAGF NPTVTVFHVY DILENVEHAY GMRAAQFHAR FMDAITPTGT 180
Patient 1 UL30 GFWPRRSRLW GGVDHAPAGF NPTVTVFHVY DILENVEHAY GMRAAQFHAR FMDAITPTGT 163
Patient 2 UL30 GFWPRRSRLW GGVDHAPAGF NPTVTVFHVY DILENVEHAY GMRAAQFHAR FMDAITPTGT 163
Patient 3 UL30 GFWPRRSRLW GGVDHAPAGF NPTVTVFHVY DILENVEHAY GMRAAQFHAR FMDAITPTGT 163
200 220 240
HSV-1 KOS UL30 VITLLGLTPE GHRVAVHVYG TRQYFYMNKE EVDRHLQCRA PRDLCERMAA ALRESPGASF 240
HSV-1 17+ UL30 VITLLGLTPE GHRVAVHVYG TRQYFYMNKE EVDRHLQCRA PRDLCERMAA ALRESPGASF 240
Patient 1 UL30 VITLLGLTPE GHRVAVHVYG TRQYFYMNKE EVDRHLQCRA PRDLCERMAA ALRESPGASF 223
Patient 2 UL30 VITLLGLTPE GHRVAVHVYG TRQYFYMNKE EVDRHLQCRA PRDLCERMAA ALRESPGASF 223
Patient 3 UL30 VITLLGLTPE GHRVAVHVYG TRQYFYMNKE EVDRHLQCRA PRDLCERMAA ALRESPGASF 223
260 280 300
HSV-1 KOS UL30 RGISADHFEA EVVERTDVYY YETRPALFYR VYVRSGRVLS YLCDNFCPAI KKYEGGVDAT 300
HSV-1 17+ UL30 RGISADHFEA EVVERTDVYY YETRPALFYR VYVRSGRVLS YLCDNFCPAI KKYEGGVDAT 300
Patient 1 UL30 RGISADHFEA EVVERTDVYY YETRPALFYR VYVRSGRVLS YLCDNFCPAI KKYEGGVDAT 283
Patient 2 UL30 RGISADHFEA EVVERTDVYY YETRPALFYR VYVRSGRVLS YLCDNFCPAI KKYEGGVDAT 283
Patient 3 UL30 RGISADHFEA EVVERTDVYY YETRPALFYR VYVRSGRVLS YLCDNFCPAI KKYEGGVDAT 283
320 340 360
HSV-1 KOS UL30 TRFILDNPGF VTFGWYRLKP GRNNTLAQPR APMAFGTSSD VEFNCTADNL AIEGGMSDLP 360
HSV-1 17+ UL30 TRFILDNPGF VTFGWYRLKP GRNNTLAQPR APMAFGTSSD VEFNCTADNL AIEGGMSDLP 360
Patient 1 UL30 TRFILDNPGF VTFGWYRLKP GRNNTLAQPR APMAFGTSSD VEFNCTADNL AIEGGMSDLP 343
Patient 2 UL30 TRFILDNPGF VTFGWYRLKP GRNNTLAQPR APMAFGTSSD VEFNCTADNL AIEGGMSDLP 343
Patient 3 UL30 TRFILDNPGF VTFGWYRLKP GRNNTLAQPR APMAFGTSSD VEFNCTADNL AIEGGMSDLP 343
380 400 420
HSV-1 KOS UL30 AYKLMCFDIE CKAGGEDELA FPVAGHPEDL VIQISCLLYD LSTTALEHVL LFSLGSCDLP 420
HSV-1 17+ UL30 AYKLMCFDIE CKAGGEDELA FPVAGHPEDL VIQISCLLYD LSTTALEHVL LFSLGSCDLP 420
Patient 1 UL30 AYKLMCFDIE CKAGGEDELA FPVAGHPEDL VIQISCLLYD LSTTALEHVL LFSLGSCDLP 403
Patient 2 UL30 AYKLMCFDIE CKAGGEDELA FPVAGHPEDL VIQISCLLYD LSTTALEHVL LFSLGSCDLP 403
Patient 3 UL30 AYKLMCFDIE CKAGGEDELA FPVAGHPEDL VIQISCLLYD LSTTALEHVL LFSLGSCDLP 403
440 460 480
HSV-1 KOS UL30 ESHLNELAAR GLPTPVVLEF DSEFEMLLAF MTLVKQYGPE FVTGYNIINF DWPFLLAKLT 480
HSV-1 17+ UL30 ESHLNELAAR GLPTPVVLEF DSEFEMLLAF MTLVKQYGPE FVTGYNIINF DWPFLLAKLT 480
Patient 1 UL30 ESHLNELAAR GLPTPVVLEF DSEFEMLLAF MTLVKQYGPE FVTGYNIINF DWPFLLAKLT 463
Patient 2 UL30 ESHLNELAAR GLPTPVVLEF DSEFEMLLAF MTLVKQYGPE FVTGYNIINF DWPFLLAKLT 463
Patient 3 UL30 ESHLNELAAR GLPTPVVLEF DSEFEMLLAF MTLVKQYGPE FVTGYNIINF DWPFLLAKLT 463
500 520 540
HSV-1 KOS UL30 DIYKVPLDGY GRMNGRGVFR VWDIGQSHFQ KRSKIKVNGM VNIDMYGIIT DKIKLSSYKL 540
HSV-1 17+ UL30 DIYKVPLDGY GRMNGRGVFR VWDIGQSHFQ KRSKIKVNGM VNIDMYGIIT DKIKLSSYKL 540
Patient 1 UL30 DIYKVPLDGY GRMNGRGVFR VWDIGQSHFQ KRSKIKVNGM VNIDMYGIIT DKIKLSSYKL 523
Patient 2 UL30 DIYKVPLDGY GRMNGRGVFR VWDIGQSHFQ KRSKIKVNGM VNIDMYGIIT DKIKLSSYKL 523
Patient 3 UL30 DIYKVPLDGY GRMNGRGVFR VWDIGQSHFQ KRSKIKVNGM VNIDMYGIIT DKIKLSSYKL 523
560 580 600
HSV-1 KOS UL30 NAVAEAVLKD KKKDLSYRDI PAYYATGPAQ RGVIGEYCIQ DSLLVGQLFF KFLPHLELSA 600
HSV-1 17+ UL30 NAVAEAVLKD KKKDLSYRDI PAYYAAGPAQ RGVIGEYCIQ DSLLVGQLFF KFLPHLELSA 600
Patient 1 UL30 NAVAEAVLKD KKKDLSYRDI PAYYAAGPAQ RGVIGEYCIQ DSLLVGQLFF KFLPHLELSA 583
Patient 2 UL30 NAVAEAVLKD KKKDLSYRDI PAYYATGPAQ RGVIGEYCIQ DSLLVGQLFF KFLPHLELSA 583
Patient 3 UL30 NAVAEAVLKD KKKDLSYRDI PAYYATGPAQ RGVIGEYCIQ DSLLVGQLFF KFLPHLELSA 583
620 640 660
HSV-1 KOS UL30 VARLAGINIT RTIYDGQQIR VFTCLLRLAD QKGFILPDTQ GRFRGAGGEA PKRPAAARED 660
HSV-1 17+ UL30 VARLAGINIT RTIYDGQQIR VFTCLLRLAD QKGFILPDTQ GRFRGAGGEA PKRPAAARED 660
Patient 1 UL30 VARLAGINIT RTIYDGQQIR VFTCLLRLAD QKGFILPDTQ GRFRGAGGEA PKRPAAARED 643
Patient 2 UL30 VARLAGINIT RTIYDGQQIR VFTCLLRLAD QKGFILPDTQ GRFRGAGGEA PKRPAAARED 643
Patient 3 UL30 VARLAGINIT RTIYDGQQIR VFTCLLRLAD QKGFILPDTQ GRFRGAGGEA PKRPAAARED 643
680 700 720
HSV-1 KOS UL30 EERPEEEGED EDEREEGGGE REPEGARETA GRHVGYQGAR VLDPTSGFHV NPVVVFDFAS 720
HSV-1 17+ UL30 EERPEEEGED EDEREEGGGE REPEGARETA GRHVGYQGAR VLDPTSGFHV NPVVVFDFAS 720
Patient 1 UL30 EERPEEEGED EDEREEGGGE REPEGARETA GRHVGYQGAR VLDPTSGFHV NPVVVFDFAS 703
Patient 2 UL30 EERPEEEGED EDEREEGGGE REPEGARETA GRHVGYQGAR VLDPTSGFHV NPVVVFDFAS 703
Patient 3 UL30 EERPEEEGED EDEREEGGGE REPEGARETA GRHVGYQGAR VLDPTSGFHV NPVVVFDFAS 703

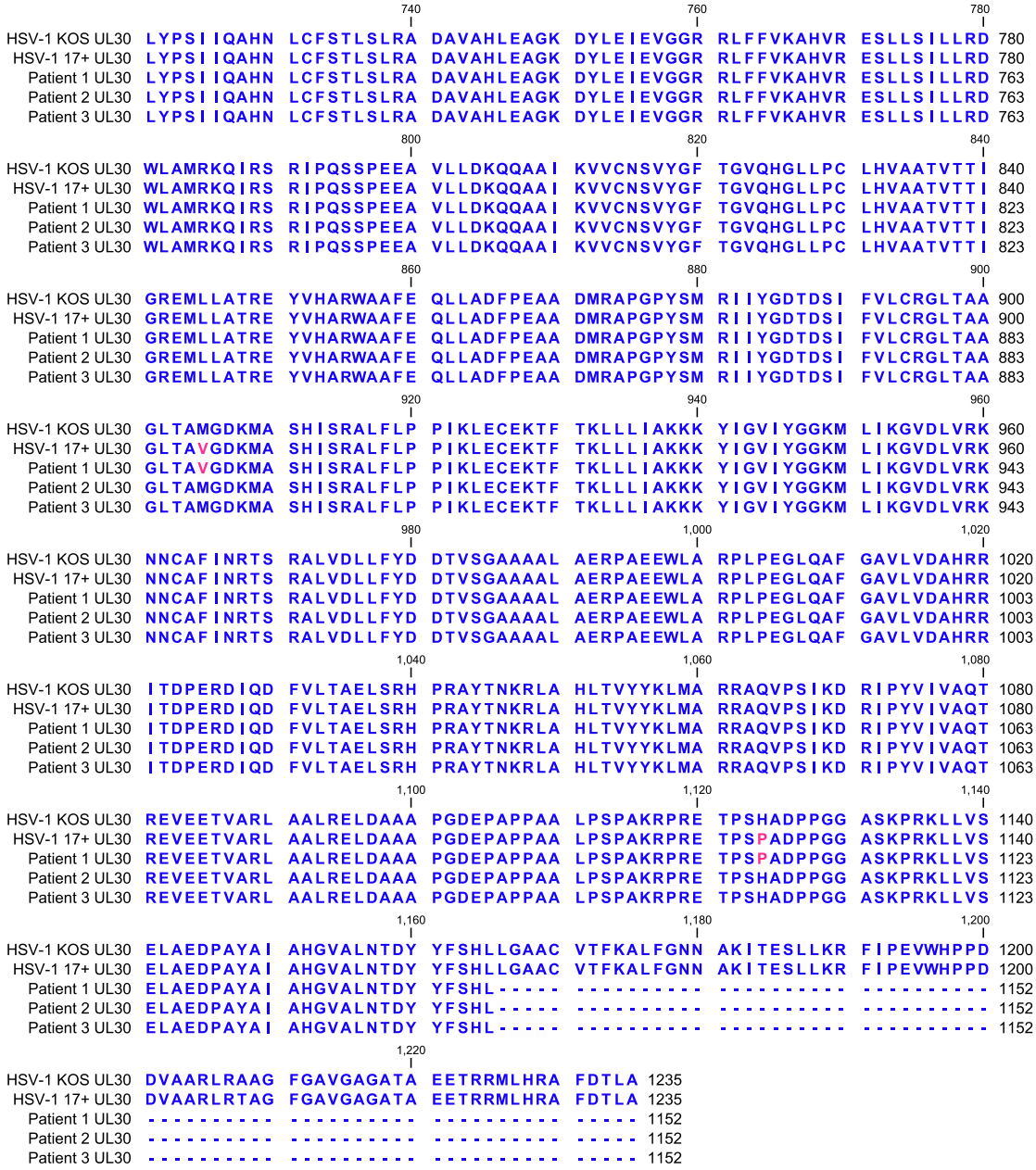

Fig. S3. Amino acids alignment for TK and DNA pol. HSV-1 strains were isolated from the three participants and sequenced for genes encoding thymidine kinase (TK, UL23) and DNA polymerase (DNA pol, UL30). Letter in red color indicated changed amino acids in TK (**A**) and DNA pol (**B**). HSV-1 KOS and 17syn+ strains were used as references. Only amino-acid changes different from both KOS and 17syn+ simultaneously are considered as ACV resistant mutations.

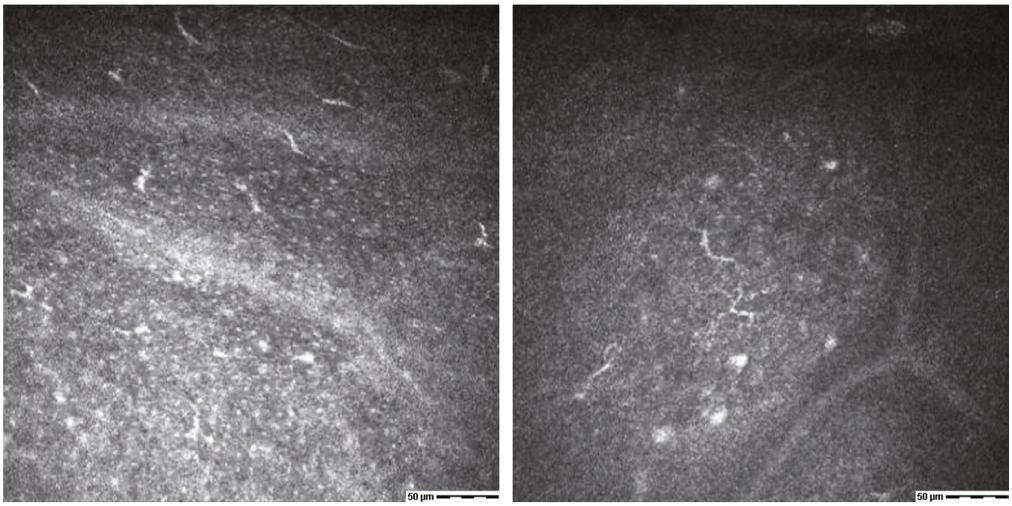

Fig. S4. Postoperative IVCM examination of patient 1. IVCM at 12-month post-injection showed very few corneal subbasal nerves in the transplanted corneal graft of patient 1.

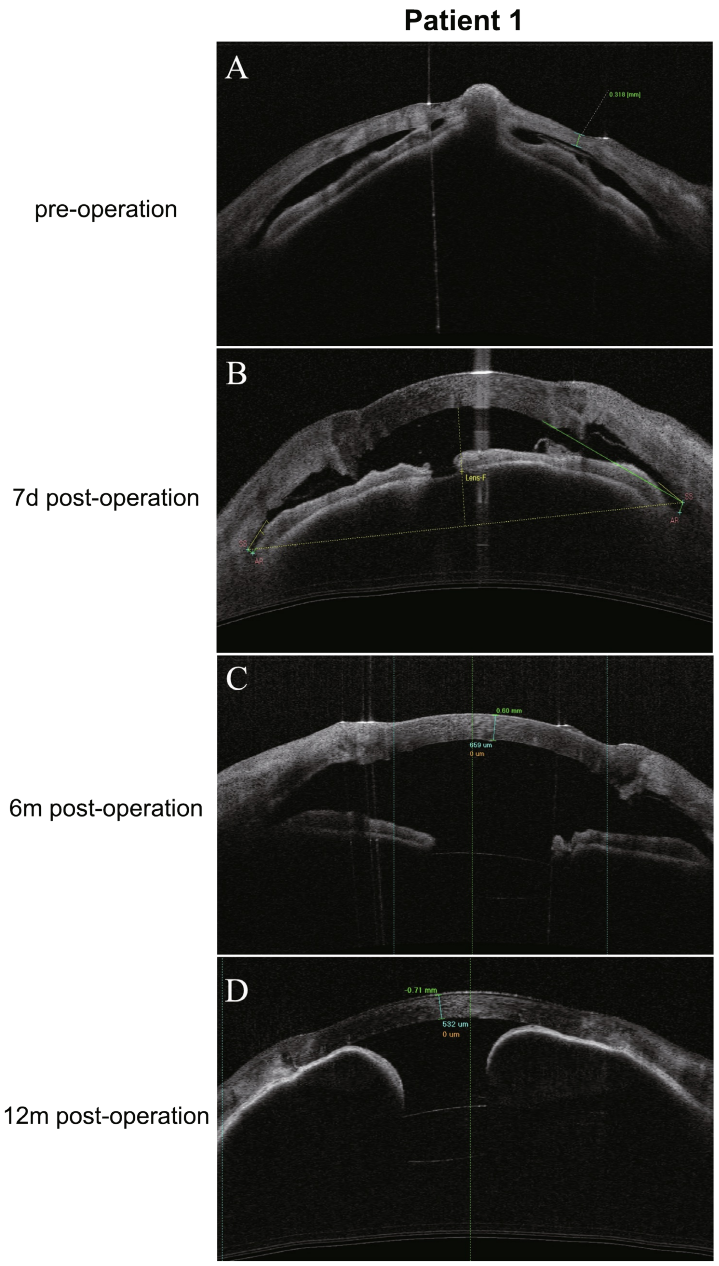

Fig. S5. Time-domain OCT of the anterior segment of patient 1. This image shows the time-domain OCT of the anterior segment of patient 1 at different time points (**A-D**). Before the injection, there was iris incarceration in the thinning area of the cornea. OCT showed a slightly shallow anterior chamber after 7 days post-injection and an iris adhesion at the 12-month visit, yet the intraocular pressure of patient 1 was within the normal range. Prophylactic laser therapy was conducted to prevent glaucoma.

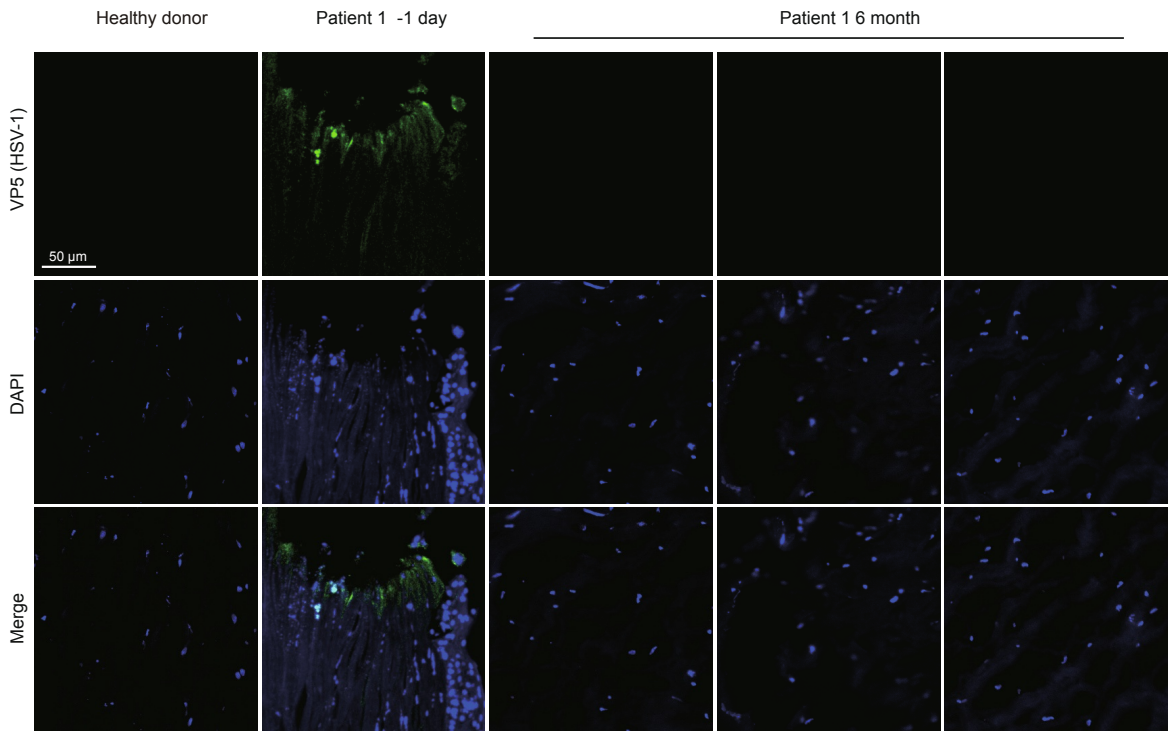

Fig. S6. Fluorescence microscopy analysis of HSV-1 in the removed corneal button. After the second corneal transplantation on the right eye of patent 1 at 6 months after PK, the removed corneal button showed no signs of HSV-1 capsid protein VP5 (green) by the fluorescence microscopy. Scale bars, 50 μm.

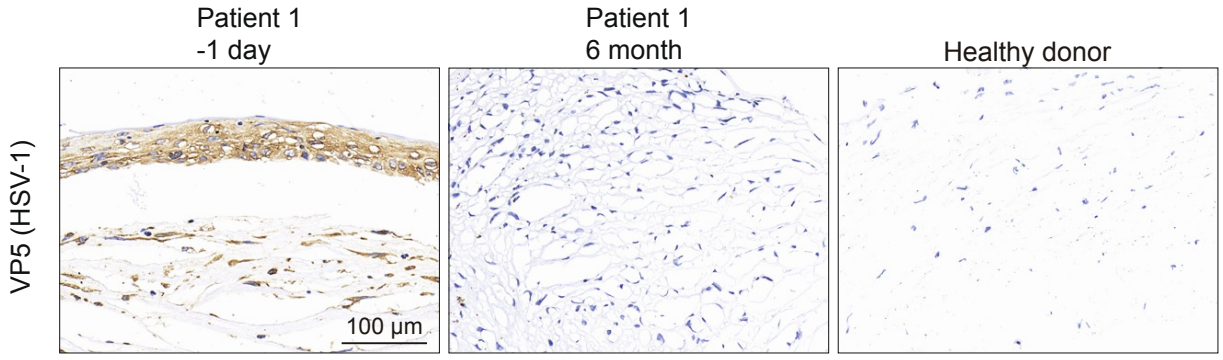

Fig. S7. Immunohistochemistry analysis of HSV-1 in the removed corneal button from patient 1. After the second corneal transplantation on his right eye 6 months after PK, the removed corneal button showed no signs of HSV-1 capsid protein VP5 (brown) by immunohistochemistry analysis.

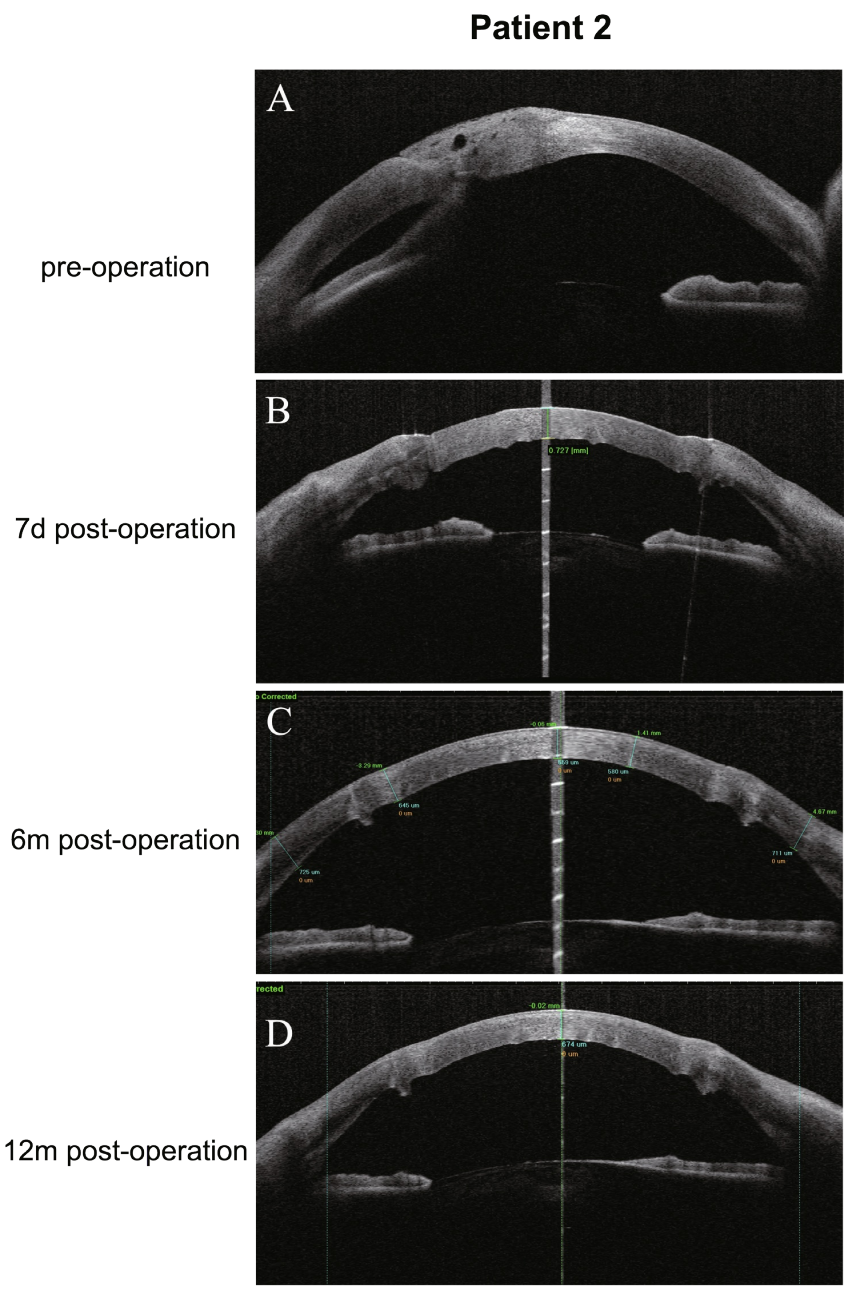

Fig. S8. Time-domain OCT of the anterior segment of patient 2. The pre-injection OCT of the anterior segment showed a possible corneal perforation site in patient 2 (**A**). Post-injection OCT images (**B-D**) indicate a deepened anterior chamber, which was maintained for over 12 months after the corneal transplantation.

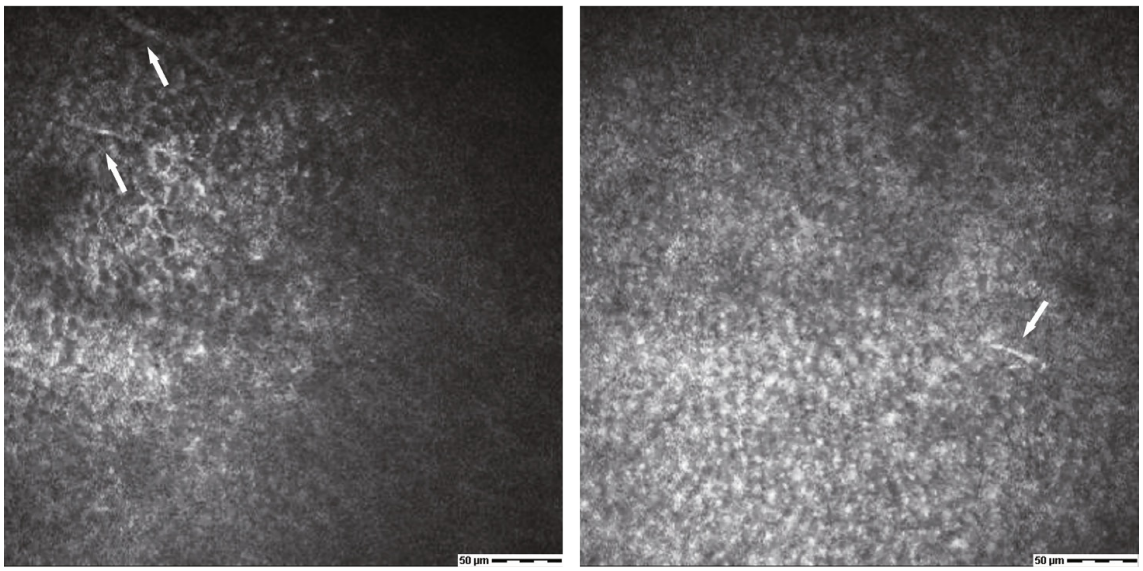

Fig. S9. Postoperative IVCM examination of patient 2. IVCM showed slight corneal nerve regeneration (white arrow) in the transplanted corneal graft at the 12 month-follow-up of patient 2.

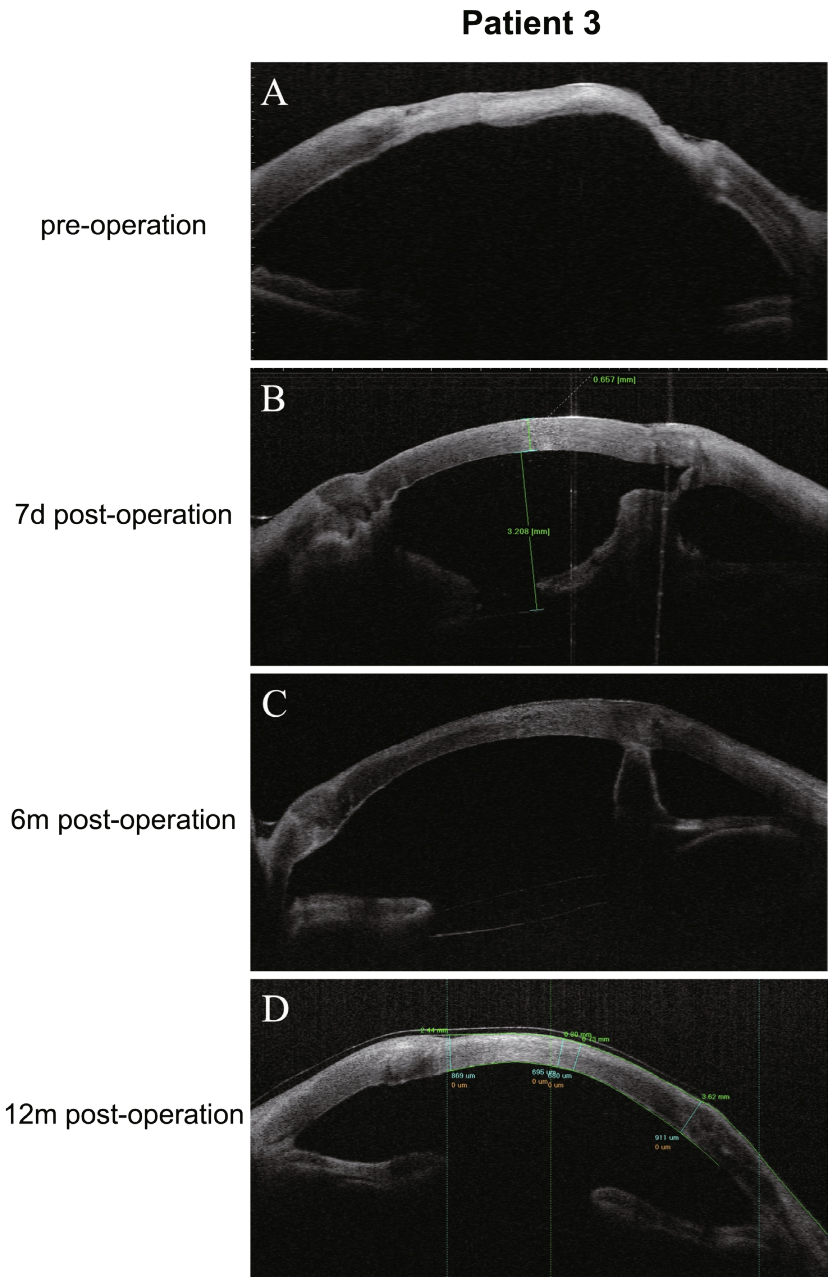

Fig. S10. Time-domain OCT of the anterior segment of patient 3. The pre-injection OCT of the anterior segment showed a corneal perforation channel in patient 3 (**A**). Post-injection OCT images (**B-D**) indicate an in-position intraocular lens and a slightly adhered iris to the posterior cornea after PK.

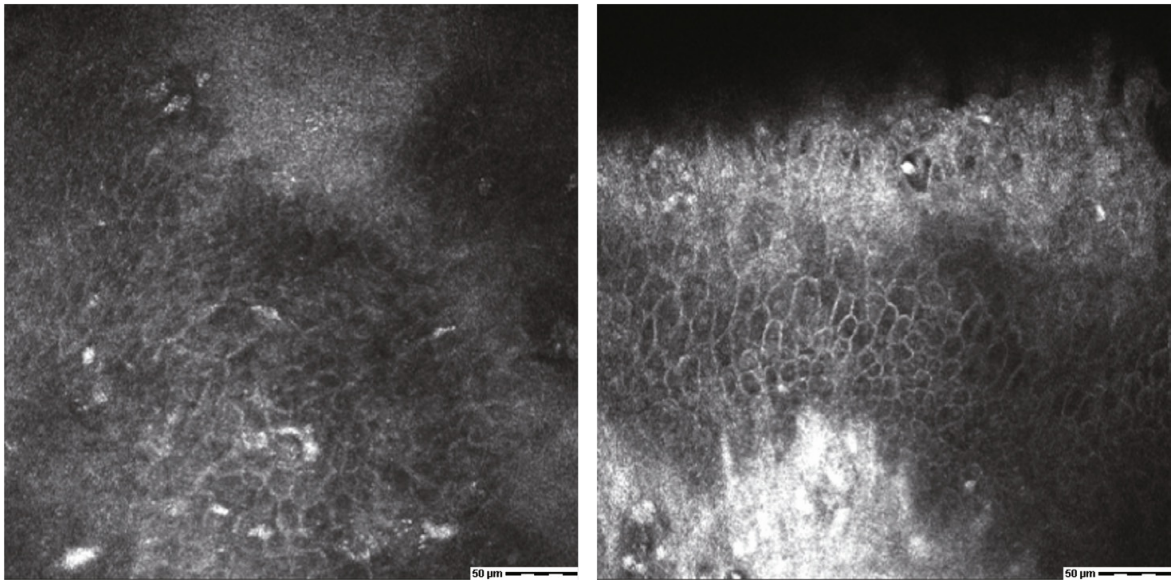

Fig.S11. Postoperative IVCM examination of patient 3. IVCM showed no signs of corneal nerve regeneration at the 12-month follow-up of patient 3. His corneal epithelium density decreased and showed irregular morphologic changes, which indicated the possibility of corneal neurological dystrophy related to HSK.

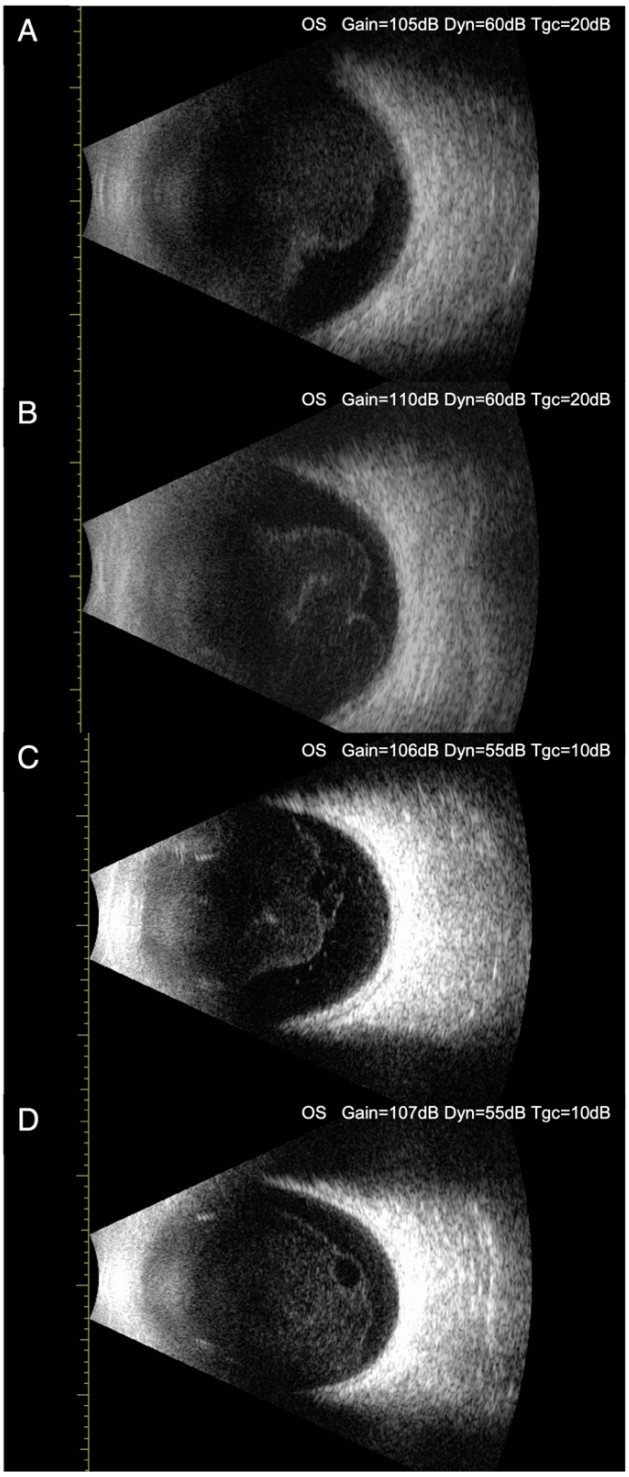

Fig. S12. Postoperative B-scan ultrasonography of patient 3. B-scan ultrasonography of the patient 3 on 7 days (**A**), 1 month (**B**), 3 months (**C**) and 6 months (**D**) post-injection. Continuous ribbon-like echo was found in the posterior vitreous body, indicating vitreous opacity with posterior detachment.

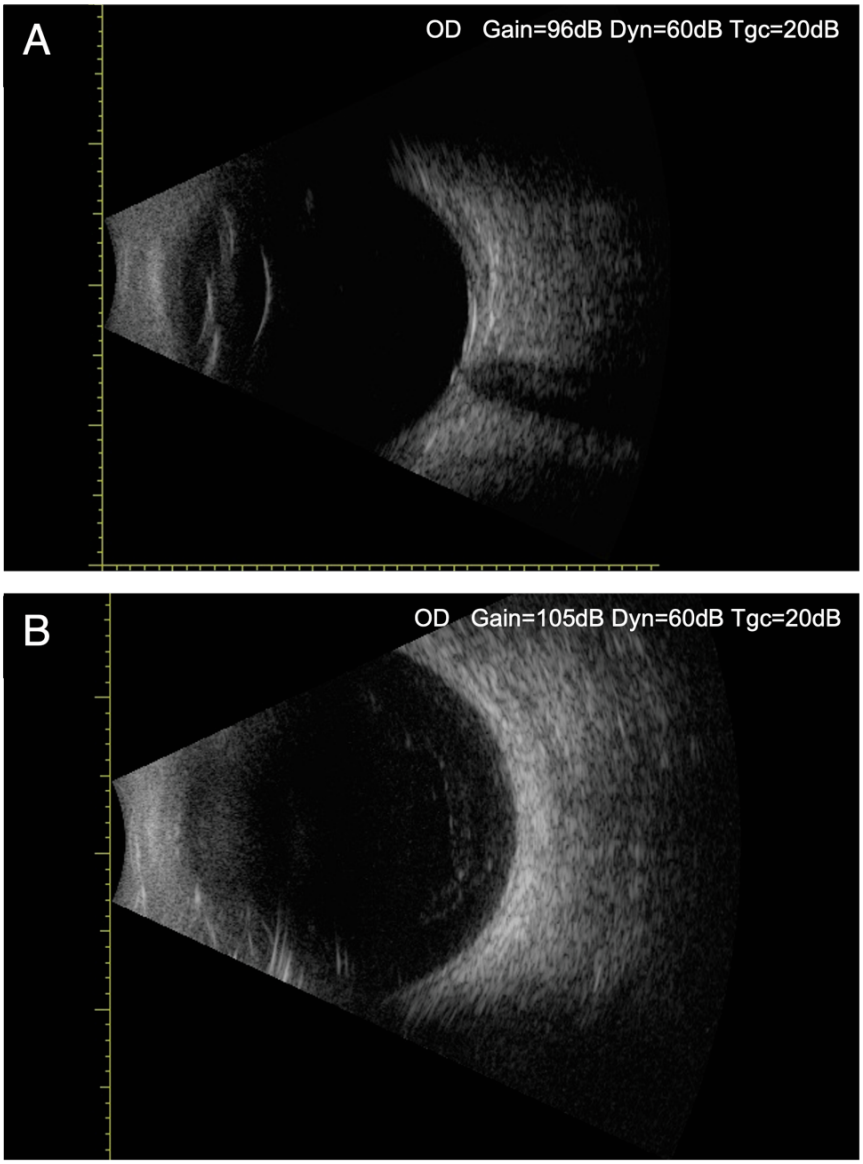

Fig. S13. Postoperative B-scan ultrasonography of patient 2. B-scan ultrasonography results of patient 2 on 6 months (**A**) and 9 months (**B**) post-injection showed no remarkable changes in the vitreous body.

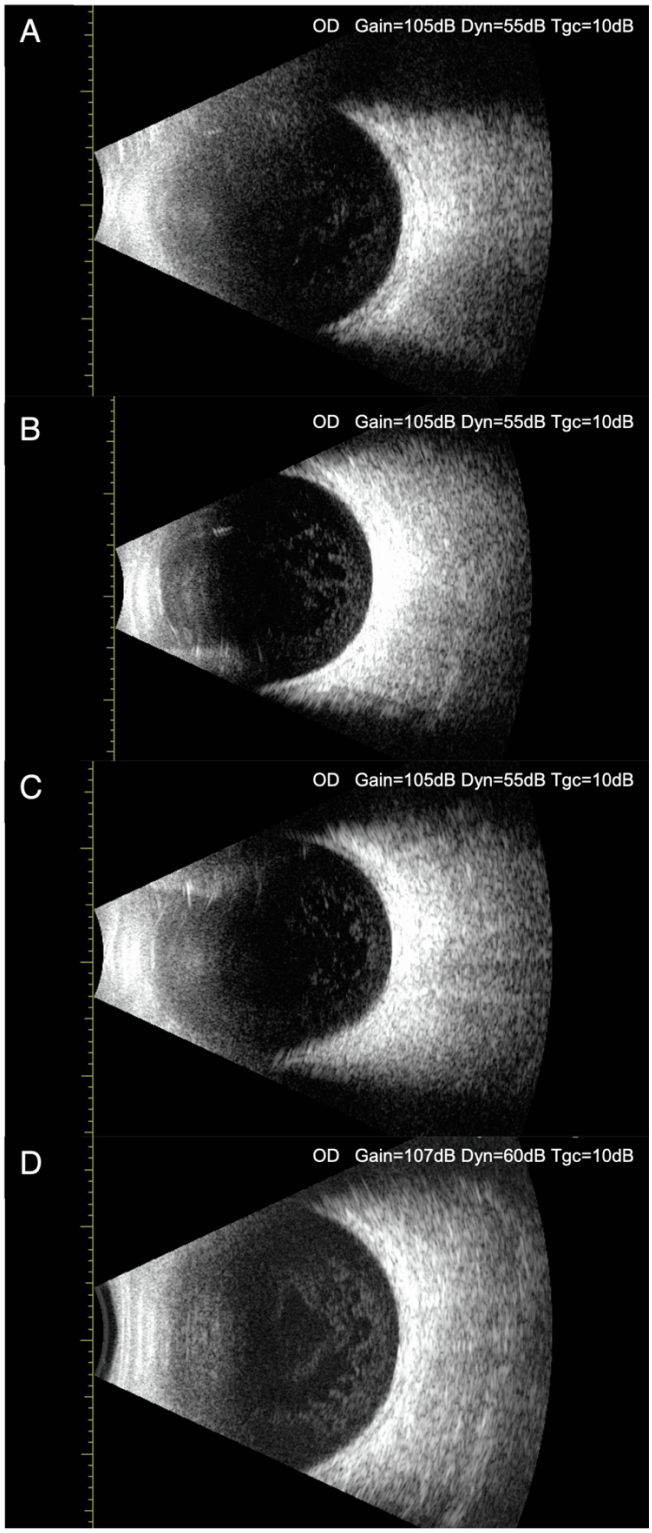

Fig. S14. Postoperative B-scan ultrasonography of patient 1. B-scan ultrasonography of patient 1 on 7 days (**A**), 1 month (**B**), 6 months (**C**) and 12 months (**D**) post-injection revealed no remarkable changes in the vitreous body.

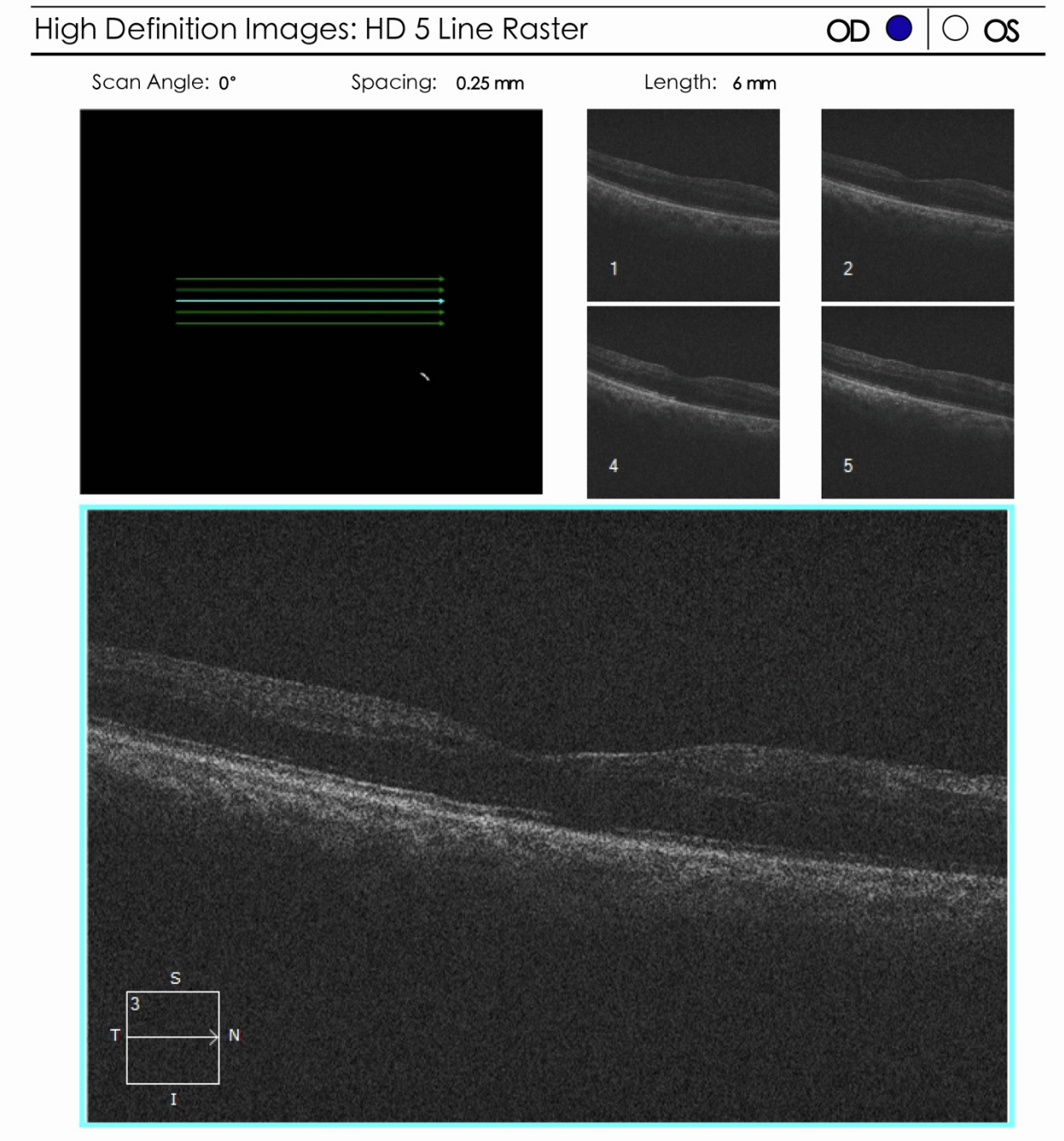

Fig. S15. Spectral-domain OCT of the retina of patient 2. The spectral-domain OCT of patient 2's retina was performed at 6 months post-injection using Cirrus OCT 5000 (Zeiss). The structure of his fundus showed no obvious exception after the administration of HELP.

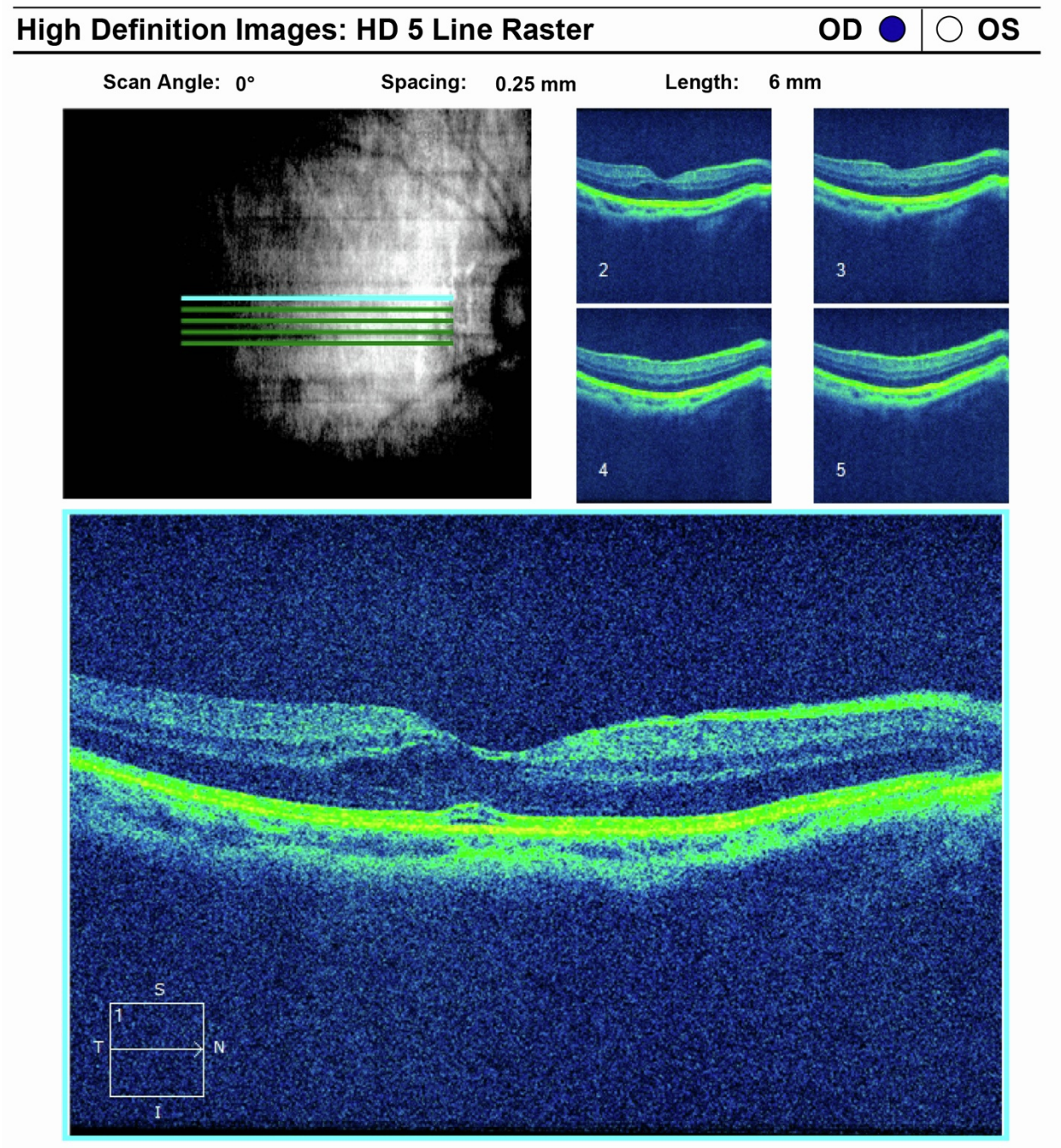

Fig. S16. Spectral-domain OCT of the retina of patient 1. The optical coherence tomography revealed mild center-involved intraretinal fluid and subfoveal fluid in the right eye of patient 1 at six months after the treatment. The ellipsoid zone was intact. We continue to follow up on this situation without any intervention.

A

Diagnosis:

1_Pattern-VEP 2.0&1.0 deg (Monitor)

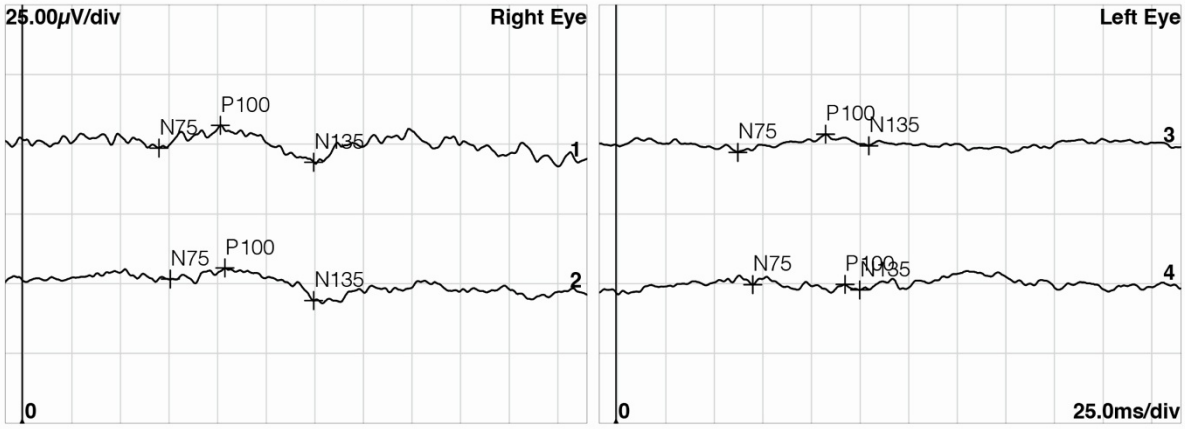

Normals	-	96-109	-	7.08µV-17.7µV	
Channel	**N75 [ms]**	**P100 [ms]**	**N135 [ms]**	**N75-P100**	**P100-N135**
1 R1 2,0 deg	70.5	102.2	150.3	8.13µV	13.3µV
2 R1 1,0 deg	76.3	104.5	150.3	3.94µV (!)	11.7µV
3 L1 2,0 deg	62.8	108.0	130.3	6.51µV (!)	4.14µV
4 L1 1,0 deg	70.5	118.0 (!)	125.6	83.5nV (!)	2.01µV

2_Pattern-VEP 30 min&15 min (Monitor)

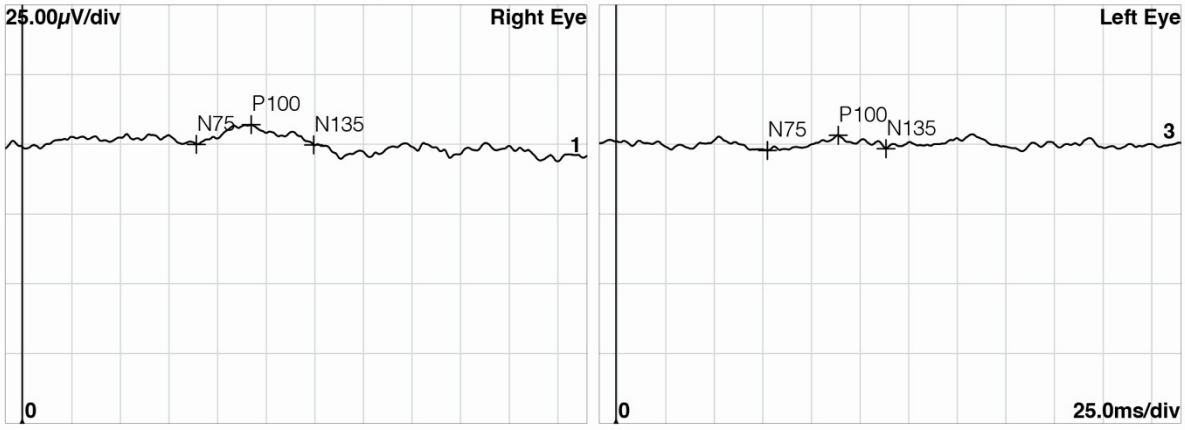

Normals	-	105-126	-	7.00µV-42.5µV	
Channel	**N75 [ms]**	**P100 [ms]**	**N135 [ms]**	**N75-P100**	**P100-N135**
1 R1 30 min	89.8	118.0	150.3	7.13µV	7.29µV
2 R1 15 min					
3 L1 30 min	78.1	114.5	139.1	5.40µV (!)	4.80µV
4 L1 15 min					

B

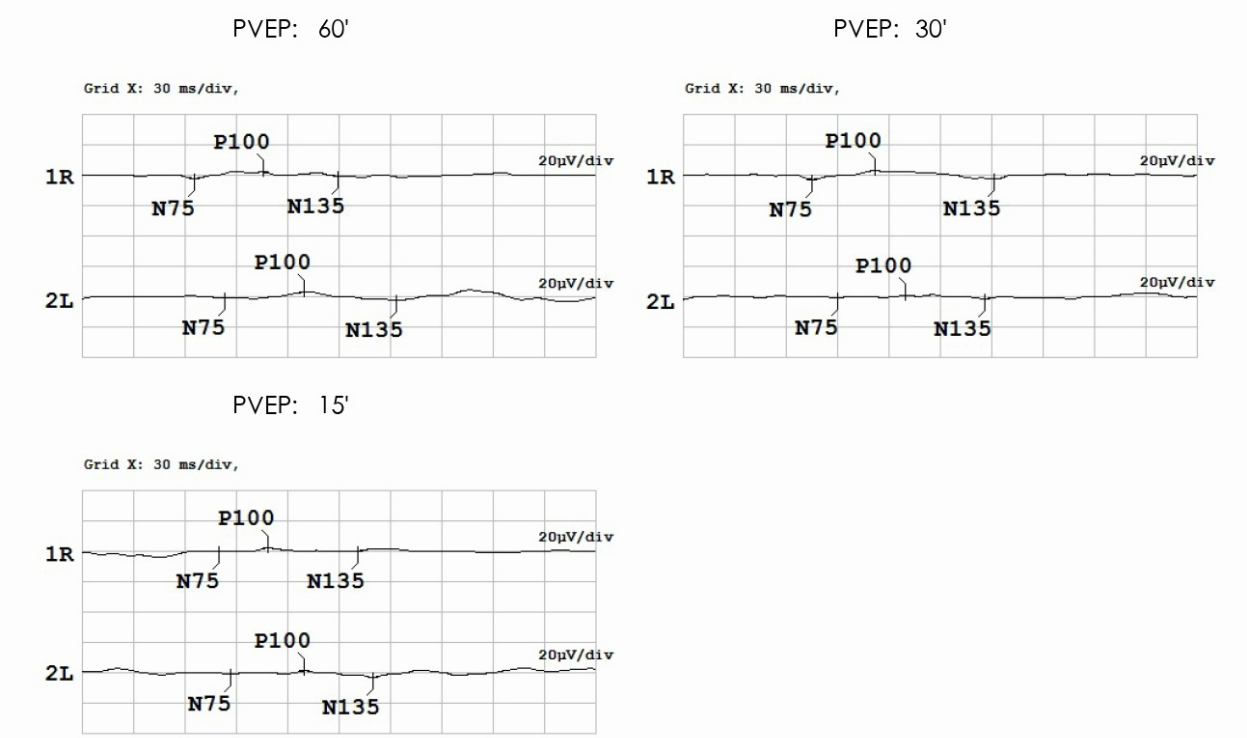

PVEP: 图形翻转.60'

No.	N75 [ms]	P100 [ms]	N135 [ms]	N75-P100 [μV]	P100-N135 [μV]
1R	66.0	106.0	149.5	4.9	3.4
2L	83.5	130.0	183.5	4.8	5.8

PVEP: 图形翻转.30'

No.	N75 [ms]	P100 [ms]	N135 [ms]	N75-P100 [μV]	P100-N135 [μV]
1R	75.5	112.0	182.0	6.3	6.0
2L	90.5	130.0	176.0	2.8	3.1

PVEP: 图形翻转.15'

No.	N75 [ms]	P100 [ms]	N135 [ms]	N75-P100 [μV]	P100-N135 [μV]
1R	80.0	109.0	161.5	3.2	1.9
2L	87.0	130.0	170.0	3.0	4.9

Fig. S17. Retina ERG of patient 3. The light-stimulated electrical activity of the retina indicates no remarkable change in terms of retinal function in patient 3 (**A**: pre-injection; **B**: six months post-injection).

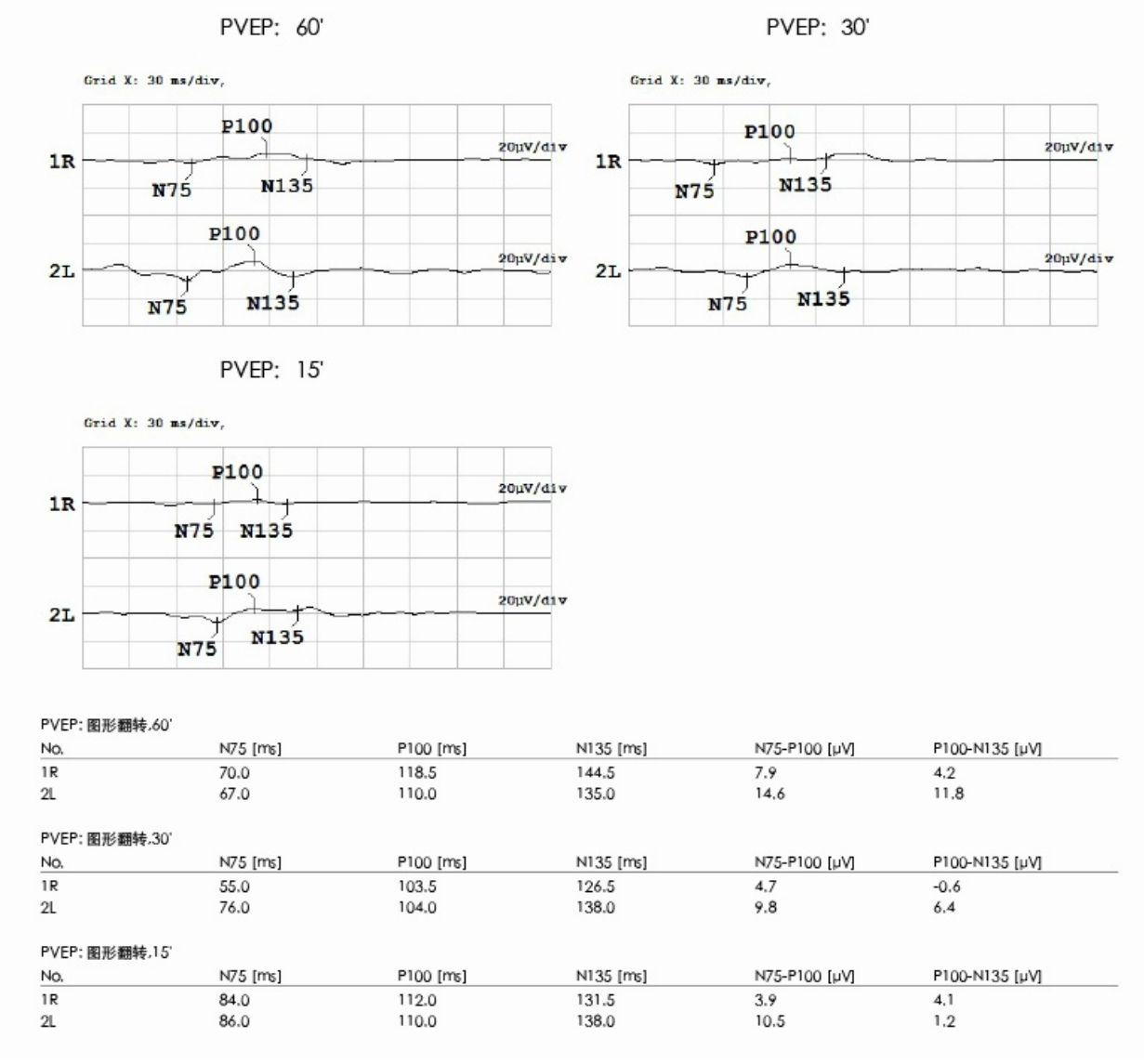

PVEP: 图形翻转.60'

No.	N75 [ms]	P100 [ms]	N135 [ms]	N75-P100 [μV]	P100-N135 [μV]
1R	70.0	118.5	144.5	7.9	4.2
2L	67.0	110.0	135.0	14.6	11.8

PVEP: 图形翻转.30'

No.	N75 [ms]	P100 [ms]	N135 [ms]	N75-P100 [μV]	P100-N135 [μV]
1R	55.0	103.5	126.5	4.7	-0.6
2L	76.0	104.0	138.0	9.8	6.4

PVEP: 图形翻转.15'

No.	N75 [ms]	P100 [ms]	N135 [ms]	N75-P100 [μV]	P100-N135 [μV]
1R	84.0	112.0	131.5	3.9	4.1
2L	86.0	110.0	138.0	10.5	1.2

Fig. S18. Retina ERG of patient 2. The light-stimulated electrical activity of retina indicates no significant change in terms of retinal function in patient 2 twelve months after the treatment.

A

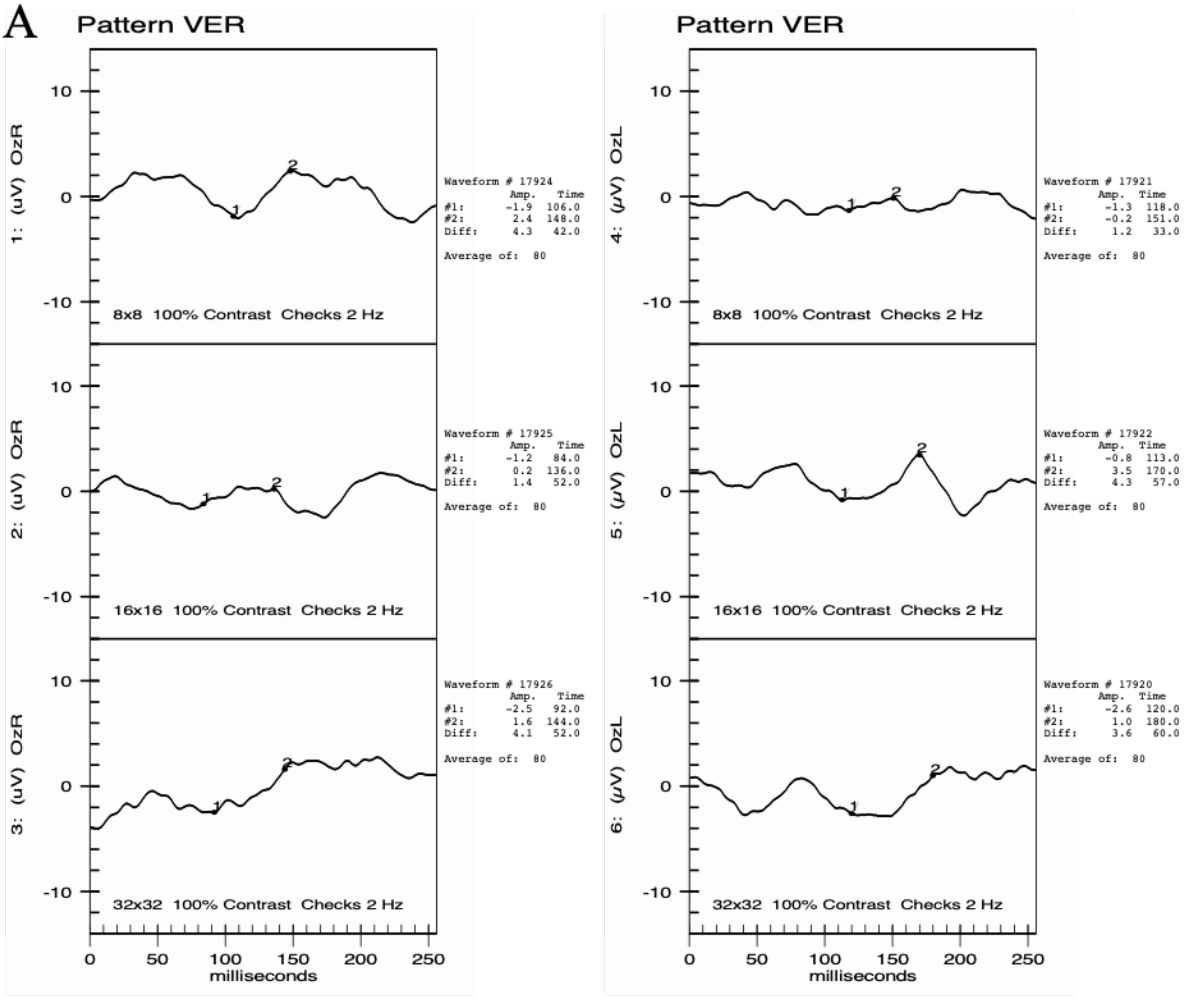
Pattern VER
1: (uV) OzR
2: (uV) OzR
3: (uV) OzR
8x8 100% Contrast Checks 2 Hz
16x16 100% Contrast Checks 2 Hz
32x32 100% Contrast Checks 2 Hz
Waveform # 17924
Amp. Time
#1: -1.9 106.0
#2: 2.4 148.0
Diff: 4.3 42.0
Average of: 80
Waveform # 17925
Amp. Time
#1: -1.2 84.0
#2: 0.2 136.0
Diff: 1.4 52.0
Average of: 80
Waveform # 17926
Amp. Time
#1: -2.5 92.0
#2: 1.6 144.0
Diff: 4.1 52.0
Average of: 80
milliseconds
Pattern VER
4: (μV) OzL
5: (μV) OzL
6: (μV) OzL
8x8 100% Contrast Checks 2 Hz
16x16 100% Contrast Checks 2 Hz
32x32 100% Contrast Checks 2 Hz
Waveform # 17921
Amp. Time
#1: -1.3 118.0
#2: -0.2 151.0
Diff: 1.2 33.0
Average of: 80
Waveform # 17922
Amp. Time
#1: -0.8 113.0
#2: 3.5 170.0
Diff: 4.3 57.0
Average of: 80
Waveform # 17920
Amp. Time
#1: -2.6 120.0
#2: 1.0 180.0
Diff: 3.6 60.0
Average of: 80
milliseconds

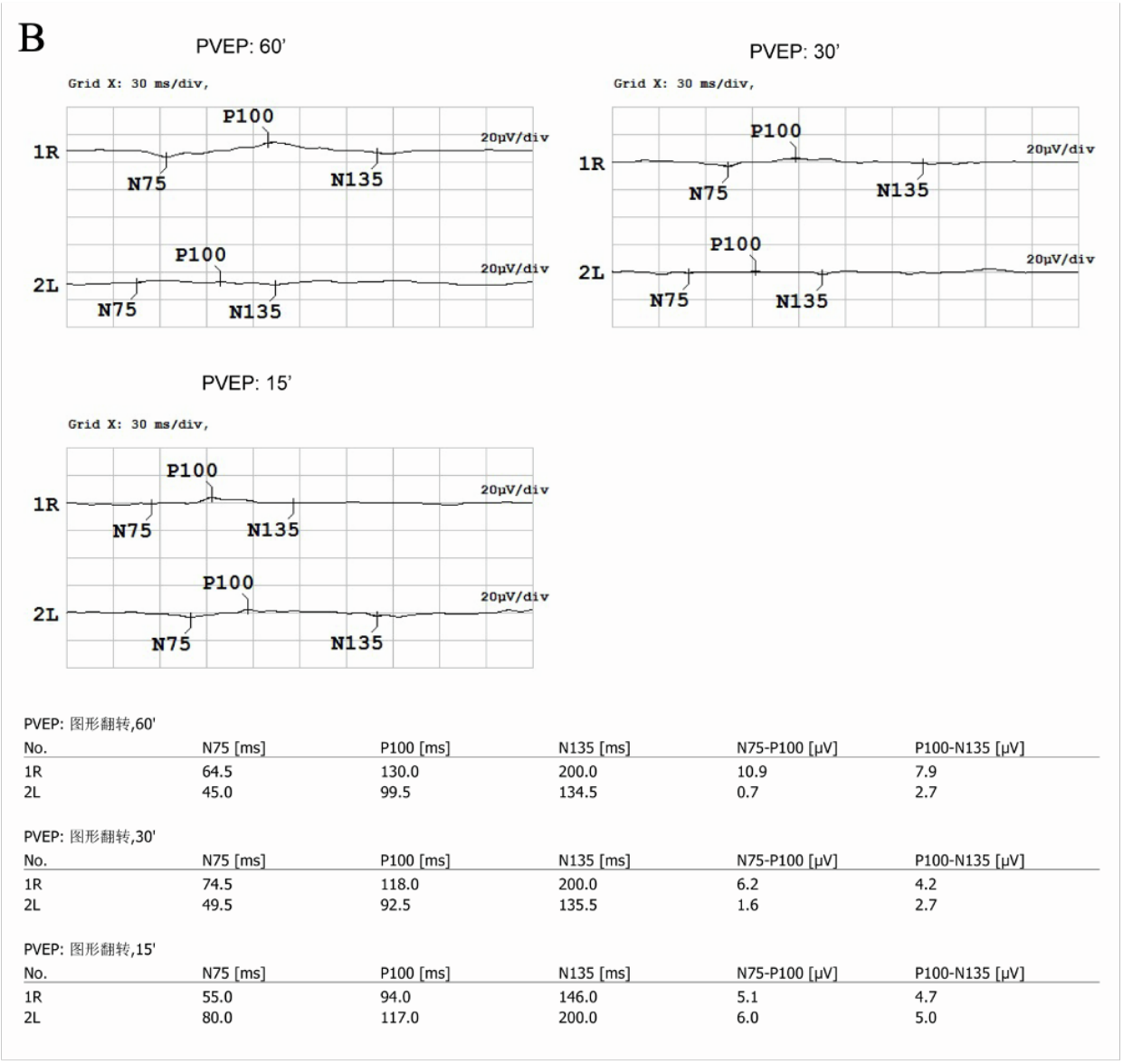

PVEP: 图形翻转,60'

No.	N75 [ms]	P100 [ms]	N135 [ms]	N75-P100 [μV]	P100-N135 [μV]
1R	64.5	130.0	200.0	10.9	7.9
2L	45.0	99.5	134.5	0.7	2.7

PVEP: 图形翻转,30'

No.	N75 [ms]	P100 [ms]	N135 [ms]	N75-P100 [μV]	P100-N135 [μV]
1R	74.5	118.0	200.0	6.2	4.2
2L	49.5	92.5	135.5	1.6	2.7

PVEP: 图形翻转,15'

No.	N75 [ms]	P100 [ms]	N135 [ms]	N75-P100 [μV]	P100-N135 [μV]
1R	55.0	94.0	146.0	5.1	4.7
2L	80.0	117.0	200.0	6.0	5.0

Fig. S19. Retinal ERG examination of patient 1. ERG detected no obvious changes of rod or cone responses to light stimulus in patient 1. (**A**: pre-injection; **B**: twelve months post-injection)

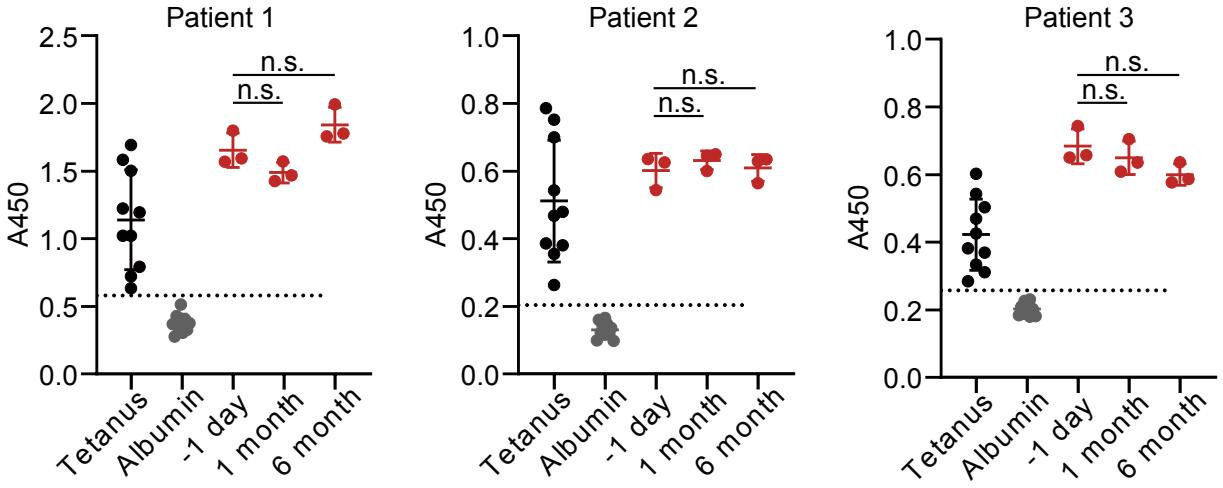

Fig. S20. ELISA results detect antibodies against SpCas9. Tetanus toxoid and human albumin in the sera from different donors served as a positive and negative control, respectively. The Cas9-specific antibodies were determined at different time points. The change in Cas9 antibody levels before and after HELP administration was insignificant. All samples above the dotted line were considered antibody-positive. The dotted line represents the mean absorbance of the negative control, human albumin, plus three s.d. from the mean. Data and error bars represent mean ± s.e.m.; n.s., non-significant; unpaired two-tailed Student's t-tests.

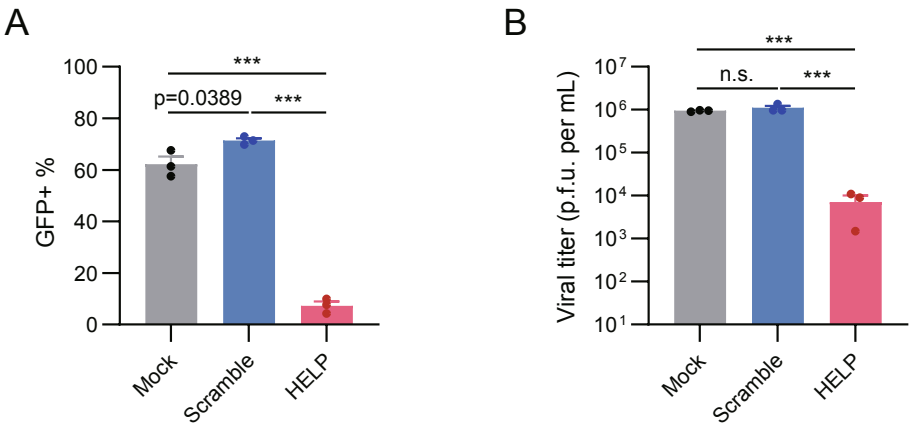

Fig. S21. In vitro antiviral activity of the clinical grade HELP. 4×10^4 293T cells were seeded in a 48-well plate and transduced with 400 ng of HELP or scramble control on the following day. The medium was refreshed 12 h post-infection (h.p.i.). 24 h after transduction, cells were infected with HSV-1-GFP at an MOI of 1. The cells and supernatants were harvested at 24 and 48 h.p.i. for flow cytometry (**A**) and plaque assay (**B**), respectively. 293T cells were transduced with HELP for 24 h and then infected with HSV-1-GFP. n=3 biologically independent samples. Data and error bars represent mean ± s.e.m.; n.s., non-significant; ***P<0.001; unpaired two-tailed Student's t-tests.

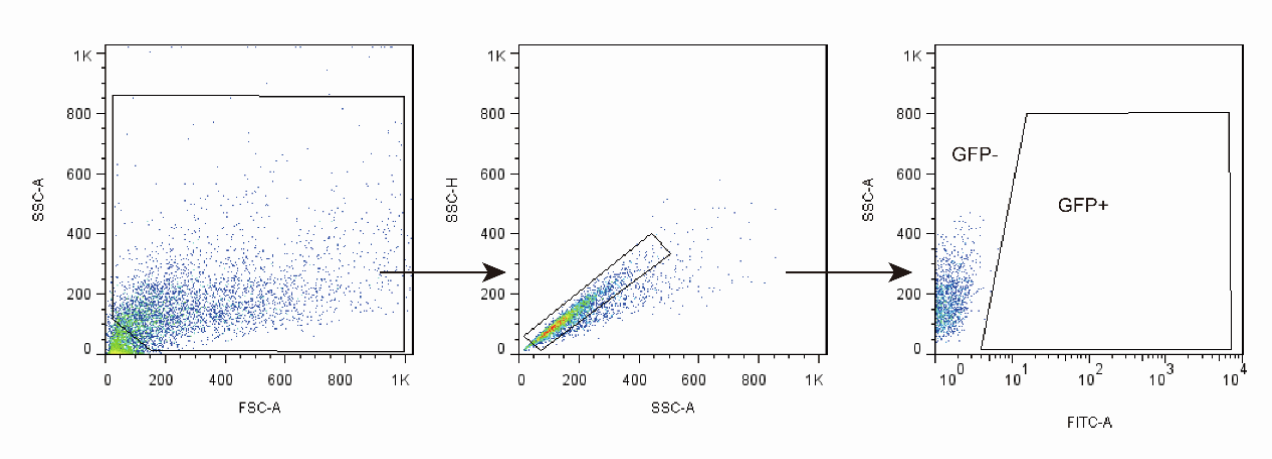

Fig. S22. Gating strategies used for cell sorting analysis. Gate strategy to sort GFP positive cells from HSV-1-GFP infected 293T cells on supplementary Fig. S21A.

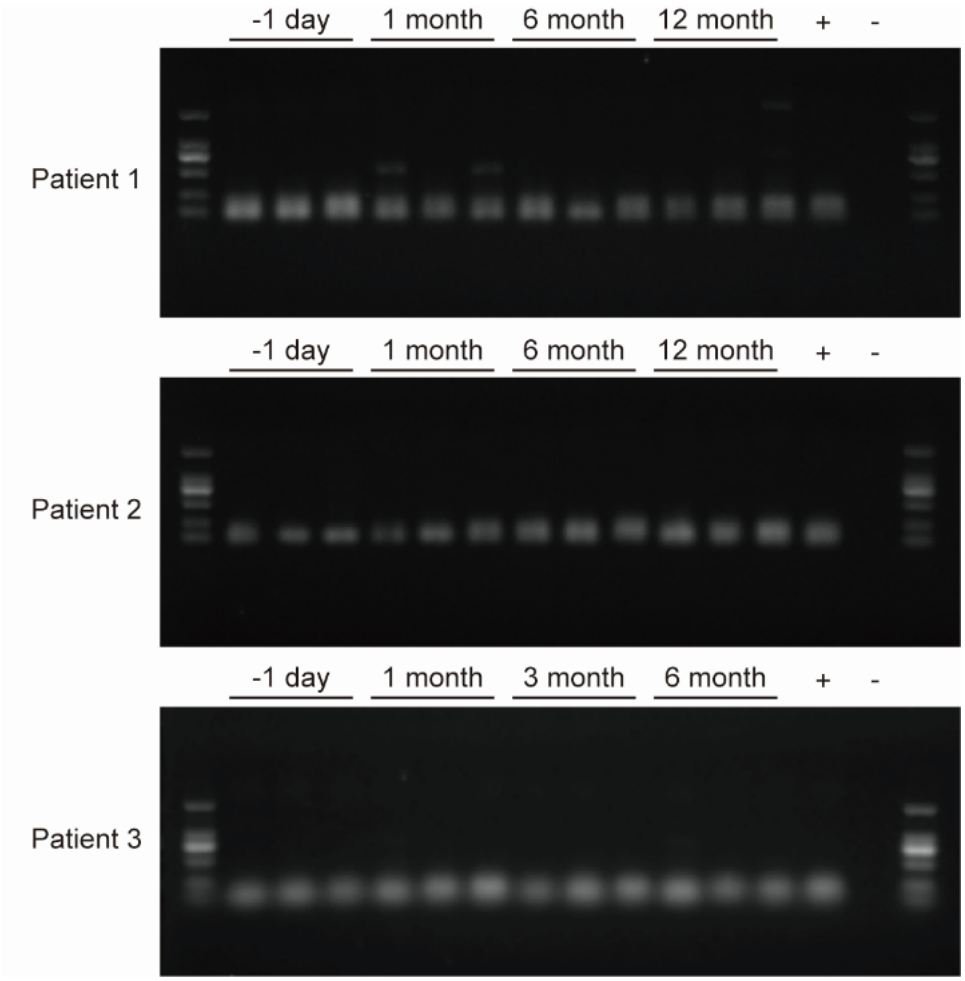

Fig. S23. Validity of patient samples. GAPDH gene in the tear swab of patients was tested by PCR to verify the validity of patient samples. Eye swab samples of 1 day pre-injection, 1 month, 6 months, 12 months post-injection of patient 1 & 2, and samples of 1 day pre-injection, 1 month, 3 months, 6 months post-injection of patient 3 were used as templates for PCR followed by nucleic acid gel electrophoresis. The results showed that GAPDH was positive in all samples, indicating that the swabs were valid.

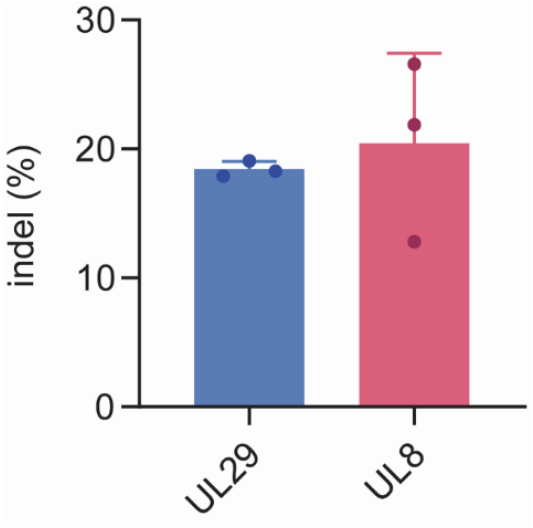

Fig. S24. Gene editing efficiency of the clinical grade HELP. TIDE analysis of indels in the HSV-1 genome. 2×10^4 293T cells were incubated with 200 ng P24 HELP, then infected with HSV-1 with MOI=1 24 h later. Virus DNA was collected at 2 days post-infection for Sanger sequencing. n=3 biologically independent samples.

A

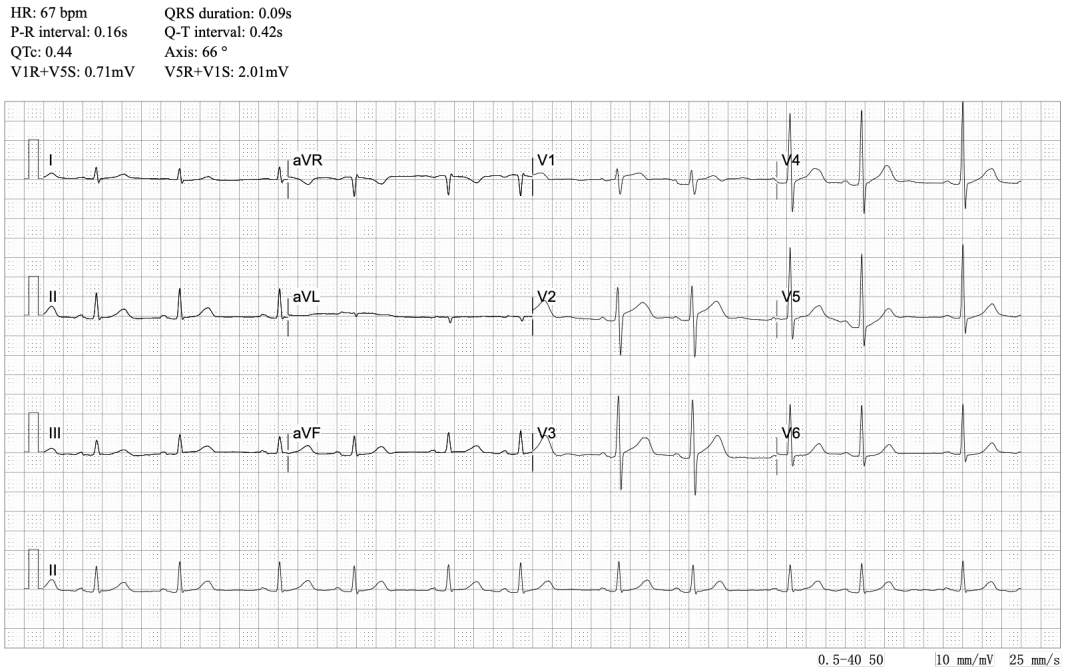

B

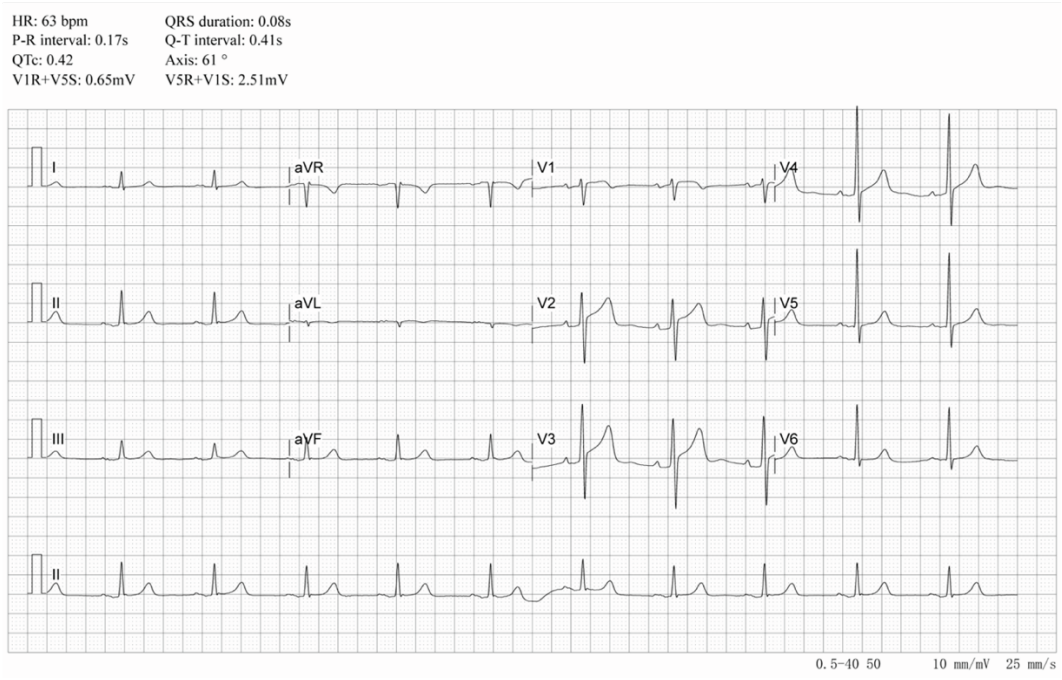

Fig. S25. The ECG examination of patient 1. The pre- and postoperative ECG of patient 1 was unremarkable. (**A**: pre-injection; **B**: twelve months post-injection)

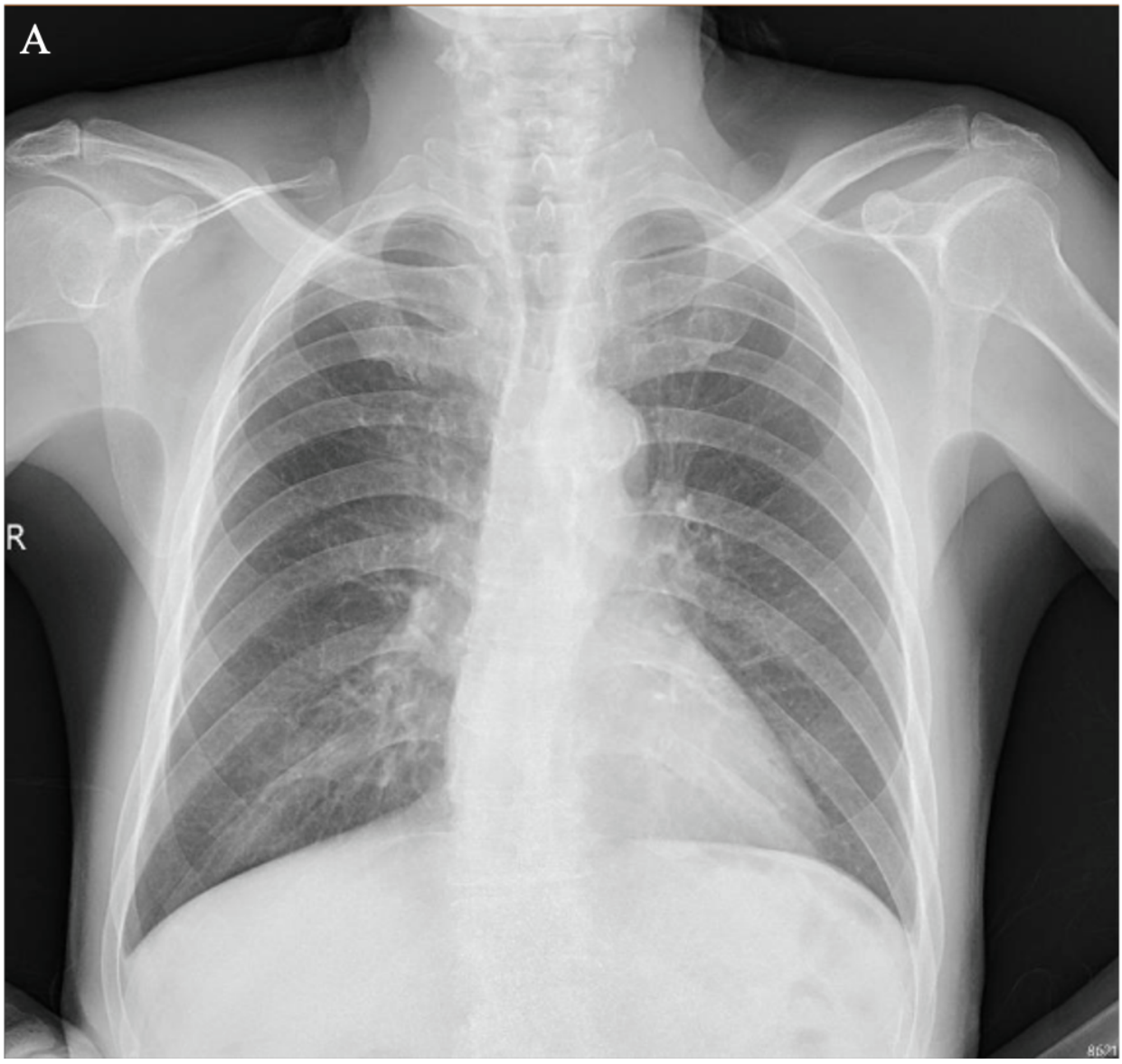
A
R

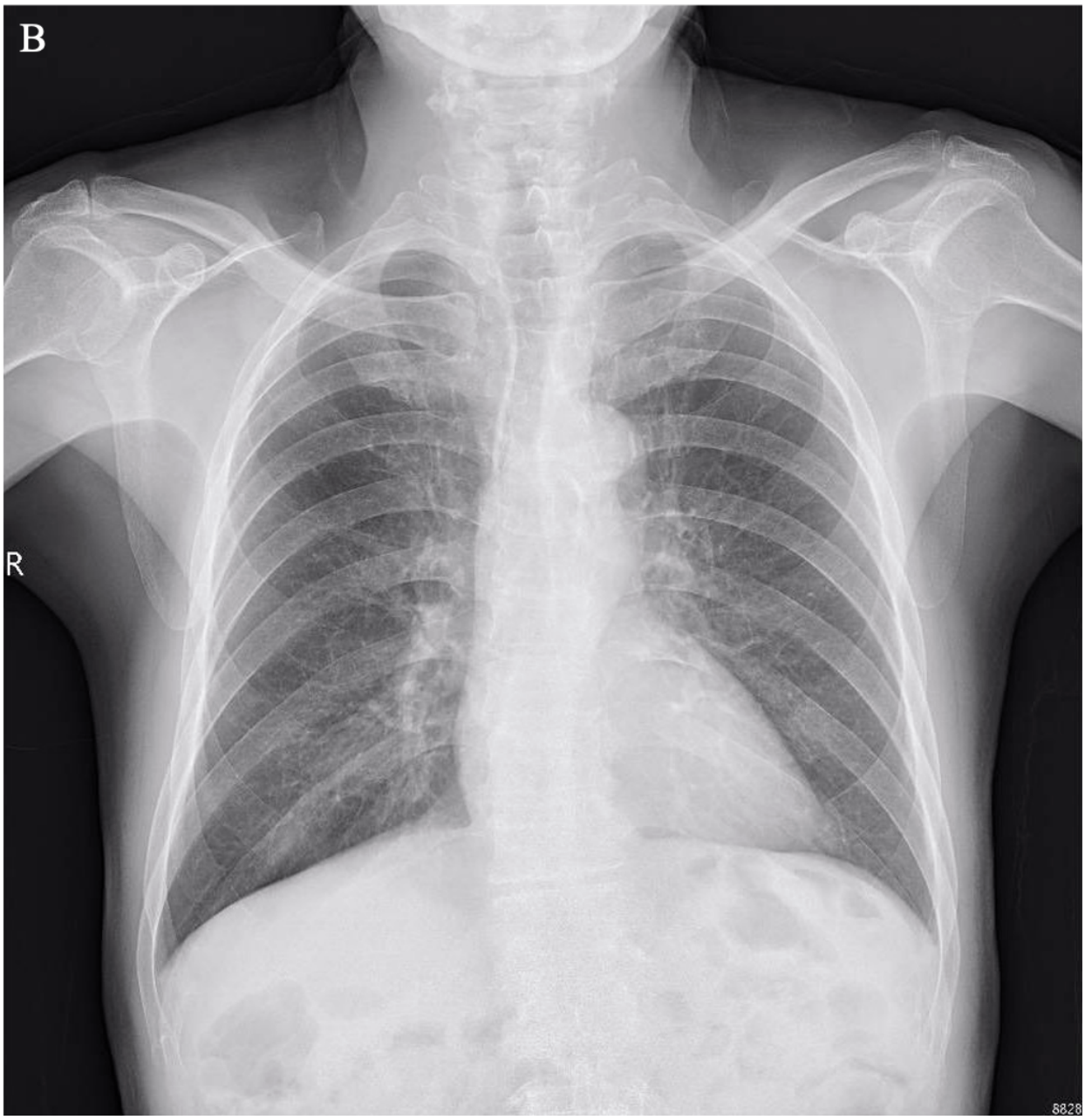

Fig. S26. Chest X-ray examination of patient 1. The Chest X-ray of patient 1 showed no remarkable changes before (**A**) and twelve months (**B**) after the injection.

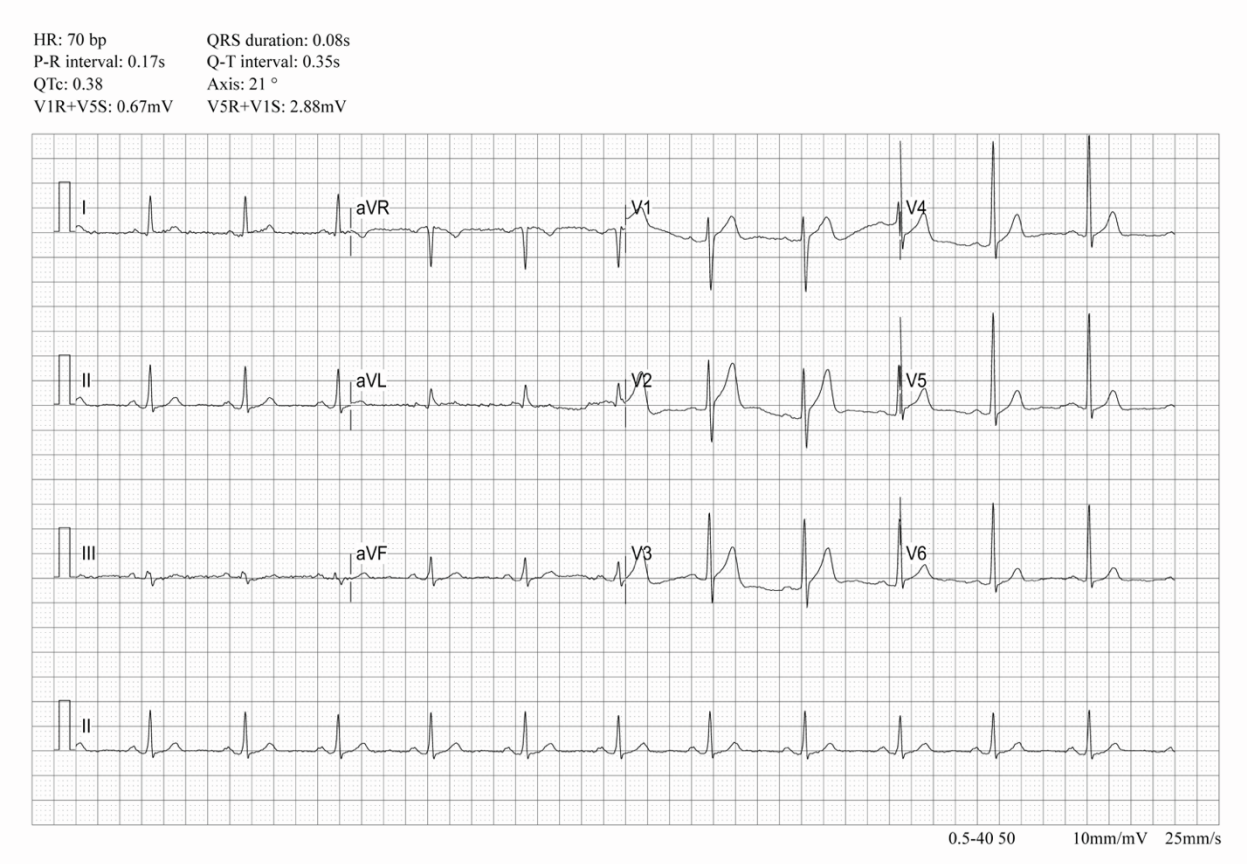

Fig. S27. The ECG of patient 2. The ECG of patient 2 showed counterclockwise transposition, indicating a possibly hypertrophic in the left ventricle. Slightly hypertrophy of the ventricle is not reckoned as a contraindication for corneal transplant surgery.

Fig. S28. Chest X-ray film of patient 2. The chest X-ray result of patient 2 was unremarkable.

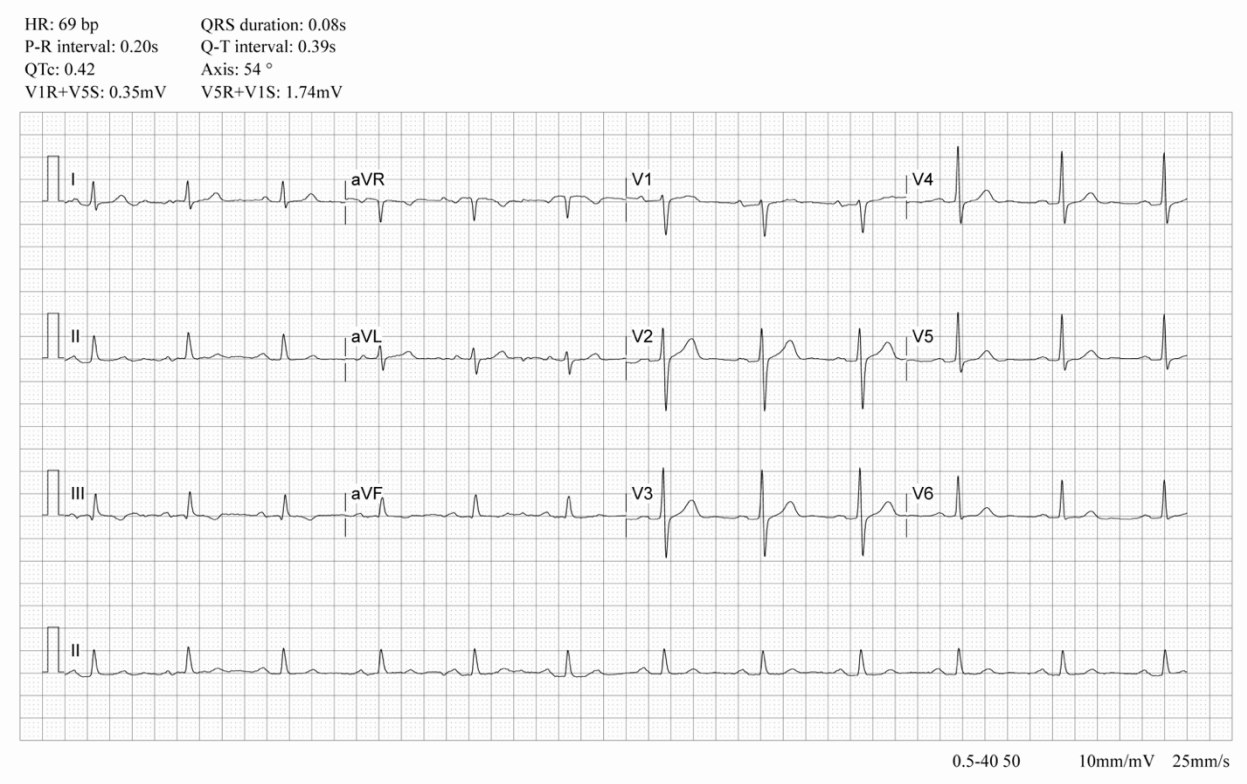

Fig. S29. The ECG examination of patient 3. The pre-operative ECG of patient 3 was unremarkable.

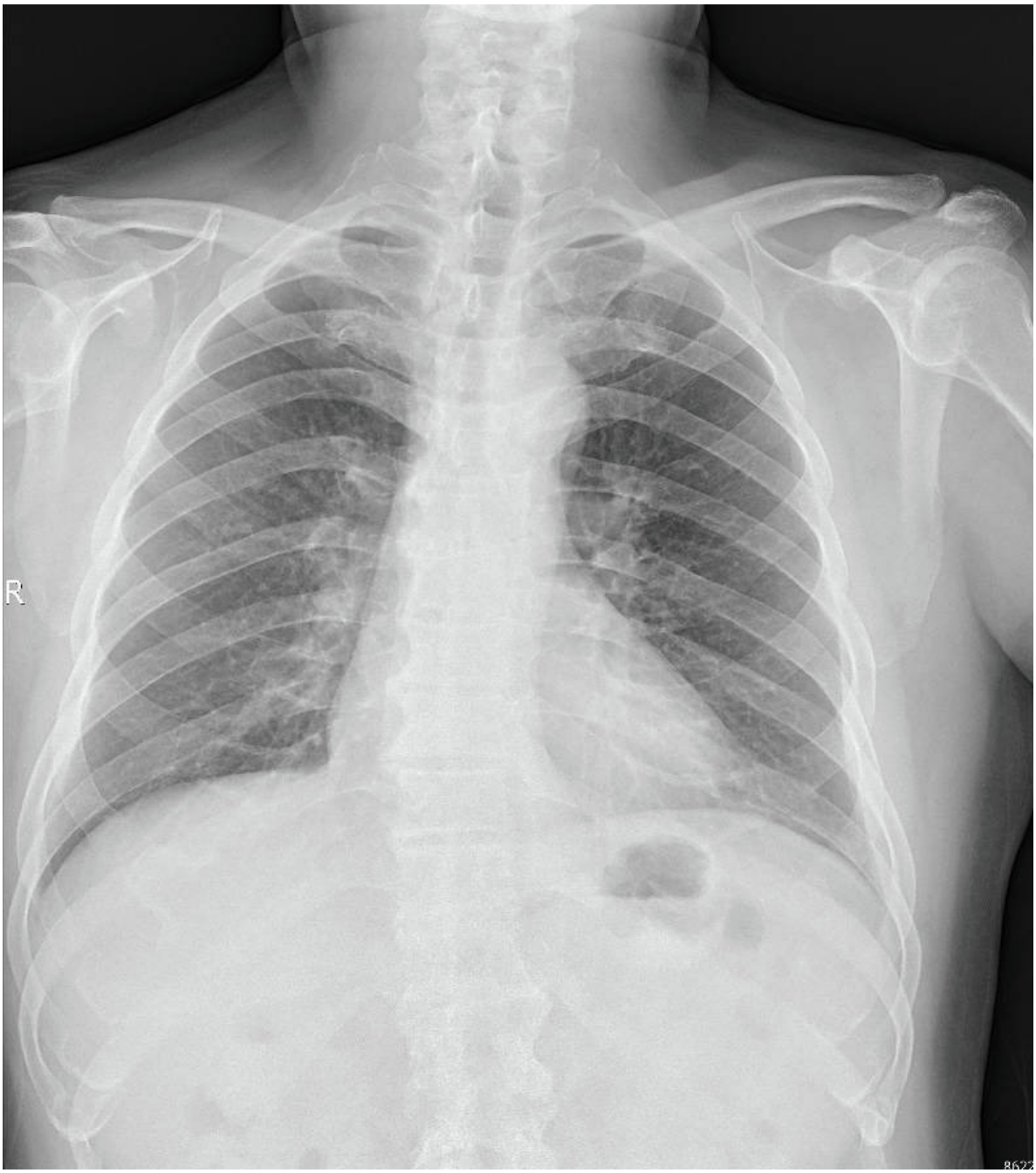

Fig. S30. Chest X-ray film of patient 3. The chest X-ray result of patient 3 was unremarkable.

Table S1. Visual acuity, intraocular pressure and virus tests.

		1 day pre-injection	7 days post-injection	1 month post-injection	2 months post-injection	3 months post-injection	6 months post-injection	12 months post-injection
Patient 1	**Best-corrected visual acuity**	Light perception	Finger count	Finger count	Finger count	Finger count	20/100	20/100
	Intraocular pressure (mmHg)	Undetectable	12.0	10.4	16	15.3	8	21.3
	HSV-1 tests (Ct value)	21.35 (Cornea) 28.37 (Aqueous) 30.55*(Tear swab)	- 24.09(Tear swab) -	28.37(Tear swab) 31.49(Tear swab) 31.08(Tear swab)	- - -	- - -	- - -	- - -
Patient 2	**Best-corrected visual acuity**	Hand motion	20/250	20/167	20/100	20/67	20/133	20/133
	Intraocular pressure (mmHg)	Undetectable	11.0	16.3	16.4	12.4	7.3	15.0
	HSV-1 tests (Ct value)	26.34 (Cornea) 36.50 (Aqueous) 35.01*(Tear swab)	- - -	- - -	- - -	- - -	- - -	- - -
Patient 3	**Best-corrected visual acuity**	Hand motion	Hand motion	Hand motion	Hand motion	Hand motion	Hand motion	Finger count
	Intraocular pressure (mmHg)	Undetectable	n.a.	15.0	24.1	18.5	18.1	19.3
	HSV-1 tests (Ct value)	34.9 (Cornea) - (Aqueous) 29.5 (Tear swab)	- - -	- - -	- - -	- - -	- - -	- - -

*Mean HSV-1 titer (Ct value) of three simultaneously sampled tear swabs; n.a., not available; -, Ct value undetectable.

Table S2. List of adverse events.

Patient	Adverse Event	Start Date	End Date	Placebo Related	Severity	Outcome	Treatment
1	corneal edema	11/2020	11/2020	possibly related	mild	resolved	concomitant medication
	conjunctival injection	11/2020	11/2020	unlikely to be related	mild	resolved	concomitant medication
	hyphema	11/2020	11/2020	unrelated	mild	resolved	none
	neurotrophic keratitis	5/2021	/	unrelated	mild	unresolved	concomitant medication
	uncontrolled corneal ulcer	9/2021	11/2021	unrelated	moderate	resolved	penetrating keratoplasty
	cataract	n.a.	11/2021	unrelated	mild	resolved	cataract surgery
	secondary glaucoma	10/2021	12/2021	unrelated	mild	resolved	concomitant medication
2	corneal edema	1/2021	1/2021	possibly related	mild	resolved	concomitant medication
	conjunctival injection	1/2021	1/2021	unlikely to be related	mild	resolved	concomitant medication
	itching	2/2021	3/2021	unrelated	mild	resolved	concomitant medication
	endophthalmitis	7/2021	7/2021	unrelated	moderate	resolved	vitrectomy and antibiotic injection
	cataract	n.a.	/	unrelated	mild	unresolved	none
3	corneal edema	5/2021	5/2021	possibly related	mild	resolved	concomitant medication
	conjunctival injection	5/2021	5/2021	unlikely to be related	mild	resolved	concomitant medication
	graft rejection	8/2021	10/2021	unrelated	mild	resolved	concomitant medication
	secondary glaucoma	7/2021	8/2021	unrelated	mild	resolved	concomitant medication
	cataract	n.a.	/	unrelated	mild	unresolved	none

Table S3. p24 antibody test.

Positive Index*	Positive control	Negative control	-1 day	1 month	3 months	6 months
Patient 1	15.3	0.49	0.45	0.45	0.45	0.45
Patient 2	13.4	0.51	0.50	0.44	0.46	0.44
Patient 3	11.62	0.49	0.46	0.49	0.5	0.47

* Calculate the mean absorbance values (OD450) for Negative Control using formula:
OD mean (negative control) = (OD (negative control 1) + OD (negative control 2)) / 2.
Calculate the cut-off value: Cut-off = OD mean (negative control) + 0.05
Calculate Positivity Index for each sample:
Positivity Index = mean OD 450 (sample) / Cut-off value.
If Positivity Index value is greater than 1.1, the result is **Positive**.
If Positivity Index value is less than 0.9, the result is **Negative**.

Table S4. Sequencing information on raw data.

Sample	Yield (Mb)	Depth (x)	Reads	Base≥Q30 (%)	Insert size (bp)
WT	192,354	64	1,282,361,462	91.60%	420.725
HELP	185,126	62	1,234,177,196	90.93%	403.405

Note:
Depth (x): The average sequencing depth (Yield bases/Human genome size).
Yield (Mb): The number of bases in raw data.
Reads: The number of paired-end reads.
Base ≥ Q30 (%): The percentage of bases with a quality score of 30 or higher. Q30 means that the sequencing error rate of a base is 0.001.

Insert size (bp): The average size of sample sequencing fragments.

Table S5. The coverage statistics of the sequence alignment.

Sample	Mapping rate	Properly mapped	Fraction of covered with ≥20x	Fraction of covered with ≥0.2 * Mean	Fraction of CDS regions covered with ≥20x
WT	92.254%	89.592%	97.168%	98.809%	98.55%
HELP	92.537%	89.771%	97.095%	98.831%	98.50%

Note:

Mapping rate (%): The percentage of total reads mapping to the reference genome.

Properly mapped: In the paired-end sequencing mode, the percentage of total reads, with both Read1 and Read2 mapping to the genome and corresponding mapping positions consistent with the fragment size distribution of the sequencing library.

Fraction of covered with ≥ 20x (%): It refers to the proportion of bases with a coverage depth not less than 20x in the genome.

Fraction of covered with ≥ 0.2 * Mean (%): It refers to the proportion of bases with a coverage depth of no less than 0.2 fold the mean depth of coverage in the genome.

Fraction of CDS regions covered with ≥ 20x (%): It refers to the proportion of bases with a coverage depth not less than 20x in the CDS regions.

Table S6. The information on potential off-target site

Pos	Strand	Sequence	Variant_Classification	Variant_type	Ref	Alt	DP	DV	AF	Distance to CDS of gene	Distance
chr8:105379575	+	GCGAGaGTAaACaacTCCCAGG	intergenic	SNP	G	T	55	3	0.0545	-10678bp to gene:DCSTAMP; +12064bp to DPYS	20

Note:
Pos: The mutation site on chromosome.
Strand: The strand where the off-target sites are located.
Sequence: Sequence of off-target sites.
Variant_Classification: The genome function regions where the mutations occurred.
Variant_type: Variant type (SNP/Indel). SNP, single nucleotide polymorphism.
Ref: The corresponding base in the reference genome (before editing) at this mutation site.
Alt: The mutated base/sequence.
DP: Sequencing depth of the locus.
DV: Sequencing depth of the mutation base.
AF: Proportion of reads carrying variant alleles.
Distance to CDS of gene: The distance between gene and the mutation.
Distance: The distance between the mutation site and the homologous region site, with negative values indicating that the mutation occurred upstream of the homologous site and positive values indicating that the mutation occurred downstream of the homologous site

Table S7. The statistics table of SV.

Group	BND	DEL	DUP	INS	INV	Total
HELP_vs _WT	7	2	0	1	0	10
WT_vs_HELP	6	1	0	0	0	7

Note:

1) Group: The first line is in the format case_vs_control, which is the experiment and control groups provided by the project. The second line is in the format control_vs_case. The WT of the project is the untreated HCSCs and HELP-treated HCSCs is the experimental group (case).
2) BND: The number of chromosomal translocation breakend variations of samples.
3) DEL: The number of large segment deletion variations of samples.
4) DUP: The number of tandem duplication variations of samples.
5) INS: The number of chromosome segment insertion variations of samples.
6) INV: The number of chromosome segment inversion variations of samples.
7) Total: Total number of structural variations detected of samples.

Table S8. SV annotation of sample group HELP_vs_WT.

Chrom	POS	FORMAT	WT	HELP	Somatic Score	SV type	Cyto Band	Gene_name	Gene count	Function_Gene	RE_gene	ExAC_delZ	ExAC_dupZ	OMIM_ID	GnomAD_pLI	ExAC_pLI	ACMG_class
chr3	60598188	PR:SR	46,0:44,0	28,2:40,3	41	DEL	p14.2	FHIT;MIR548BB	2	Intron/exonic	AAGAB(HI=3/morbid/RE=mTL_miRNA);ABHD5(morbid/RE=mTL_miRNA);.....	0.44589193	-0.556419	.	0.0057055	0.0013918	3
chr8	48662203	PR:SR	15,0:46,5	31,6	40	DEL	q11.21	.	0	intergenic	.	.	.	.	.	.	3
chr11	1628828	PR	75,0	31,6	64	BND	p15.5	KRTAP5-3	1	exonic	.	.	.	.	0.16438	0.26291	.
chr11	50325994	PR	62,0	24,0:43,8	60	BND	p11.12	.	0	intergenic	.	.	.	.	.	.	.
chr11	71238526	PR	75,0	74,8	48	BND	q13.4	KRTAP5-7	1	exonic	.	.	.	.	0.090951	0.58196	.
chr16	21031742	PR:SR	2,0:18,0	51,7	38	INS	p12.3	DNAH3	1	intron	.	-2.253479	0.84066663	.	1.54E-64	9.63E-51	.
chr16	35157286	PR	62,0	74,8	49	BND	p11.1	.	0	intergenic	.	.	.	.	.	.	.
chr4	187503324	PR	45,0	4,0:12,7	44	BND	q35.2	.	0	intergenic	.	.	.	.	.	.	.
chr4	190110388	PR	45,0	51,7	44	BND	q35.2	.	0	intergenic	.	.	.	.	.	.	.
chrY	9986510	PR	231,1	199,7	33	BND	p11.2	.	0	intergenic	.	.	.	.	.	.	.

Note:

Chrom: Name of the chromosome.

POS: The starting site of chromosome of structural variation.

FORMAT: The FORMAT column from a VCF file. PR indicates spanning paired-read support for the ref and alt alleles in the order listed. SR indicates split reads for the ref and alt alleles in the order listed

WT: The support reads of control sample which is shown in the format indicated by column “Format”

HELP: The support reads of case sample which is shown in the format indicated by column “Format”.

SomaticScore: Somatic variant quality score.

SV_type: Types of structural variation.

CytoBand: Cytogenic band annotation.

Gene_name: Gene symbol.

Gene_count: Number of overlapped genes with the copy number variation segment.

Function_Gene: The gene function regions where the variant occurred.

RE_gene: Name of the genes regulated by a regulatory element overlapped with the SV to annotate.

ExAC_delZ: Positive delZ_ExAC (Z score) from ExAC indicate gene intolerance to deletion.

ExAC_dupZ: Positive dupZ_ExAC (Z score) from ExAC indicate gene intolerance to duplication.

OMIM_ID: OMIM unique six-digit identifier.

GnomAD_pLI: Score computed by gnomAD indicating the probability that a gene is intolerant to a loss of function variation.

ExAC_pLI: Score computed by ExAC indicating the probability that a gene is intolerant to a loss of function variation. ExAC considers pLI >= 0.9 as an extremely LoF intolerant gene.

ACMG_class: SV ranking class into 1 of 5: class 1 (benign) class 2 (likely benign) class 3 (variant of uncertain significance) class 4 (likely pathogenic) class 5 (pathogenic).

Table S9. SV annotation of sample group WT_vs_HELP.

Chrom	POS	FORMAT	HELP	WT	SomaticScore	SV_type	Cyto Band	Gene_name	Gene_count	Function_Gene	RE_gene	ExAC_delZ	ExAC_dupZ	OMIM_ID	GnomAD_pLI	ExAC_pLI	ACMG_class
chr5	149029138	PR:SR	13,0:10,0	16,0:8,5	30	DEL	q32	.	0	intergenic	.	.	.	.	.	.	3
chr10	24500527	PR:SR	29,0:18,1	28,0:15,6	47	BND	p12.2	KIAA1217	1	intron	.	1.17216141	0.58181469	.	0.00023185	0.014168	.
chr10	58939351	PR	80,1	61,9	30	BND	q21.1	.	0	intergenic	.	.	.	.	.	.	.
chr15	47872183	PR:SR	47,0:63,0	48,2:54,2	34	BND	q21.1	SEMA6D	1	intron	.	0.50209124	-0.2822914	.	0.93948	0.99947	3
chr3	50478844	PR:SR	47,0:63,0	48,2:54,2	34	BND	p21.31	CACNA2D2	1	intron	.	1.68574942	1.51141627	607082	0.99997	0.99969	3
chr5	84159932	PR:SR	29,0:18,1	28,0:15,6	47	BND	q14.3	.	0	intergenic	.	.	.	.	.	.	.
chr9	123131688	PR	80,1	61,9	30	BND	q33.2	.	0	intergenic	.	.	.	.	.	.	.

Table S10. The primers for UL8 and UL29 amplification.

Target sites	gRNA Sequence (5'-3')	Primer names	Sequence (5'-3')
UL8	GGGGCAGCCATACCGCGTAA	Y1-F	gagccgtagaaatcccgcag
		Y2-R	aaacctcaccaaacagacaa
UL29	GCGAGCGTACACGTATCCC	Y3-F	gggtgtagtccgaaaagccaa
		Y4-R	cacgcccccaggtaaagtgta

Table S11. The quality report of HELP.

Source	OBiO Technology (Shanghai) Corp., Ltd.	**Specification**	0.25 ml/vial
Test Category	**Test**	**Result**	
Quantification	p24 protein content	1.19E+04 ng p24/ml	
Safety	Bacteria	Negative	
	Mycoplasma	Negative	
Conclusion	Qualified		

Table S12. Intraocular bacterial and fungal culture results of patient 2. Gram+ cocci were found in the right eye of patient 2 during the vitrectomy 6 months after PK.

Culture	Presence	Species
Bacteria	+	Gram-positive cocci
Fungus	-	-

Table S13. Blood tests of patient 1. The blood tests of patient 1 showed slight anemia, hypoproteinemia, and diabetes before the injection. We observed no abnormal changes which were related to the injection in these blood tests at 12-month follow-up.

Code	Pre-Injection	Twelve Months Post-Injection	Normal Range	Unit
White blood cell count	5.24	4.39	4.0~10.0	10^9/L
Red blood cell count	2.71 ↓	3.47 ↓	4.3~5.8	10^12/L
Hemoglobin	106 ↓	122 ↓	130~175	g/l
Packed red blood cell volume	30.7 ↓	36.9 ↓	40~50	%
Red blood cell volume distribution width-coefficient of variation	15.1 ↑	15.2 ↑	10.0~15.0	%
Red blood cell volume distribution width-standard deviation	62.3 ↑	59.8 ↑	35.0~50.0	fL
Mean corpuscular volume	113.3 ↑	106.3 ↑	80.0~100.0	fL
Mean corpuscular hemoglobin	39.1 ↑	35.2 ↑	27.0~33.0	Pg
Mean corpuscular hemoglobin concentration	345	331	320~360	g/l
Platelet count	175	213	100~400	10^9/L
Platelet distribution width	9.7	11.1	9.0~17.00	
Thrombocytocrit	0.17	0.22	0.16~0.22	%
Mean platelet volume	9.7	10.2	9.0~16.0	fL
Platelet-larger cell ratio	21.6	25.0	14.0~46.0	%
Percentage of neutrophil	61.6	56.2	50.0~70.0	%
Percentage of lymphocyte	32.1	30.8	20.0~40.0	%
Percentage of eosinophil	1.5	3.0	0.5~5.0	%
Percentage of monocyte	4.4	8.9 ↑	3.0~8.0	%
Percentage of basophil	0.4	1.1 ↑	0.0~1.0	%
Neutrophil count	3.23	2.47	2.0~7.0	10^9/L
Lymphocyte count	1.68	1.35	0.8~4.0	10^9/L
Monocyte count	0.23	0.39	0.10~0.80	10^9/L
Eosinophil count	0.08	0.13	0.00~0.50	10^9/L
Basophil count	0.02	0.05	0.00~0.10	10^9/L
Code	**Pre-Injection**	**Twelve Months Post-Injection**	**Normal Range**	**Unit**
Alanine aminotransferase	22	31	0~65	u/l
Aspartate aminotransferase	25	30	15~37	u/l
Total protein	67	71	64~82	g/l
Albumin	47	43	35~54	g/l
Globulin	20	28	20~40	g/l
Albumin/globulin	2.4	1.5	1.2~2.5	

γ-Glutamyltransferase	55		37		15~85	u/l
Prealbumin	150	↓	200		200~400	mg/l
Alkaline phosphatase	134		137	↑	50~136	u/l
Blood urea nitrogen	6.8	↑	9.2	↑	2.5~6.4	mmol/l
Creatinine	78		90		53~115	umol/l
Uric acid	0.42	↑	0.38	↑	0.202~0.417	mmol/l
Total bilirubin	10		6		0~17	umol/l
Connect bilirubin	5		2		1~5	umol/l
Total bile acid	14.5	↑	14.4	↑	0.0~10.0	umol/l
High density lipoprotein	1.73		1.86		0.910~2.060	mmol/l
Low density lipoprotein	1.33		2.21		0.00~3.36	mmol/l
Apoprotein A	1.53		1.28		1.100~1.700	g/l
Apoprotein B	0.56	↓	0.76	↓	0.800~1.550	g/l
Apoprotein E	35		38		27~45	mg/l
Lipoprotein small a	25		42		0~300	mg/l
Small dense low density lipoprotein	0.74		1.20		0.26~1.36	mmol/l
Calcium	2.21		2.21		2.04~2.74	mmol/l
Phosphorus	1.24		1.15		0.80~1.60	mmol/l
Potassium	4.6		4.8		3.5~5.4	mmol/l
Sodium	145		143		135~147	mmol/l
Chloride	109	↑	103		96~108	mmol/l
Carbon dioxide binding capacity	22		24		21~32	mmol/l
Lactate dehydrogenase	172		153		81~234	u/l
Creatine kinase	75		95		39~308	u/l
Complement 3c	0.73	↓	0.71	↓	0.9~1.8	g/l
Complement 4	0.20		0.16		0.1~0.4	g/l
Complement 1q	108.7	↓	117.7	↓	159~233	mg/l
Total complement	68.7	↑	62.7	↑	32.5~58.3	u/ml
Haptoglobin	56.50		92.00		32~205	mg/dl
Blood glucose	6.1		6.9	↑	3.9~6.1	mmol/l
Total cholesterol	3.04		4.54		2.80~5.20	mmol/l
Triacylglycerol	0.77		0.70		0.34~2.26	mmol/l

Code	**Pre-Injection**	**Twelve Months Post-Injection**	**Normal Range**	**Unit**
Prothrombin time	13.7	12.7	11.0~14.5	sec
International normalized ratio	1.03	0.98	0.80~1.20	INR
Activated partial thromboplastin time	35.9	32.6	28~45	s
Thrombin time	16.3	17.2	14.0~21.0	s

Fibrinogen	2.70		3.01	2.00~4.00	g/l
D-Dimer	0.67	↑	0.75	↑	0.00~0.50	ug/ml
Prothrombin time ratio	95		105	70~150	%

Code	**Pre-Injection**		**Twelve Months Post-Injection**		**Normal Range**	**Unit**
Glycated hemoglobin	6.2	↑	6.2	↑	4.0~6.0	%

*Red font denotes an elevated clinical index than the normal range; pink font denotes a decreased clinical index than the normal range. Similarly hereinafter.

Table S14. Urine tests of patient 1. The pre-injection and twelve months post-injection routine urinalysis of patient 1 was unremarkable.

Code	Pre-Injection	Twelve Months Post-Injection	Normal Range	Unit
Urine glucose	-	-	-	
Ketone body	-	-	-	
Occult blood	-	-	-	
Protein	-	-	-	
Nitrite	-	-	-	
Bilirubin	-	-	-	
Specific gravity	>=1.030 ↑	1.020	1.003~1.030	
Urine PH value	6.0	6.0	5.0~6.5	
Urobilinogen	16	16	3.0~16.0	umol/l
Leukocyte	-	-	-	
White blood cell count	2	2	0~28	/ul
Red blood cell count	1	6	0~17	/ul
Squamous epithelial cells	-	2	0~28	/ul
Non-squamous epithelial cells	-	1	0~6	/ul
Trichomonas	-	-	0~1	/ul
Kidney epithelial cells	-	-	0~6	/ul
Transparent tube	-	-	0~2	/ul
Particle tube	-	-	0~1	/LPF
Cell tube	-	-	0~1	/LPF
Triphosphate crystal	-	-		
Calcium oxalate crystal	-	-		
Leucine crystal	-	-		
Cystine crystals	-	-		

Table S15. Infectious diseases tests of patient 1. The four transfusion-associated contagion tests (hepatitis B, hepatitis C, syphilis, AIDS) of patient 1 were unremarkable.

Code	Pre-Injection	Twelve Months Post-Injection
Hepatitis B virus surface antigen	Negative	Negative
Hepatitis B virus surface antibody	Negative	Negative
Hepatitis B virus e antigen	Negative	Negative
Hepatitis B virus e antibody	Negative	Negative
Hepatitis B virus core antibody	Negative	Negative
Hepatitis B virus antibody-immunoglobin M	Negative	Negative
Hepatitis B virus pre-S1 antigen	Negative	Negative
Hepatitis C virus antibody	Negative	Negative
Treponema pallidum particle agglutination test	Negative	Negative
Rapid plasma regain test	Negative	Negative
Human immunodeficiency virus antibody	Negative	Negative

Table S16. Blood tests of patient 2. The blood tests of patient 2 indicated mild hyperlipidemia, which had no obvious influence on the implementation of the surgery. We observed no notable changes related to the injection in these blood tests at 12-month follow-up.

Code	Pre-Injection	Twelve Months Post-Injection	Normal Range	Unit
White blood cell count	7.17	10.16 ↑	4.0~10.0	10^9/L
Red blood cell count	4.73	4.69	4.3~5.8	10^12/L
Hemoglobin	148	144	130~175	g/l
Packed red blood cell volume	44.0	43.1	40~50	%
Red blood cell volume distribution width-coefficient of variation	12.1	12.9	10.0~15.0	%
Red blood cell volume distribution width-standard deviation	41.6	43.1	35.0~50.0	fL
Mean corpuscular volume	93.0	91.9	80.0~100.0	fL
Mean corpuscular hemoglobin	31.3	30.7	27.0~33.0	Pg
Mean corpuscular hemoglobin concentration	336	334	320~360	g/l
Platelet count	229	236	100~400	10^9/L
Platelet distribution width	9.3	9.8	9.0~17.00	
Thrombocytocrit	0.21	0.22	0.16~0.22	%
Mean platelet volume	9.1	9.2	9.0~16.0	fL
Platelet-larger cell ratio	17.7	18.4	14.0~46.0	%
Percentage of neutrophil	64.3	77.8 ↑	50.0~70.0	%
Percentage of lymphocyte	28.7	18.3 ↓	20.0~40.0	%
Percentage of eosinophil	1.0	0.3 ↓	0.5~5.0	%
Percentage of monocyte	5.6	3.1	3.0~8.0	%
Percentage of basophil	0.4	0.5	0.0~1.0	%
Neutrophil count	4.61	7.9 ↑	2.0~7.0	10^9/L
Lymphocyte count	2.06	1.86	0.8~4.0	10^9/L
Monocyte count	0.40	0.32	0.10~0.80	10^9/L
Eosinophil count	0.07	0.03	0.00~0.50	10^9/L
Basophil count	0.03	0.05	0.00~0.10	10^9/L
Code	**Pre-Injection**	**Twelve Months Post-Injection**	**Normal Range**	**Unit**
Alanine aminotransferase	17	19	0~65	u/l
Aspartate aminotransferase	17	15	15~37	u/l
Total protein	70	68	64~82	g/l
Albumin	46	42	35~54	g/l
Globulin	24	26	20~40	g/l
Albumin/globulin	1.9	1.6	1.2~2.5	

γ-Glutamyltransferase	33		37	15~85	u/l
Prealbumin	320		350	200~400	mg/l
Alkaline phosphatase	71		80	50~136	u/l
Blood urea nitrogen	5.5		7.5 ↑	2.5~6.4	mmol/l
Creatinine	69		62	53~115	umol/l
Uric acid	0.25		0.32	0.202~0.417	mmol/l
Total bilirubin	16		10	0~17	umol/l
Connect bilirubin	5		2	1~5	umol/l
Total bile acid	2.5		11.2 ↑	0.0~10.0	umol/l
High density lipoprotein	1.24		1.61	0.910~2.060	mmol/l
Low density lipoprotein	4.36	↑	4.72 ↑	0.00~3.36	mmol/l
Apoprotein A	1.46		1.24	1.100~1.700	g/l
Apoprotein B	1.51		1.55	0.800~1.550	g/l
Apoprotein E	52	↑	46 ↑	27~45	mg/l
Lipoprotein small a	41		47	0~75	nmol/l
Small dense low density lipoprotein	3.11	↑	2.70 ↑	0.26~1.36	mmol/l
Calcium	2.34		2.25	2.04~2.74	mmol/l
Phosphorus	1.18		0.99	0.80~1.60	mmol/l
Potassium	4.2		4.0	3.5~5.4	mmol/l
Sodium	140		142	135~147	mmol/l
Chloride	104		101	96~108	mmol/l
Carbon dioxide binding capacity	23		21	21~32	mmol/l
Lactate dehydrogenase	168		182	81~234	u/l
Creatine kinase	122		128	39~308	u/l
Complement 3c	1.03		1.04	0.9~1.8	g/l
Complement 4	0.20		0.32	0.1~0.4	g/l
Complement 1q	154.5	↓	169.4	159~233	mg/l
Total complement	67.9	↑	63.5 ↑	32.5~58.3	u/ml
Haptoglobin	93.30		110.50	32~205	mg/dl
Blood glucose	5.6		6.1	3.9~6.1	mmol/l
Total cholesterol	6.12	↑	7.04 ↑	2.80~5.20	mmol/l
Triacylglycerol	2.33	↑	1.81	0.34~2.26	mmol/l

Code	**Pre-Injection**	**Twelve Months Post-Injection**	**Normal Range**	**Unit**
Prothrombin time	13.3	12.4	11.0~14.5	sec
International normalized ratio	0.99	0.95	0.80~1.20	INR
Activated partial thromboplastin time	35.3	33.0	28~45	s
Thrombin time	18.7	19.7	14.0~21.0	s

Fibrinogen	2.98	2.74	2.00~4.00	g/l
D-Dimer	0.24	0.23	0.00~0.50	ug/ml
Prothrombin time ratio	102	110	70~150	%
Code	**Pre-Injection**	**Twelve Months Post-Injection**	**Normal Range**	**Unit**
Glycated hemoglobin	5.9	5.9	4.0~6.0	%

Table S17. Routine urine test of patient 2. The routine urinalysis of patient 2 was unremarkable.

Code	Pre-Injection	Twelve Months Post-Injection	Normal Range	Unit
Urine glucose	-	-	-	
Ketone body	-	-	-	
Occult blood	-	-	-	
Protein	-	-	-	
Nitrite	-	-	-	
Bilirubin	-	-	-	
Specific gravity	>=1.030 ↑	1.025	1.003~1.030	
Urine PH value	5.5	6.0	5.0~6.5	
Urobilinogen	3.2	16	3.0~16.0	umol/l
Leukocyte	-	-	-	
White blood cell count	6	6	0~28	/ul
Red blood cell count	2	2	0~17	/ul
Squamous epithelial cells	2	1	0~28	/ul
Non-squamous epithelial cells	-	1	0~6	/ul
Trichomonas	-	-	0~1	/ul
Kidney epithelial cells	-	-	0~6	/ul
Transparent tube	-	-	0~2	/ul
Particle tube	-	-	0~1	/LPF
Cell tube	-	-	0~1	/LPF
Triphosphate crystal	-	-		
Calcium oxalate crystal	-	-		
Leucine crystal	-	-		
Cystine crystals	-	-		

Table S18. Transfusion-associated contagion tests of patient 2. The contagion tests of patient 2 showed specific antibodies to the hepatitis B virus. The other three transfusion-associated contagion tests (hepatitis C, syphilis, AIDS) were negative.

Code	Pre-Injection	Twelve Months Post-Injection
Hepatitis B virus surface antigen	Negative	Negative
Hepatitis B virus surface antibody	Weak Positive	Weak Positive
Hepatitis B virus e antigen	Negative	Negative
Hepatitis B virus e antibody	Negative	Negative
Hepatitis B virus core antibody	Positive	Positive
Hepatitis B virus antibody-immunoglobin M	Negative	Negative
Hepatitis B virus pre-S1 antigen	Negative	Negative
Hepatitis C virus antibody	Negative	Negative
Treponema pallidum particle agglutination test	Negative	Negative
Rapid plasma regain test	Negative	Negative
Human immunodeficiency virus antibody	Negative	Negative

Table S19. Blood tests of patient 3. The blood tests of patient 3 indicated mild hyperlipidemia, which had no obvious influence on the implementation of the surgery.

Code	Pre-Injection	Six Months Post-Injection	Normal Range	Unit
White blood cell count	5.45	4.83	4.0~10.0	10^9/L
Red blood cell count	5.28	4.89	4.3~5.8	10^12/L
Hemoglobin	159	152	130~175	g/l
Packed red blood cell volume	46.1	42.8	40~50	%
Red blood cell volume distribution width-coefficient of variation	11.9	12.4	10.0~15.0	%
Red blood cell volume distribution width-standard deviation	37.6	39.0	35.0~50.0	fL
Mean corpuscular volume	87.3	87.5	80.0~100.0	fL
Mean corpuscular hemoglobin	30.1	31.1	27.0~33.0	Pg
Mean corpuscular hemoglobin concentration	345	355	320~360	g/l
Platelet count	151	105	100~400	10^9/L
Platelet distribution width	10.8	12.2	9.0~17.00	
Thrombocytocrit	0.14 ↓	0.11 ↓	0.16~0.22	%
Mean platelet volume	9.5	10.7	9.0~16.0	fL
Platelet-larger cell ratio	21.5	30.8	14.0~46.0	%
Percentage of neutrophil	62.3	57.7	50.0~70.0	%
Percentage of lymphocyte	29.7	32.4	20.0~40.0	%
Percentage of eosinophil	1.7	2.3	0.5~5.0	%
Percentage of monocyte	5.9	7.3	3.0~8.0	%
Percentage of basophil	0.4	0.3	0.0~1.0	%
Neutrophil count	3.40	2.21	2.0~7.0	10^9/L
Lymphocyte count	1.62	1.24	0.8~4.0	10^9/L
Monocyte count	0.32	0.28	0.10~0.80	10^9/L
Eosinophil count	0.09	0.09	0.00~0.50	10^9/L
Basophil count	0.02	0.01	0.00~0.10	10^9/L
Code	**Pre-Injection**	**Six Months Post-Injection**	**Normal Range**	**Unit**
Alanine aminotransferase	29	53	0~65	u/l
Aspartate aminotransferase	18	26	15~37	u/l
Total protein	76	65	64~82	g/l
Albumin	49	40	35~54	g/l
Globulin	27	24	20~40	g/l
Albumin/globulin	1.8	1.66	1.2~2.5	
γ-Glutamyltransferase	37	49	15~85	u/l

Prealbumin	350		310		200~400	mg/l
Alkaline phosphatase	95		103		50~136	u/l
Blood urea nitrogen	6.6	↑	5.6		2.5~6.4	mmol/l
Creatinine	78		77		53~115	umol/l
Uric acid	0.32		0.37		0.202~0.417	mmol/l
Total bilirubin	16		16		0~17	umol/l
Connect bilirubin	7	↑	3		1~5	umol/l
Total bile acid	6		2		0.0~10.0	umol/l
High density lipoprotein	1.16		0.84	↓	0.910~2.060	mmol/l
Low density lipoprotein	2.79		2.24		0.00~3.36	mmol/l
Apoprotein A	1.29		1.00	↓	1.100~1.700	g/l
Apoprotein B	1.000		0.800		0.800~1.550	g/l
Apoprotein E	39		35		27~45	mg/l
Lipoprotein small a	38		42		0~75	nmol/l
Small dense low density lipoprotein	1.90	↑	1.87	↑	0.26~1.36	mmol/l
Calcium	2.32		2.32		2.04~2.74	mmol/l
Phosphorus	0.97		1.23		0.80~1.60	mmol/l
Potassium	4.3		4.4		3.5~5.4	mmol/l
Sodium	140		139		135~147	mmol/l
Chloride	102		105		96~108	mmol/l
Carbon dioxide binding capacity	26		23		21~32	mmol/l
Lactate dehydrogenase	149		175		81~234	u/l
Creatine kinase	75		98		39~308	u/l
Complement 3c	1.07		1.12		0.9~1.8	g/l
Complement 4	0.31		0.29		0.1~0.4	g/l
Complement 1q	195.5		210.4		159~233	mg/l
Total complement	82.5	↑	84.7	↑	32.5~58.3	u/ml
Haptoglobin	86.50		98.20		32~205	mg/dl
Blood glucose	5.7		4.7		3.9~6.1	mmol/l
Total cholesterol	4.36		3.68		2.80~5.20	mmol/l
Triacylglycerol	1.23		2.24		0.34~2.26	mmol/l

Code	**Pre-Injection**	**Six Months Post-Injection**	**Normal Range**	**Unit**
Prothrombin time	13.3	11.1	11.0~14.5	sec
International normalized ratio	1.00	0.94	0.80~1.20	INR
Activated partial thromboplastin time	37.7	32.8	28~45	s
Thrombin time	18.0	16.8	14.0~21.0	s
Fibrinogen	3.43	2.72	2.00~4.00	g/l

D-Dimer	0.28	0.31	0.00~0.50	ug/ml
Prothrombin time ratio	99	97	70~150	%

Code	**Pre-Injection**	**Six Months Post-Injection**	**Normal Range**	**Unit**
Glycated hemoglobin	5.3	4.89	4.0~6.0	%

Table S20. Routine urine test of patient 3. The routine urinalysis of patient 3 was unremarkable.

Code	Pre-Injection Results		Normal Range	Unit
Urine glucose	-		-	
Ketone body	-		-	
Occult blood	-		-	
Protein	-		-	
Nitrite	-		-	
Bilirubin	-		-	
Specific gravity	>=1.030	↑	1.003~1.030	
Urine PH value	7.0	↑	5.0~6.5	
Urobilinogen	3.2		3.0~16.0	umol/l
Leukocyte	-		-	
White blood cell count	1		0~28	/ul
Red blood cell count	1		0~17	/ul
Squamous epithelial cells	-		0~28	/ul
Non-squamous epithelial cells	-		0~6	/ul
Trichomonas	-		0~1	/ul
Kidney epithelial cells	-		0~6	/ul
Transparent tube	-		0~2	/ul
Particle tube	-		0~1	/LPF
Cell tube	-		0~1	/LPF
Triphosphate crystal	-			
Calcium oxalate crystal	-			
Leucine crystal	-			
Cystine crystals	-			

Table S21. Transfusion-associated contagion tests of patient 3. The contagion tests of patient 3 showed specific antibodies to the hepatitis B virus. The other three transfusion-associated contagion tests (hepatitis C, syphilis, AIDS) were negative.

Code	Pre-Injection Results
Hepatitis B virus surface antigen	Negative
Hepatitis B virus surface antibody	Positive
Hepatitis B virus e antigen	Negative
Hepatitis B virus e antibody	Positive
Hepatitis B virus core antibody	Positive
Hepatitis B virus antibody-immunoglobin M	Negative
Hepatitis B virus pre-S1 antigen	Negative
Hepatitis C virus antibody	Negative
Treponema pallidum particle agglutination test	Negative
Rapid plasma regain test	Negative
Human immunodeficiency virus antibody	Negative

Video S1. HELP Administration method. Each formulation, 0.2 mL in total, was drawn into a 27g ophthalmic syringe for the intrastromal injection. Penetrating keratoplasty was performed following the routine procedures. After sewing up the donor cornea, the graft bed of the recipient was injected with the HELP formulation in 6-8 locations.

Supplemental Results of Whole Genome Sequencing (WGS)

The sequencing depth of sequencing data of the two samples (HELP-treated group and WT group) was sufficient (62x and 64x, respectively) with good sequencing quality (Q30 > 90%) (Table S4). After sequence alignment, the results showed that mapping rate to human genome (hg19) was greater than 92%, and the fraction of covered with ≥20x and 0.2*Mean were greater than 97%. The fraction of CDS regions covered with ≥20x was greater than 98%. These results indicating a good quality of the sequencing data (Table S5).

The analysis of off-target sites showed that there were few potential off-target sites. In the HELP-treated cells, no potential off-target sites of UL8 sgRNA were identified, and one potential off-target site of UL29 sgRNA was identified, which was a SNP located at chr8:105,379,595 in the intergenic region and far from CDS (>10K) with low mutation frequency of 0.0545 (Table S6).

Structural variants (SVs) analysis revealed ten SVs in the HELP-treated HCSCs sample after filtering out the data of untreated HCSCs sample (WT sample), and seven SVs in the WT sample after filtering out the data of HELP-treated HCSCs sample. All the structural variants have low risk of affecting the gene function and causing pathogenicity (Table S7-9). Considering the structural variants result, it is presumed that these SVs probably occur due to the nature of the cells rather than HELP treatment.